STRUCTURAL MONITORING AND WIND TUNNEL STUDIES OF A LOW WOODEN BUILDING

Ioannis Zisis

A Thesis

In

The Department

of

Building, Civil and Environmental Engineering

Presented in Partial Fulfillment of the Requirements
for the Degree of Master of Applied Science (Building Engineering) at
Concordia University
Montreal, Quebec, Canada

December 2006

Your file Votre référence
ISBN: 978-0-494-28895-5
Our file Notre référence
ISBN: 978-0-494-28895-5

ABSTRACT

STRUCTURAL MONITORING AND WIND TUNNEL STUDIES OF A LOW WOODEN BUILDING

IOANNIS ZISIS

Low rise wooden buildings are the most common residential housing type for North America. The behavior of these structures subjected to wind load is examined in the present study. Coupling of three individual research methods is used in order to better understand and assess the subject.

Full-scale monitoring is the first part of the study. A test building was constructed in Fredericton, NB and was equipped with weather, pressure and load monitoring instrumentation. The behavior of this structure has been monitored since spring 2006. The recorded data have been analyzed and pressure and force coefficients have been computed.

The second part of the study, deals with the wind tunnel experiments of the test building. A 1:200 scale model was constructed and tested at the Building Aerodynamics laboratory of Concordia University. The building model was tested for a total number of 15 angles of wind attack and the pressure results were transformed into mean and peak local and area-averaged pressure coefficients.

Numerical analysis was used as a supplementary tool for this study. A 3-D linear model was created and finite-element analysis was performed for the selected wind directions. Using the computed stresses at the points of interest (location of full-scale load cells), the force coefficients were evaluated.

Pressure distribution comparisons between the full-scale and the wind tunnel results show good agreement. Small discrepancies were attributed to the direction fluctuations of the full-scale records. The force coefficient comparison between the full-scale and the finite element analysis show generally good agreement as well.

ACKNOWLEDGMENTS

I would like to gratefully acknowledge all the individuals who contributed each with a unique way to the completion of this study.

Special thanks are due to Dr. Theodore Stathopoulos for the excellent guidance and advice through out this study and my family Georgios, Efstathia and Periklis Zisis for the continuous support and encouragement.

I would also like to acknowledge my friends in Greece and Canada for the many enjoyable moments we spent during the last two years.

Finally, I would like to particularly thank my friend Georgios Gerontakos for his sincere support, Kai Wang and Dean McCarthy for their great help with the wind tunnel tests and full-scale measurements respectively and Panagiota Karava for reviewing this thesis.

TABLE OF CONTENTS

LIST OF FIGURES

LIST OF SYMBOLS

c_f	force coefficient
$c_{f,mean}$	mean force coefficient
$c_{f,min}$	minimum force coefficient
$c_{f,max}$	maximum force coefficient
c_p	pressure coefficient
$c_{p,i}$	internal pressure coefficient
$c_{p,mean}$	mean pressure coefficient
$c_{p,min}$	minimum pressure coefficient
$c_{p,max}$	maximum pressure coefficient
$c_{p,rms}$	root-mean-square pressure coefficient
g	gravitational acceleration
h_g	gradient height
k	Von Karman constant
H	wall height
$I(z)$	turbulence intensity

L_u^x	longitudinal integral scale of turbulence
L_x	wall length
n	frequency
p	pressure
p_a	atmospheric pressure
p_i	internal pressure
p_{mean}	mean pressure
p_{min}	minimum pressure
p_{max}	maximum pressure
p_s	stagnation pressure
q	dynamic pressure
$R_u(\tau)$	autocoveriance function
R_X	reaction at x direction
S_V	spectral density function of velocity
$V, V(z)$	wind speed
$\overline{V}, \overline{V(z)}$	mean wind speed
$V(t)$	fluctuating component of wind speed
V_1	wind speed at height z_1
V_H	wind speed at building height
V_g	gradient wind speed

V_*	shear or friction velocity
u, v, w	denote wind speed components on x, y and z directions
z	height from ground level
z_g	gradient height
z_0	roughness length
α	power law exponent
δ	boundary layer thickness
θ	wind incidence angle
ρ	ambient air density
σ	standard deviation
σ_u	standard deviation of the mean wind speed

CHAPTER 1

INTRODUCTION

1.1 OVERVIEW

The structural response of low-rise wooden buildings subjected to environmental loads is assumed to be a relatively straightforward phenomenon. This is not always the case though, especially in the last couple of decades where a rapid development of wood construction has been observed. The advancement of computer technology and the numerous commercial analysis and design software packages can be considered as reasons for this augmented "know-how" confidence. Many studies have tried also to define the structural response of wooden buildings in the most accurate and sophisticated way. Outcomes of these studies usually enrich the building code provisions and provide the structural engineers with the appropriate knowledge and experience for a safe and economical design.

Low-rise wooden buildings are not always simple rectangular structures. More recently, the demand for unique and innovating architectural design, lead to complex structural systems where the use of new wood-based materials was necessary. On the other hand the prescriptive building codes are often based on simplifications and assumptions, especially when they deal with low-rise buildings. This analysis

approach may lead to over-estimated or under-estimated design solutions with a direct impact to the construction cost or to the safety of the occupants.

Environmental loads are by their nature random; therefore use of statistics and dynamic analysis are important tools for a better understanding of their impact on structures. Past studies uncovered many uncertainties of the wind nature, particularly as far as interaction with buildings is concerned. Unfortunately, most of these studies were conducted only on scale models, in a simulated environment (wind tunnel) and the rest were based on computer software analysis. Very few studies were able to couple full-scale with model scale and numerical analysis extensive research results.

1.2 SCOPE AND OBJECTIVES

The NSERC Collaborative Research and Development (CRD) Project "Load Paths in Wood Buildings" awarded to four Canadian Universities including Concordia, entails the monitoring and collection of data from three light frame wood buildings to assess the application of environmental loads and their actual transferring through the buildings' elements to their foundation. Structure 1 is an existing industrial single-storey, light-frame shed located in Saint Foy, Quebec and owned by Forintek Canada Corp. This shed was monitored for wind pressures and structural responses to natural, as well as artificial loading, since 2002 (Doudak et al. 2005). Structure 2 has been constructed in Fredericton, New Brunswick and is going to be the case study for this thesis. Structure 3 is a single-storey, light-frame building with post frame construction and duo-pitch roof in Winnipeg, Manitoba.

Scope of this project is to determine how environmental loads affect a typical wood building. The main loading considered in this study is wind. Understanding the interaction between the wind load and the structure is considered critical in the evaluation of wind load paths in buildings. Full-scale measurements on Structure 2, wind tunnel studies and numerical analysis are used to understand and define the nature of this complex subject. Through this study, the importance of the wind-induced pressure acting on the surface of a building will be examined, i.e. how this pressure is distributed on the structure and, finally, how the structural system resists to the applied load.

Main objectives of the current thesis are to collect and interpret full-scale data, to conduct wind tunnel tests and analyze measured data and to create a linear numerical model for comparison and verification of the full- and model-scale results. General objectives of the CRD project are in addition to the above, the development of more complex numerical models, which in conjunction with model simulated studies they will be used for sophisticated but economic analysis of wooden structures. Appropriate generalization of these complex models will be made in order to contribute to future building codes, by providing them with simple structural models, which every structural engineer will be able to use. In general, a better understanding of the structural behavior of low-rise wooden buildings is going to be achieved. A schematic overview of the project objectives is shown in Figure 1.2.1.

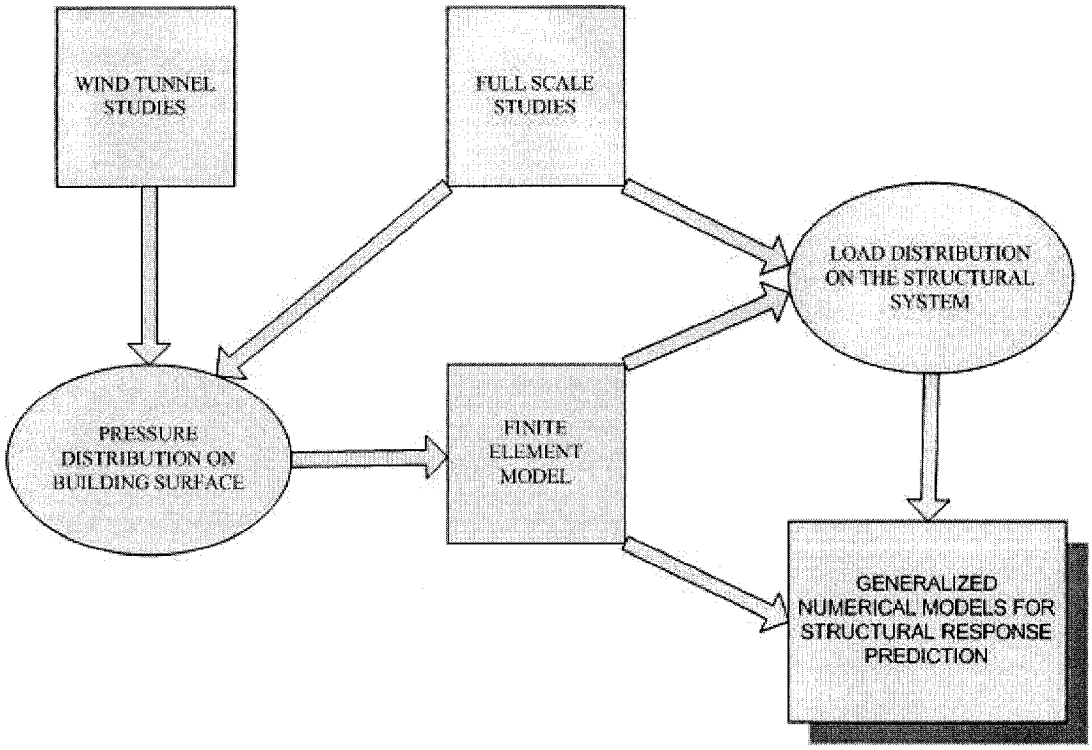

Figure 1.2.1 Schematic overview of research project objectives

1.3 THESIS STRUCTURE

In the following chapters, a detailed description of the objectives of this study will be made and results will be presented. In more detail, the thesis structure is going to be as follows:

- Chapter 2: A literature survey along with some basic wind engineering concepts is discussed.

- Chapter 3: The wind tunnel studies are presented in detail. The wind tunnel facilities and the model construction are discussed. The simulation and testing procedure are described.

- Chapter 4: This chapter is dealing with the full-scale studies. The facilities and the instrumentation are presented in detail and a discussion about the data interpretation technique follows.

- Chapter 5: The finite element analysis is the main subject of this chapter. Details about the numerical modeling of the test building and the input loading data are presented.

- Chapter 6: Presentation of results, comparisons and discussion are the scope of this chapter. In addition, comments are made concerning the comparison of the results.

A conclusion chapter is the last part of this thesis where recommendations for future research are also included. Two appendices with supplementary results complete this work.

CHAPTER 2

LITERATURE REVIEW

2.1 INTRODUCTION

In the last 2-3 decades very few full-scale wind pressure monitoring studies have been carried out. For most of them the results compared with model scale tests and computer based analysis. The outcomes of these studies are generally in good agreement but there are also points still waiting for further research. The agreement mentioned above is mainly associated with the mean structural response and specifically with the mean surface pressures on the building. However peak response and load distribution is an area with a lot of complexity.

The several difficulties on performing full-scale studies are the main reasons for this lack of intensive research in this scientific area. Some of these difficulties are the cost of full-scale monitoring studies, the unforeseen character of natural wind, the requirement of different disciplines interaction (wind, structural and electrical engineers) and the need of sophisticated and strong capabilities software. The very few projects that had coupled full-scale wind pressure monitoring with wind tunnel studies will be presented in detail in this chapter. For easier understanding of the material presented, a brief discussion about basic wind engineering concepts will first follow.

2.2 WIND ENGINEERING BASICS

2.2.1 The Atmospheric Boundary Layer

The atmosphere consists of different layers which interchange with respect to height or the distance from the ground level. Since common structures rest on the ground level and have a height of a few meters, only the very first of the atmospheric layers, the so called atmospheric boundary layer, is of main interest. This layer has a depth between a few hundred meters to several kilometers, depending mainly on the terrain characteristics, such as topography and roughness.

The basic characteristic of the atmospheric boundary layer is that the wind speed increases with respect to the height – see Figure 2.2.1. Thus, the surface wind speed at the ground level (zero reference height) is assumed to be zero and as the height increases and reaches the end of the atmospheric boundary layer, the wind speed is maximum. This maximum speed is usually referred as gradient wind speed.

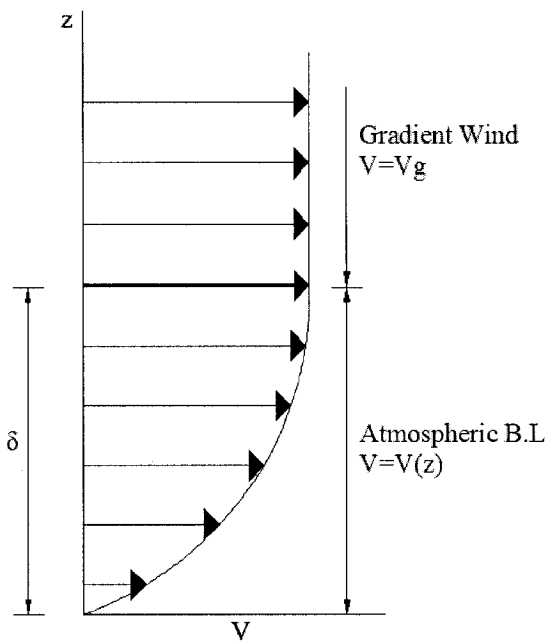

Figure 2.2.1 Atmospheric boundary layer

Above the atmospheric boundary layer, the wind speed is assumed to be constant. In bibliography, the greek letter δ is commonly used to define the thickness of the boundary layer. There are two main approaches for the approximation of the wind speed profile. The first is the logarithmic law (Eq. 2.1) and the second is the power law (Eq. 2.2).

$$V(z) = \frac{1}{k} V_* \times \ln \frac{z}{z_0} \tag{2.1}$$

$$V(z) = V_1 \times \left(\frac{z}{z_1} \right)^{\alpha} \tag{2.2}$$

The surface roughness is a very important characteristic for the development of the wind speed profile. The effect of the surface roughness can be easily seen at the logarithmic law equation; larger values of roughness shift the wind speed profile to greater heights. This can also be shown using the power law, by setting as reference height the thickness δ of the atmospheric boundary layer and as reference wind speed the gradient speed (Eq. 2.3).

$$V(z) = V_g \times \left(\frac{z}{\delta} \right)^{\alpha} \tag{2.3}$$

The values of α and δ are directly affected by the terrain roughness. A summary of suggested values for the above characteristics of the atmospheric boundary layer in codes and standards can be found in Table 2.1.

Table 2.1 Power law exponent, terrain roughness and boundary layer thickness suggested values (from Liu 1991)

Exposure Category	Power Law Exponent (α)	Terrain Roughness (z_0) - cm	Atmospheric B.L. Thickness (δ) - m
A	0.33	80	457
B	0.22	20	366
C	0.14	3.5	274
D	0.1	0.7	213

Another very important characteristic of the wind is the turbulence. Wind is a flow with many fluctuations and random behavior. For this reason, it is of great importance to use the definitions of the mean, peak and RMS wind speed so as to better understand this phenomenon. The first and most important definition is the mean wind speed: the average over certain duration of a wind speed record. The most common averaging periods are the 10-minutes and 1-hour mean values. Although the mean wind speed is useful for describing climate characteristics, structural engineers are mainly interested for the peak values of the wind speed. The peak wind speeds can be defined with a number of different ways, again depending the duration of the record and also the statistical tools used. In general, for a random wind speed record, the peak wind speed for a given return period is inversely proportional to the averaging time.

In order to describe the turbulence of a given terrain, the turbulence intensity was introduced. As mentioned previously, the wind speed has a fluctuating nature; especially for the regions near the ground surface the flow is highly fluctuating and the speed can be described by:

$$V(z,t) = \overline{V}(z) + V(t) \tag{2.4}$$

where $\overline{V}(z)$ is the constant component of the wind speed and V(t) the fluctuations.

The longitudinal turbulence intensity is defined as:

$$I(z) = \frac{\sqrt{\overline{V^2(z,t)}}}{\overline{V}(z)} \tag{2.5}$$

where $\sqrt{\overline{V^2(z,t)}}$ is the root mean square value of the wind speed at the elevation z

In addition to the turbulence intensity, some other characteristics are used to describe the wind flow. These are the integral scales of turbulence and the spectrum of turbulence expressed by its power spectral density. The fluctuation of the wind flow results from the superposition of eddies on the mean wind. Each of these eddies has a characteristic amplitude and frequency n and all together contribute to the total kinetic energy of the fluctuating motion.

The integral scales of turbulence measure the average size of eddies. Since there are three dimensions and three different components for the flow fluctuations (longitudinal, transverse and vertical) a total of nine different scales of turbulence exist. The most common is the longitudinal scale of turbulence, defined as:

$$L_u^x = \frac{1}{\sqrt{\overline{V^2}}} \int_0^\infty R_u(\tau)\, d\tau \tag{2.6}$$

where $R_u(\tau)$: autocoveriance function of the fluctuation V(z,t)

The spectrum of wind turbulence is used to describe the total energy generated by the eddies and for convenience purposes this is defined by

$$V_1 = \sqrt{\overline{V(t)^2}} = \int_0^\infty S_1(n)\,dn \tag{2.7}$$

The most common expressions of the power spectra of longitudinal velocity used for structural design purposes are the following (from Simiu and Scanlan, 1996):

- Davenport Equation:

$$\frac{nS(z,n)}{V_*^2} = 4\frac{x^2}{(1+x^2)^{\frac{4}{3}}} \tag{2.8}$$

where: $x = \frac{1200 \times n}{V(10)}$,

n in (Hz) and V(10) the mean wind speed in m/sec at z=10m

- Von Karman Equation:

$$\frac{nS(n)}{V_*^2} = 4\frac{\beta\frac{nL_u^x}{U}}{\left[1+70.8\left(\frac{nL_u^x}{V}\right)^2\right]^{\frac{5}{6}}} \tag{2.9}$$

2.2.2 Wind Induced Pressures and Forces on Buildings

A structure exposed to the natural wind is subjected to wind induced pressures leading to wind induced forces and moments. Scope of wind engineers is to fully define the surface pressure on the building and translate this pressure to actual load. In order to define the wind pressure on structures there is a need for a reference pressure

which the wind pressure is going to be compared. This reference pressure is the ambient atmospheric pressure and is simply the air pressure at the examined location assuming that the structure was not present. It is of great importance in wind engineering studies (especially full-scale studies) to be able to measure the ambient atmospheric pressure without any effects of separation or wake of adjacent structures or buildings. As a result of using the atmospheric pressure as reference, both positive (pressure) and negative (suctions) pressures act on the surface of the buildings.

In order to define the pressure and suctions acting on the surface of the structure, the wind flow is assumed to be steady and uniform. Applying Bernoulli's equation for the flow:

$$p_a + \frac{1}{2}\rho V^2 = p_s \tag{2.10}$$

where p_s is the stagnation pressure

For convenience, dimensionless coefficients have been introduced and these coefficients help to evaluate and compare the effects of wind on structures. Thus, the mean pressure coefficient is defined as:

$$c_{p,mean} = \frac{p_{mean} - p_a}{\frac{1}{2}\rho V^2} \tag{2.11}$$

Peak and RMS pressure coefficients are defined as:

$$c_{p,peak} = \frac{p_{peak} - p_a}{\frac{1}{2}\rho V^2} \tag{2.11}$$

$$c_{p,rms} = \frac{p_{rms} - p_a}{\frac{1}{2}\rho V^2} \tag{2.12}$$

Internal pressure coefficient is defined as:

$$c_{p,i} = \frac{p_i - p_a}{\frac{1}{2}\rho V^2} \tag{2.13}$$

2.2.3 Boundary Layer Wind Tunnels

The need to better understand the effects of wind on structures urged engineers to find a way to simulate wind in a controlled environment and examine the response of structural models inside this environment. A specially constructed wind tunnel, the boundary layer wind tunnel, is used for this reason and the basic requirements of these tunnels is sufficient length, width and height in order to simulate properly the characteristics of the atmospheric boundary layer (velocity profile, turbulence intensity and power spectra of turbulence).

Wind tunnel studies are a very detailed and difficult task. A number of similarity parameters should be considered during a wind tunnel study. The basic scale factors

are the length, velocity, air density, frequency and time factors. It should be noted that these parameters are not independent from each other.

Wind tunnel models are of different scales and different material, depending on the scope of the study. Sophisticated equipment is used in order to conduct with accuracy a wind tunnel study.

2.3 THE AYLESBURY EXPERIMENT

One of the first studies carried out on a full-scale structure was the Aylesbury test building. This study started at 1970's and the data collected were used and compared with wind tunnel studies for nearly the following 3 decades. The test building was a two-storey house, located in Aylesbury, UK. It was a rectangular-shaped building (13.0 x 7.0 meters) and had a variable pitch roof (range of 5 to 45 degrees). Details of the full-scale experiments are presented by Eaton et al. (1975 and 1976).

Full-scale data were collected by the Building Research Establishment (BRE-UK). The frequency response of the transducers used was up to 32 Hz. The ambient atmospheric pressure was used as reference and a special manhole located approximately 80 meters east of the house was used for this reason. The total number of transducers used was 72.

Several wind tunnel tests were conducted, in order to compare the results with the full-scale data from the Aylesbury project. The most complete study was the Aylesbury Comparative Experiment (Sill et al. 1989 and 1992). This study compares full-scale measurements with wind tunnel results from 17 different laboratories. The most important outcome of this comparison was the problematic behavior of the

reference static pressure box location and construction. This was found to be the main reason for the differences between the model scale and the full-scale results. Another interesting point of this experiment was the difference of the results between the different wind tunnel studies, which for some cases it was up to 40%.

It appears that the Aylesbury project was the forerunner for the wind pressure monitoring in full-scale low rise buildings. The location of the reference static pressure box in the full-scale house was the weakest point of this study. The interpretation and analysis of the full-scale and model scale data was also another reason for the discrepancy between the results, especially for the peak pressures.

2.4 THE SILSOE STRUCTURE (BRE)

Another important project, connecting full-scale with model scale studies, started in the Silsoe Research Institute (formerly AFRC Institute of Engineering Research) in the late 1980's. The Silsoe experimental building was located at the Silsoe Institute, Wrest Park, Silsoe, UK on a relatively open field site. This building was designed specifically for wind pressure monitoring. A basic characteristic of the building was the choice of curved or sharp eave detail configuration. The house was of rectangular shape, 24 meters long by 13.9 wide and the ridge height was 5.3. The duo pitch roof had a 10-degree inclination. Two main sets of full-scale pressure data were collected. The first set of measurements was collected by SRI (Silsoe Research Institute) with a total of 77 pressure taps installed on the surface of the house. The second main set was measured by BRE (British Research Establishment) a few years later, using a

new independent set of instrumentation. For this case, 32 pressure taps were connected to the transducers and simultaneous measurements were made.

The researchers, having already the experience of previous full-scale studies and knowing the problems created by the reference static pressure box location, decided to mount the reference pressure probe 20 meters upstream of the house at the same height with the ridge. This distance and position was assuring that the influence of the building was negligible.

The full-scale measurements were supported by several wind tunnel studies. Two most important such studies, were conducted at the UWO and the BRE wind tunnel facilities. Two models were constructed at the BRE, one with curved and one with sharp eaves. Both models were made at 1:100 geometric scale. The same models but with different tubing sensor systems were used for both studies at UWO and BRE wind tunnels. The curved-eave model had a total of 81 pressure taps and the sharp-eave model a total of 74 pressure taps. For both tests, special attention was given for the accurate simulation of the upstream terrain characteristics and different tests covered a number of upstream terrain configurations.

Most of the comparisons referred mainly to the mean pressure coefficients. Some references (Richardson, 1991) mention that the flow separation and recirculation cannot be properly simulated in the wind tunnel tests. As a result, underestimated peak response was predicted in the wind tunnel measurements.

The experience gained through this study was significant, not only for the full-scale but for the wind tunnel tests as well. For first time in full-scale studies, it was shown that architectural details are of great importance and they can affect the surface pressure distribution significantly. Many of the full-scale results, especially for the mean pressure coefficients, were in good agreement with the simulated tests. A couple

of CFD studies, for the verification of the results, is also another worth mentioning point regarding the value of this project.

2.5 THE TEXAS TECH UNIVERSITY PROJECT (TTU)

In the late 1980's a very important and long lasting full-scale study was undertaken by the Texas Tech University (Levitan et al. 1992a and 1992b). A permanent laboratory had been constructed in order to assess the wind effects on a low-rise building. The experimental house was located on Texas Tech University land in Lubbock, Texas. The terrain surrounding the house was open and relatively flat. The building is known under the name of WERFL (Wind Engineering Research Field Laboratory). The prefabricated metal house is a low rise rectangular structure with external dimensions of 9.1 x 13.7 x 4.0 meters (B x L x H). The roof is almost flat and the house is rested on a concrete slab. The very unique characteristic of this building is that it is not anchored to the concrete slab. Instead a special mechanism provides the building with the ability to rotate about its center. This system gives the opportunity to the researchers to control the wind angle of attack. WERFL was equipped with state of the art instrumentation (at the time it was constructed).

The total number of the pressure taps installed on the surface of the building was more than 100. The pressure taps were connected to three different types of transducers. At the early stage of the testing only 47 transducers were though available. The first set of transducers had a full-scale range of +/- 1.38 kPa, the second +/- 2.21 kPa and the last one +/- 1.24 kPa. The reference pressure for the measurements was the ambient atmospheric pressure. As mentioned previously, this

was one of the main problems for other full-scale studies. For this particular study, a box below ground was used. This box had a lid with a small hole and was located 23 meters west of the center of the test building. Special attention was given to the location of the reference pressure box so as not to be affected by the building.

The meteorological instrumentation used in this study consisted of 49 meters high meteorological tower located 46 meters west of the building. This tower was equipped with a number of instruments installed at six different levels (1, 2.5, 4, 10, 21, 49 meters). Some of the instruments used were three-cup anemometers, wind direction, barometric pressure, relative humidity and temperature sensors.

The high end equipment made for first time possible to collect a huge amount of meteorological and wind pressure data. Records of 15 minutes test runs were used to compute the basic wind characteristics, such as power law exponent (α=0.14-0.16), roughness length (z_0=1.5-1.8 cm) and turbulence intensity (I=19-20% at 4 meters height). Concerning the pressure records, a data acquisition system (DAS) was operating continuously. The trigger was set at 9 m/sec wind speed. If the wind speed was exceeding this limit then a 20-second calibration run for the transducers was performed and right after, a 15-minute duration record was scanned. A sophisticated data validation system was introduced in this study, so as to assure the quality of the record data. A stationarity check was also performed before the detailed analysis of the recorded data. Until 1992 a considerable amount of full-scale data was available for validation with model-scale studies.

As expected, many different wind tunnel studies were carried out all around the world. Different scale models were used and significant improvement of the wind tunnel testing techniques was the result of this effort. A summary of the model scale studies follows.

A 1:100 and 1:50 model of the WERFL were tested at the Colorado State University by Cohran and Cermak (1992). The comparison with the full-scale results showed good agreement with the exception of the peak pressure coefficients for the regions to the end and corner roof locations. For these regions the model study underestimated the extreme-peak pressure coefficients by up to a factor of two. The mean pressure coefficients were in good agreement though.

Another wind tunnel study was carried out at the Building Research Institute in Japan by Okada and Ha (1992). Three different geometric scale models (1:65, 1:100 and 1:150) were tested and the mean pressure coefficients were again found in good agreement with the field measurements. There is though a small disagreement for high local wind pressure on the windward wall. Concerning the peak and RMS pressure coefficients, the wind tunnel tests clearly underestimate the full-scale results. This was attributing to the difference in the turbulence intensity between the full-scale and the wind tunnel simulation. It should be noted that the reference static pressure box was barely affected by the house in this study.

The UWO wind tunnel study for the WERFL tested two models of 1:50 and 1:100 scale in a boundary layer wind tunnel. The results of this study follow the same direction with the previous wind tunnel tests. Finally, additional worth mentioning wind tunnel studies worth mentioning were conducted at WindTech's boundary layer wind tunnel (Rofail 1995) for a 1:50 and 1:100 scale models. A 1:50 model was tested at the facilities of Clemson University (Tieleman et al. 1998) with similar results as the rest of the wind tunnel tests.

2.6 THE LOAD PATHS ON WOOD BUILDINGS PROJECT (STRUCTURE 1 – QUEBEC CITY)

This study is part of the current project "Load Paths in Wood Buildings" – see section 1.2 - and refers to the first of the three wooden structures which was tested during this project. It is an existing industrial single storey, light frame shed, located in Saint Foy, Quebec and owned by Forintek Canada Corp. This building is a typical storage shed, constructed in 1998 - Figure 2.6.1. It has a rectangular plan with external dimensions of 8.0x15.0. The roof is flat and has a height of 5.1 meters with a 0.5 meters high parapet.

Figure 2.6.1 Forintek building

The area surrounding the building consists mainly of similar low-rise storage and industrial buildings and low dense plantation. The test building is equipped with 20 pressure taps, 14 of which located on the walls and the rest on the roof. The pressure

taps are connected with sensitive differential pressure transducers, which were calibrated at the Building Aerodynamics Laboratory of Concordia University. The ambient atmospheric pressure was used as reference pressure for the transducers and it was measured in a box located about 25 meters from the test building. Structure 1 is also equipped with LVDT (Linear Variable Displacement Transducers) that can measure the displacements of the structure at desired key points. Meteorological data have been collected by a weather station close to the south-west face of the building. The station is equipped with a propeller anemometer, mounted at 10 meters above the ground. In addition to this station, data are also provided by two other stations; the local airport, located west of the building site and Laval's University weather station.

Wind pressure records have been collected but only for a few wind directions. The lack of high winds for other directions made the collection of more pressure data almost impossible. Mean and peak pressure coefficients were calculated so as to compare them with wind tunnel testing results.

The model scale tests were conducted at the Building Aerodynamics Laboratory of Concordia University. A 1:200 building model was constructed and tested – see Figure 2.6.2. The model was equipped with 20 pressure taps located at the same points as the full-scale structure, as shown in Figure 2.6.3. A surroundings model was also constructed and the upstream terrain characteristics were simulated based on the full-scale wind data.

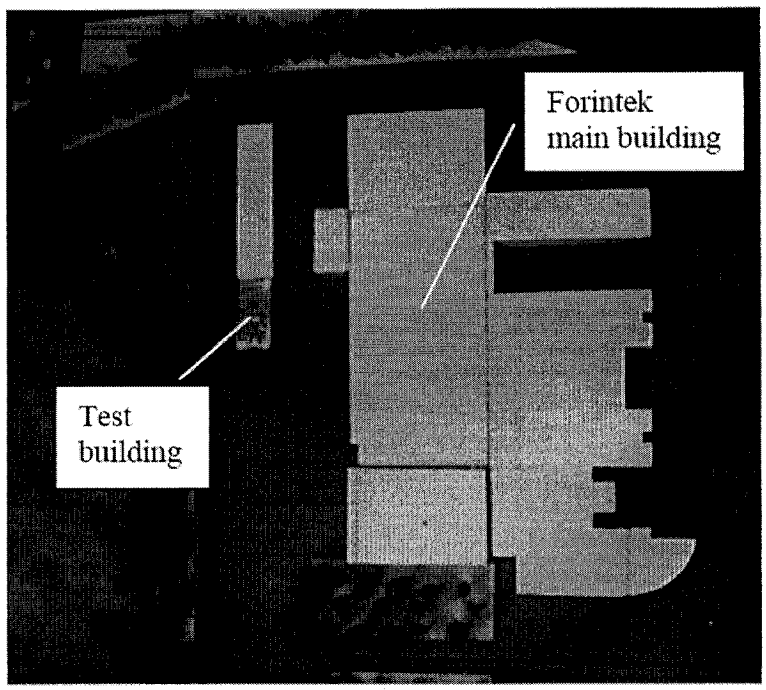

Figure 2.6.2 Wind tunnel model and surroundings

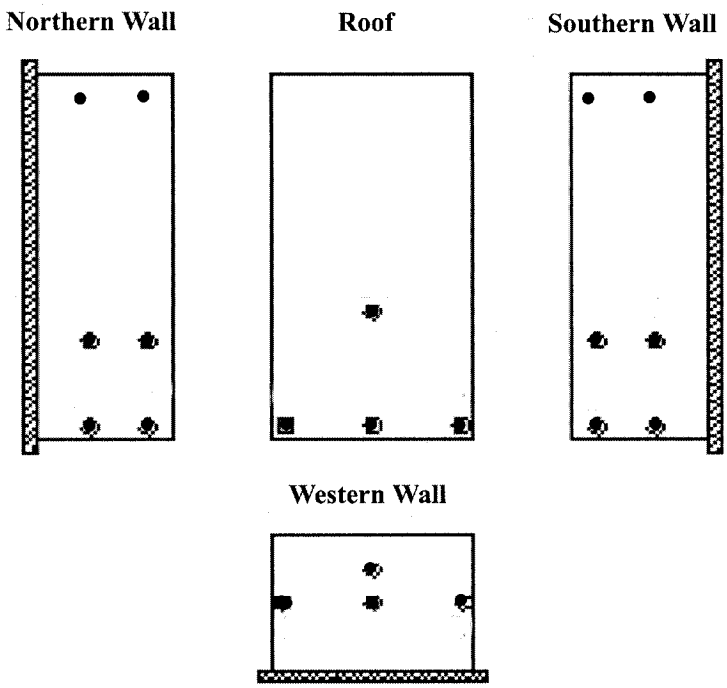

Figure 2.6.3 Pressure tap location in the wind tunnel model

Wind tunnel data were obtained for more than 15 directions using an interval of 10-15 degrees. The data were recorded at a frequency of 250 Hz. Mean and peak pressure coefficients were calculated and compared with good agreement with the full-scale results. A typical comparison record is presented in Figure 2.6.4.

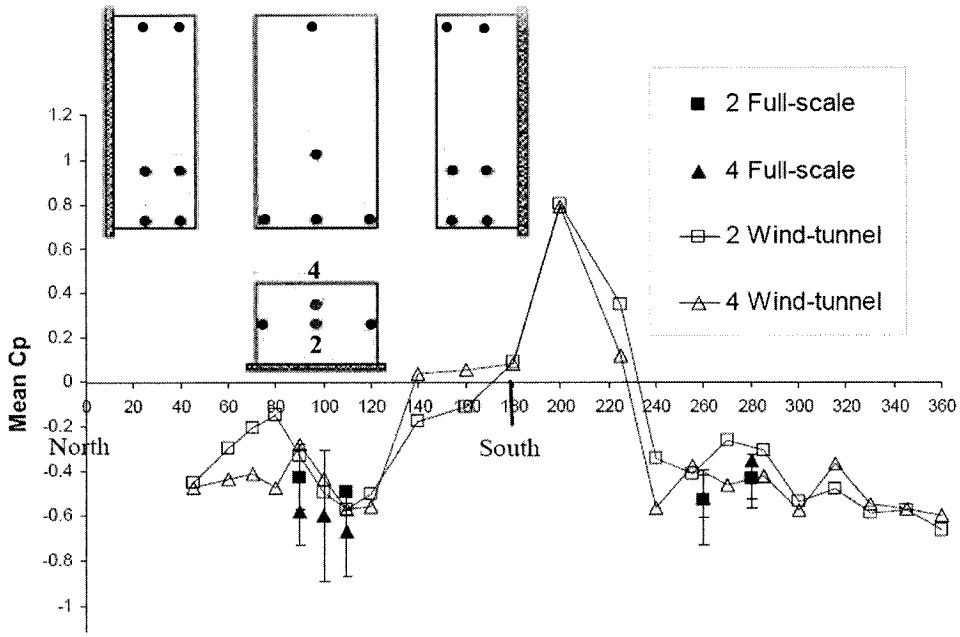

Figure 2.6.4 Comparison of full-scale and wind tunnel results (pressure taps 2 and 4) – after Doudak 2005

A finite element model was also prepared and used for comparison with the full and model-scale results. The outcomes of this study are presented in detail by Doudak et al. (2005a, 2005b and 2005c).

CHAPTER 3

WIND TUNNEL STUDIES

3.1 GENERAL

The wind tunnel tests were of great importance for the scope of this study. The appropriate simulation and testing of the full-scale building was the first part of this multilateral project. This chapter is dealing with all the necessary information concerning the wind tunnel studies. Detailed description of the facilities, construction of the building and surroundings model, boundary layer simulation for wind tunnel testing, instrumentation and equipment description, wind tunnel testing, output data interpretation and finally pressure distribution results, are presented in each of the sections of this chapter.

3.2 WIND TUNNEL FACILITIES

The wind tunnel tests were conducted in the Building Aerodynamics Laboratory (B.A.L.) located in the Engineering Complex at Concordia University. It is an open circuit, blow down tunnel 12.0 meters long and has a test section 1.8 meters wide and 1.8 meters high – see Figures 3.2.1 and 3.2.2. The wind speed of the wind tunnel

ranges between 4.0 and 14.0 m/sec. A turntable of 1.20-meter diameter is located on the test section of the tunnel and allows testing of models for different angles of attack. The floor of the wind tunnel is covered with carpet. This is the standard configuration and represents the open country (flat) terrain simulation. Different terrain simulations are also possible by adding panels with roughness elements on the floor area between the fan and the test section. Construction details and further characteristics of the tunnel were presented by Stathopoulos (1984).

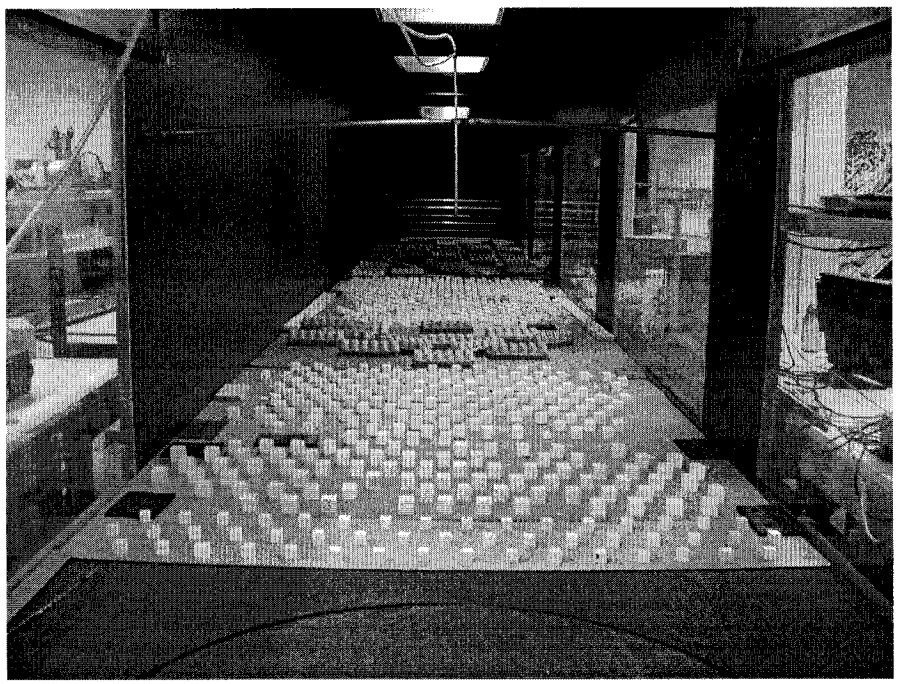

Figure 3.2.1 Front view of the boundary layer wind tunnel

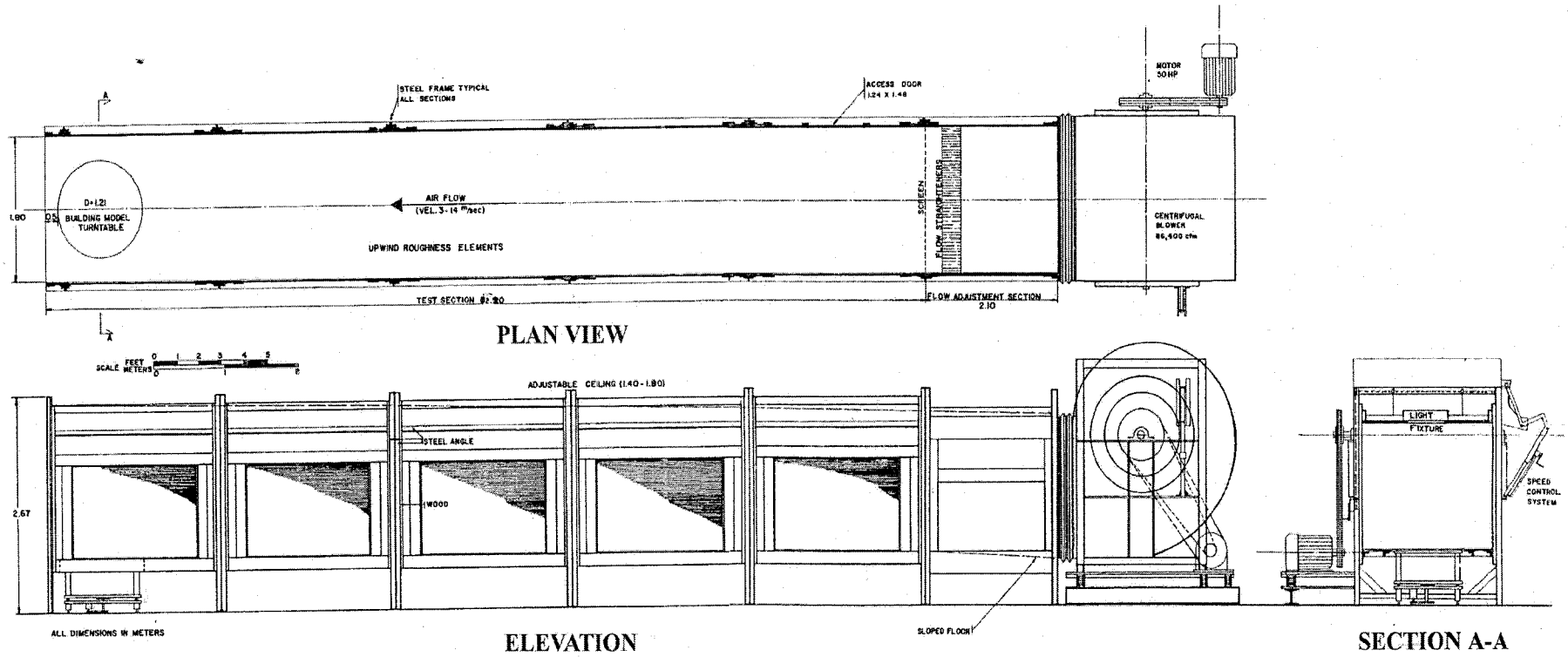

Figure 3.2.2 The boundary layer wind tunnel at Building Aerodynamics Laboratory-Concordia University, after Stathopoulos (1984)

3.3 BUILDING AND SURROUNDING MODEL

Taking into consideration the size of the full-scale building and surrounding structures, a geometric scale of 1:200 was selected for the wind tunnel studies.

A metallic 1:200 model of the building was constructed. The model has external dimensions of 86.5 mm by 42.5 mm (length – width) and a total height of 24.35 mm (ridge height). The gabled roof has a slope of 4:12. The thickness of the metallic elements used to construct the model is approximately 1.5 mm. The model is equipped with 130 pressure taps located on the wall and roof surface. A detailed exploded plan and elevation view of the model building is shown in Figure 3.3.1.

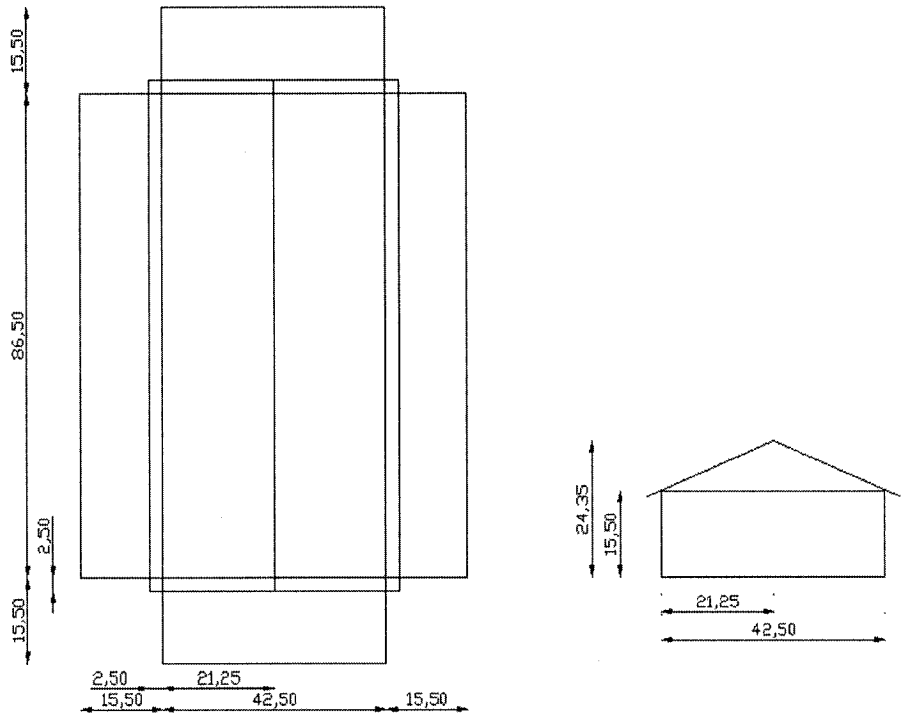

Figure 3.3.1 Exploded plan and elevation view of the wind tunnel building model

The pressure taps are made of 15 mm long brass tubes with an internal diameter of 0.8 mm and are mounted on the inside surface of the building model. Flexible urethane tubing is used to connect the brass tubes with the transducers – see Figure 3.3.2. The length of the urethane tubing is approximately 620 mm with a brass restrictor placed at the 10/24 of the length (10:14 length ratio) in order to minimize the frequency response effect during the measurements. Special attention was given to the details of the wall edges and roof eaves; sharp edges can simulate accurately the flow separation during the wind tunnel tests. The pressure taps were given a special identity name consisting of 1-2 letters, indicating the surface and a number indicating the location – see Figure 3.3.3 and Table 3.1.

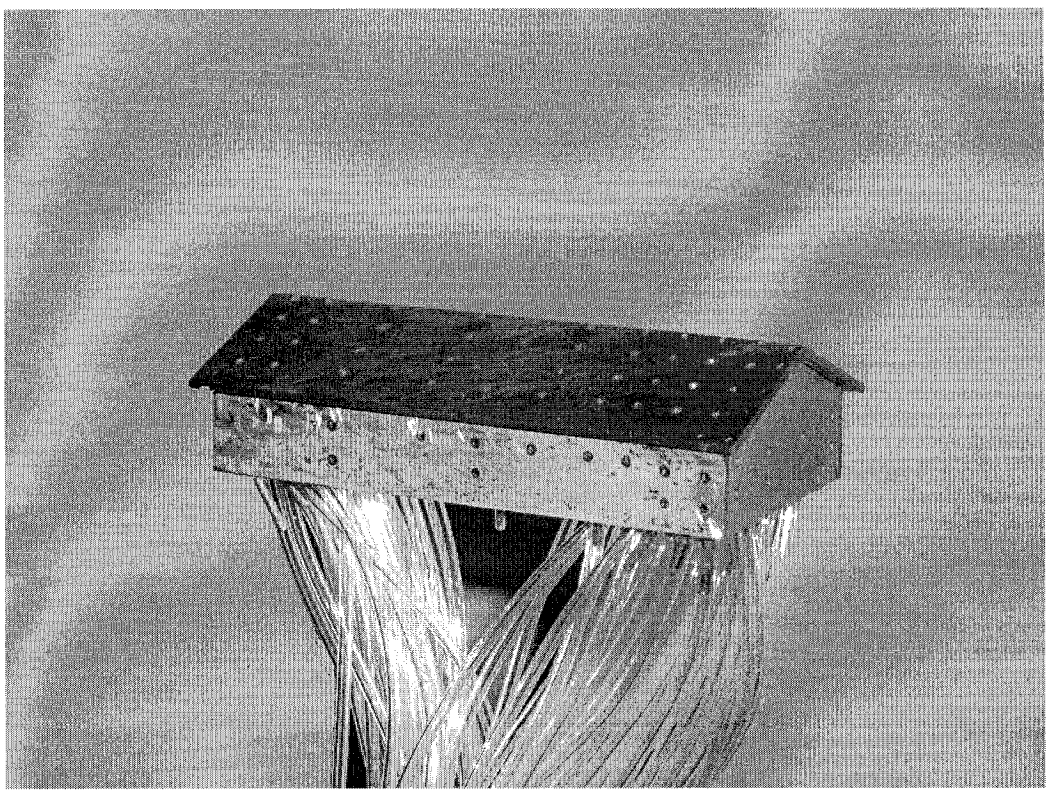

Figure 3.3.2 Wind tunnel building model (tubing and pressure tap detail)

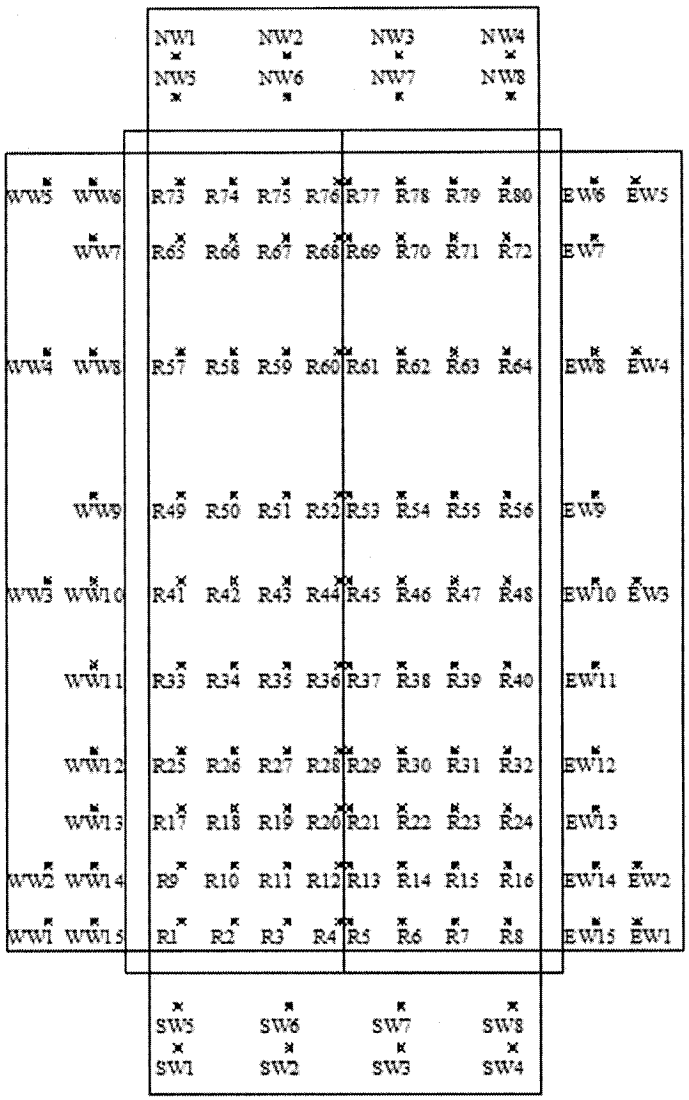

Figure 3.3.3 Pressure tap notation in the wind tunnel building model

Wall Location	Ref. Name
North Wall	NW
West Wall	WW
West Roof	WR
East Roof	ER
East Wall	EW
South Wall	SW

Table 3.1 Pressure taps identity name

In addition to the building model, a proximity model of 1:200 scale was constructed. Wind tunnel measurement results are affected significantly by the details of the surrounding area of the test building. Considering the scale of the test building and the size of the wind tunnel test section, a circular wooden base of 1.60 m diameter and 3.0 mm thickness was used to place all surrounding structures and tree elements on it. The plan view of the wooden base is shown in Figure 3.3.4.

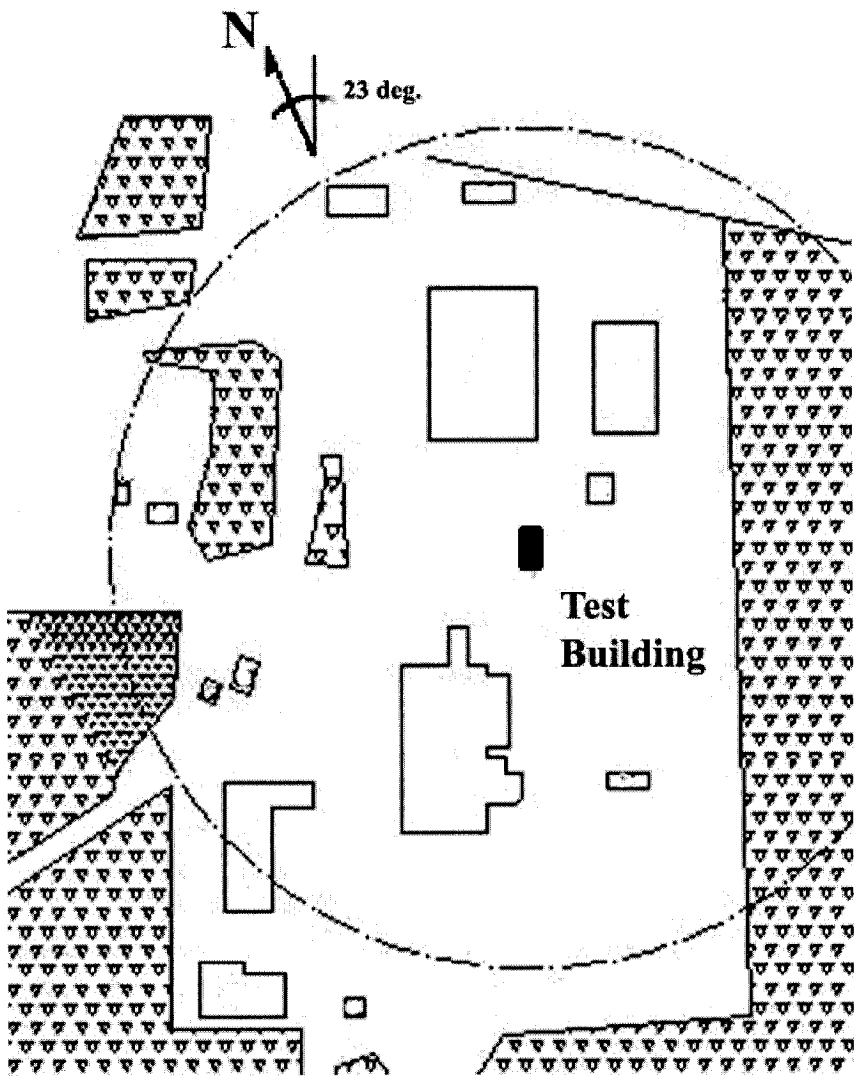

Figure 3.3.4 Surroundings model

Styrofoam was used for the construction of the surrounding building models and wooden sticks and wire wool (scourer) for the vegetation. A space at the center of the wooden base was left open in order to be able to place the test building model and pass underneath the turntable all the tubing system – see Figure 3.3.5. Finally, screws were used to mount the base on the turntable.

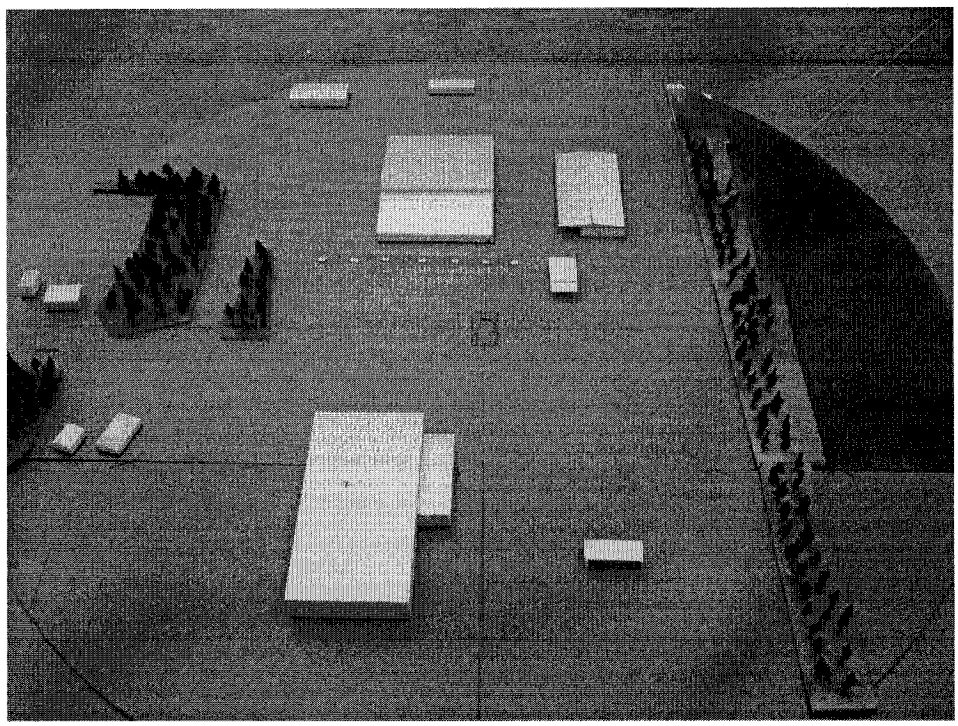

Figure 3.3.5 Surroundings model wooden base with adjacent structures and plantation

3.4 ATMOSPHERIC BOUNDARY LAYER / TERRAIN SIMULATION

One of the most important aspects of a wind tunnel study is the simulation of the atmospheric boundary layer. Accurate representation of the upstream terrain characteristics is essential for the success of the tests. This section discusses in detail the modeling procedure and the wind tunnel set up.

As mentioned in Chapter 2, wind is a highly fluctuating random process. Wind engineers call this behavior as wind turbulence. This property along with the wind velocity profile, are the main simulation parameters for an accurate wind tunnel study. The B.A.L wind tunnel has as default setting the carpet roughness, which corresponds to an open terrain simulation. The full-scale measurements for the current study showed that for most of the wind attack angles, the terrain is between the open country and suburban category. The values of the exponent alpha (α – power law) were found to be between 0.21-0.23 and the corresponding turbulence intensity values, at the roof height, approximately 27 %.

In order to simulate these terrain characteristics in the wind tunnel, a different setting than carpet roughness was used. Wooden panels with Styrofoam cubes (U and S panels) and egg-boxes (CB panels) were placed on the wind tunnel floor. The detailed configuration and panel details are shown in Figure 3.4.1 and 3.4.2.

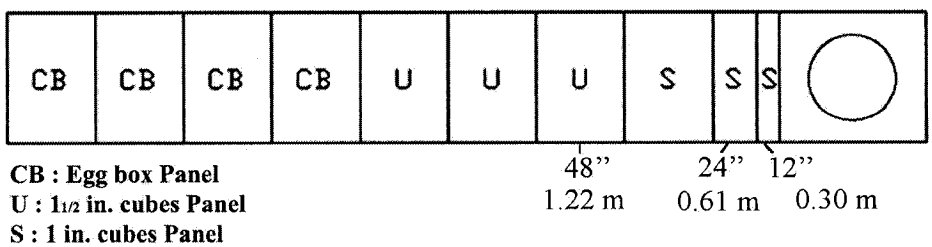

Figure 3.4.1 Wind tunnel panel configuration

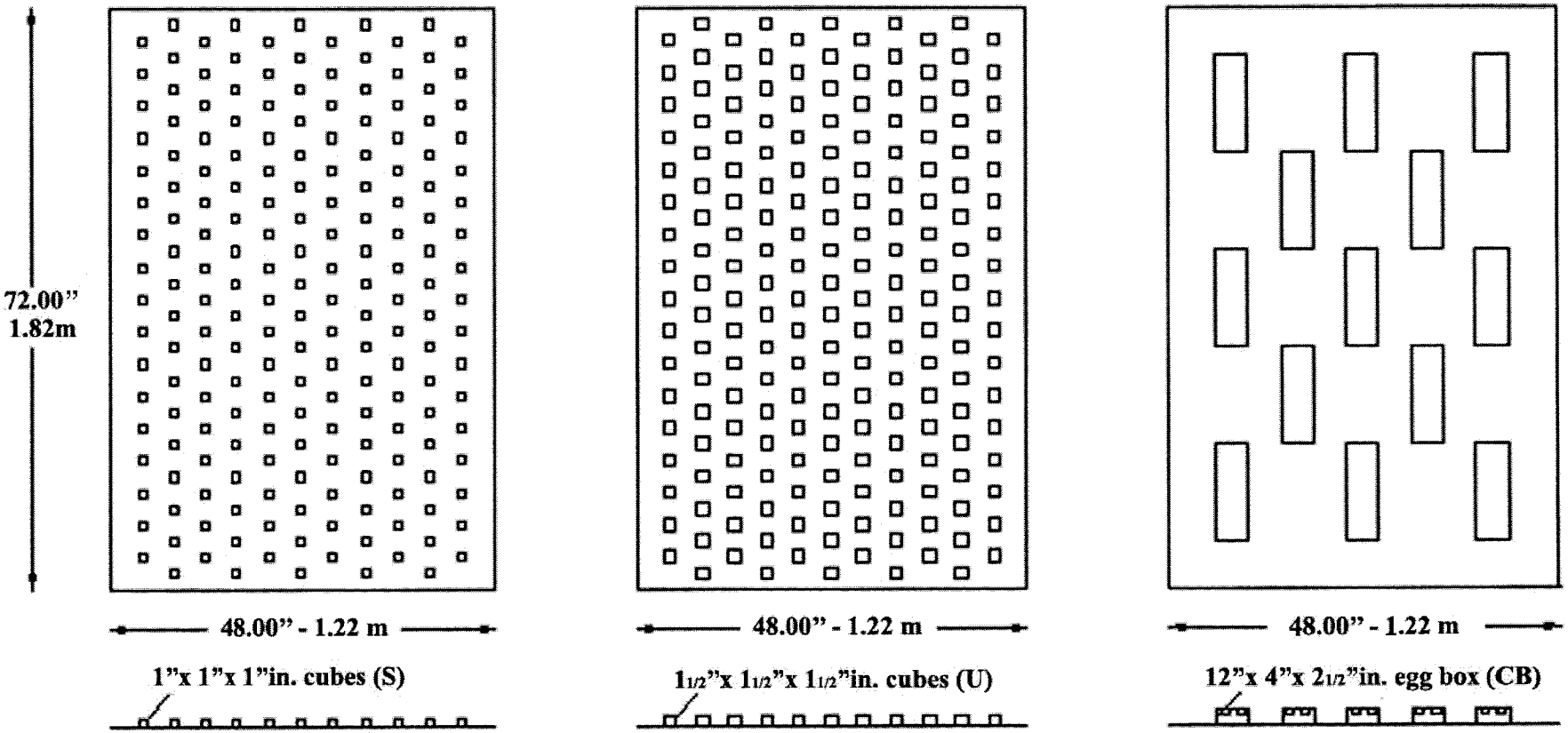

Figure 3.4.2 Roughness simulation panels

Using the above terrain roughness simulation, the wind velocity was measured at different heights at the centre of the wind tunnel test section without the model in place. The analysis of the measured speeds gave the longitudinal wind velocity (V/Vg) which is also compared with the theoretical curve obtained from the power law for α=0.22 and is presented in Figure 3.4.3. The turbulence intensity profile (Vrms/Vz) is shown in Figure 3.4.4. For comparison purposes, the profiles suggested by ASCE (7-05) and Simiu & Scanlan (1996) have been added.

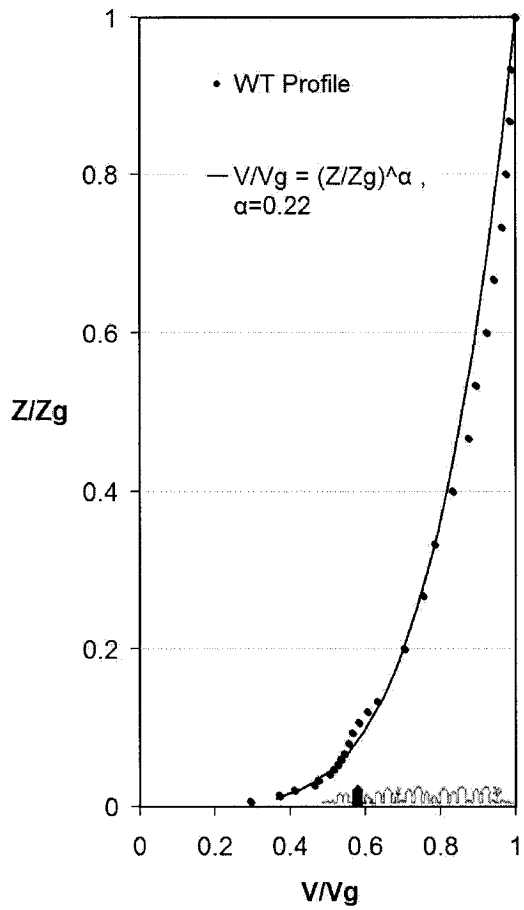

Figure 3.4.3 Wind velocity profile

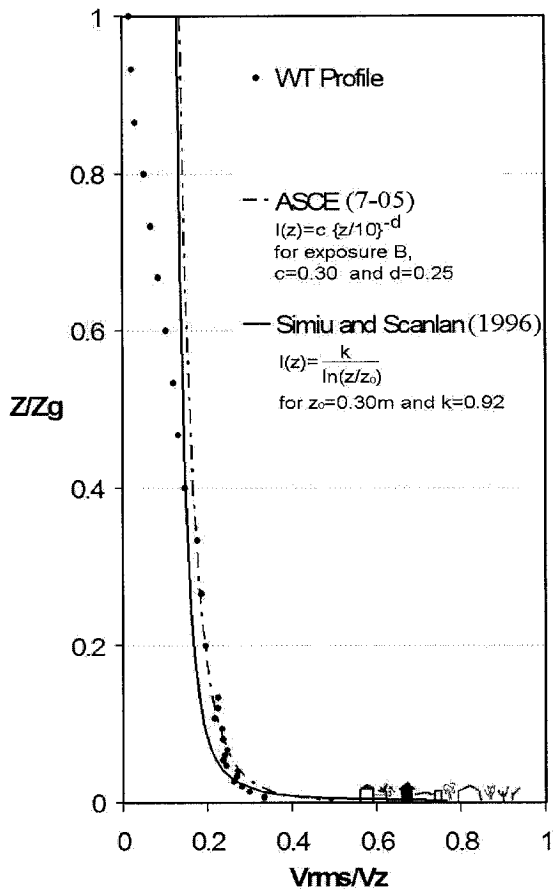

Figure 3.4.4 Turbulence intensity profile

For both profiles, a good agreement with the suggested theoretical profiles exists, particularly at the lower levels.

3.5 INSTRUMENTATION/ EQUIPMENT

The B.A.L. is equipped with sophisticated wind tunnel testing instrumentation. For the specific study, the equipment used is presented in this section so as to better understand the wind tunnel test methodology.

Two main types of instruments were used during the wind tunnel tests. First, wind velocities were measured using a hotwire anemometer. The system used consists of a hotwire probe and a data acquisition system (DATA 6100b). The second type of equipment used, is a system of sensitive pressure scanners. This system consists of a digital service module from Scanivalve (DSM3000) and two electronic pressure scanners (ZOC33/64 Px). The DSM is a stand-alone pressure scanning system which incorporates a CPU, RAM, hard disk and other interface boards – see Figure 3.5.1.

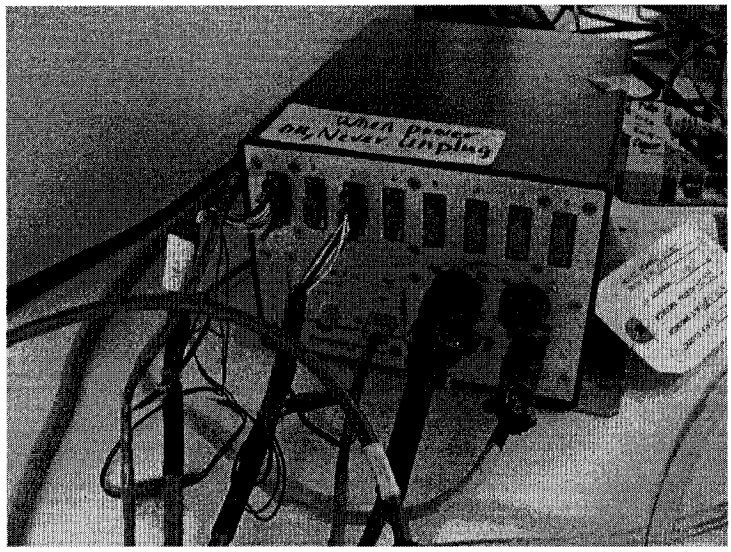

Figure 3.5.1 DSM main unit

The operating system DSM use is Windows 95 and has the capability of interfacing up to 8 ZOC modules. DSM can also communicate and actually be controlled by a host computer through Ethernet. The ZOC33/64 Px modules are electronic pressure scanners which can accept up to 64 pneumatic inputs. Each ZOC module incorporates 64 individual piezoresistive pressure sensors, calibration valving, a high speed multiplexer and an instrumentation amplifier. For insulation reasons, the ZOC module is placed inside a thermal unit helping the module to maintain a constant temperature

during the scan procedure. Main advantage of the ZOC modules is their compact size, which is of great importance for wind tunnel applications. The system of DSM with the ZOC modules is capable of high frequency scanning for up to 512 channels simultaneously.

For the scope of the current study, the DSM was connected through Ethernet port to a host computer with higher process and storage space capabilities. An instrumentation schematic of the wind tunnel set up is presented in Figure 3.5.2.

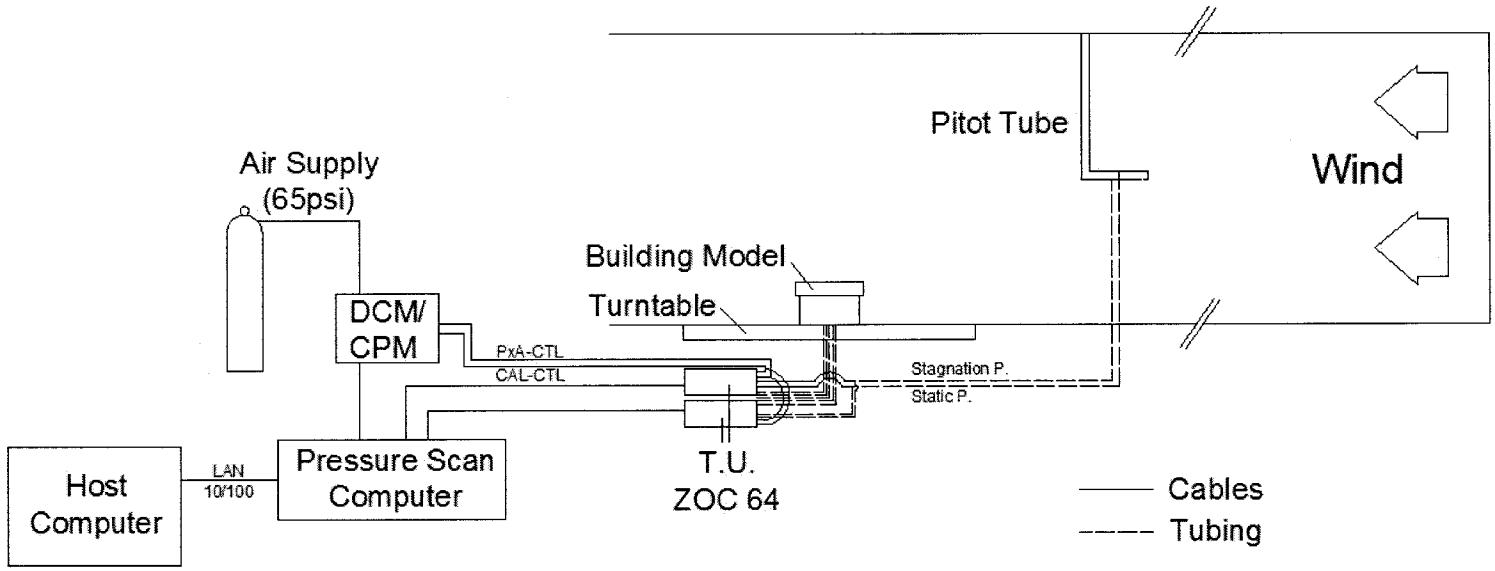

Figure 3.5.2 Instrumentation schematic of the wind tunnel experiments

3.6 WIND TUNNEL TESTING

After the construction of the test building and surroundings model, as well as the set up of the wind tunnel for the upstream terrain simulation, the wind tunnel tests were carried out. Two rounds of experiments (tests A + B) were carried out for validation and repeatability purposes. Details of these tests are discussed in this section.

For the first set of measurements 124 pressure taps of the model were used. Two ZOC modules (S/N 344 and 345), each connected to 62 pressure taps, were used. The modules were connected through cables to the main DSM unit and a host computer was responsible for the final control of the pressure scan system. Two software, provided by Scanivalve were installed to the host computer, DSM-Link and BTel: the first one was used for low and moderate frequency scans and the second for high frequency testing.

After careful examination and consideration of the past and present full-scale climatic data, a total number of 15 wind attack angles were decided to be examined – see Figure 3.6.1. A 40 μsec period and 1760 frames per second settings were used, resulting to a scanning frequency of 160 Hz.

The procedure followed for each direction is summarized below:

- Set up turntable orientation
- Perform a zero-calibration for all channels (initial CalZ)
- Turn on wind tunnel fan
- Open data log file, scan, close and save data log file
- Turn off wind tunnel fan
- Perform a zero calibration (final CalZ)

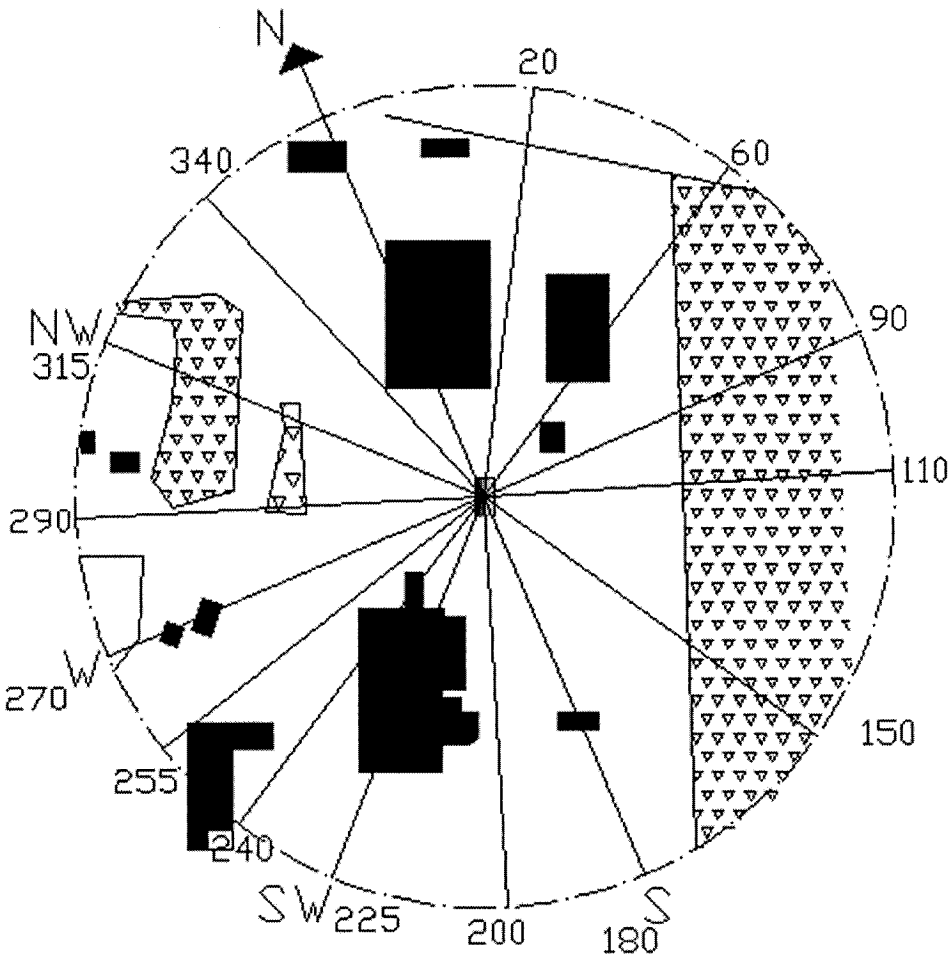

Figure 3.6.1 Wind attack angles

A scan was performed just after the initial and before the final zero calibration, in order to compute the error-drift of the sensors. Each scan record was given a characteristic name of two numbers: the first indicating the wind direction and the second the sampling frequency. The first round of measurements was completed after scanning each of the 15 different directions and saving the data according to the above notation.

The second set of tests (test B) was conducted after the completion of the first set of measurements. These tests were performed with higher frequency but not for simultaneous pressure records. For test B, the pressure taps were divided in three different groups which are shown in Figure 3.6.2. The first group consisted of 32 pressure taps and the second and third of 42 pressure taps. The reason of this grouping was to enable the capability of scanning fewer pressure taps simultaneously but with higher frequency.

A 120 μsec period and 3000 frames per second settings were used for the first group and 90 μsec period and 3000 frames per second for the second and third group, all resulting to a scanning frequency of 260 Hz.

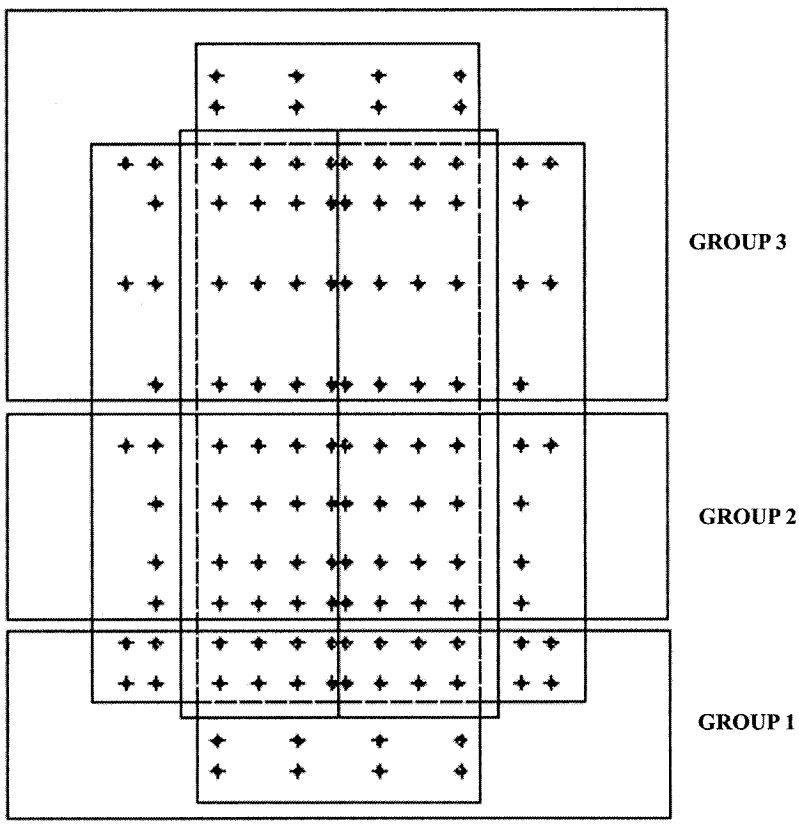

Figure 3.6.2 Pressure taps groups for test B

At the end of both tests, the experimental building and surroundings model were removed from the test section of the wind tunnel and by using the hotwire anemometer the wind velocity and turbulence intensity profile was computed. These two profiles were in absolute agreement with the initial profiles computed at the very early stage of the wind tunnel studies.

3.7 DATA PROCESSING / ANALYSIS / INTERPRETATION

After performing the wind tunnel tests, the next step was the analysis of the output data. A detailed description of the procedure followed to convert the scanned data into pressure coefficients is presented below.

In Chapter 2, the definition of pressure coefficient was presented as follows:

- Mean pressure coefficient: $c_{p,mean} = \frac{p_{mean} - p_a}{\frac{1}{2}\rho V^2}$

- Peak pressure coefficient: $c_{p,peak} = \frac{p_{peak} - p_a}{\frac{1}{2}\rho V^2}$

The data acquisition system was exporting the pressure data in psi units, therefore a special routine was followed in order to obtain the desired mean and peak pressure coefficients. The units used in these equations are kPa for the pressure, kg/m^3 for the air density and m/sec for the wind speed. The data saved for each wind direction were

differential pressure values. These data were either in binary or text (ASCI) format and Microsoft Access and Excel was used to open and analyze them. The procedure is almost the same for both the mean and peak data analysis and can be summarized in the following steps:

- Import error-drift record into Excel and calculate the average value for each channel.
- Import main scan record (124 pressure taps for test A and 32+42+42 for test B) and subtract the corresponding error-drift for each of the channels.
- Mean pressure coefficients:

  Compute the mean pressure for each channel's record.

  Peak pressure coefficients:

  Compute the average of the ten minimum and maximum values from each channel's record.
- Calculate the mean and peak pressure coefficients by using equations 2.11 and 2.12.

3.8 RESULTS

Mean, minimum and maximum pressure coefficient contour plot results for the 0-degree wind direction are presented in Figure 3.8.1. For the specific wind direction, the computed mean pressure coefficients are positive (pressure) for the windward (north) wall and negative for the other walls and the roof (suction). The regions of high suction

are located close to the roof ridge and the edges of the structure. The minimum pressure coefficient critical values reach -4.0 for the east part of the roof whereas maximum pressure coefficients in the order of +1.8 have been measured on the windward wall.

Similar pressure coefficient contours for all other wind directions are presented in Appendix A.

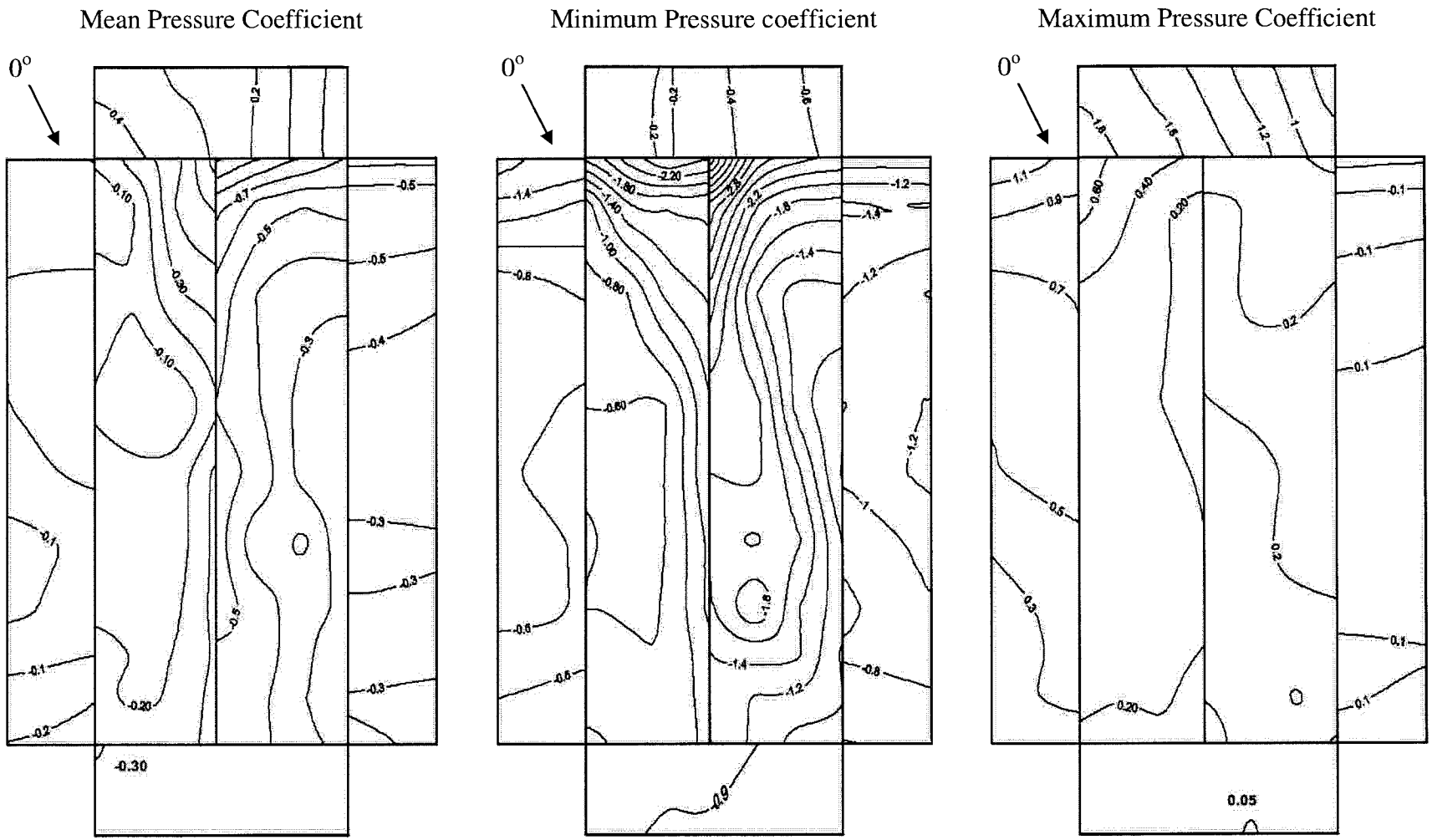

Figure 3.8.1 Pressure coefficient contour plots for 0-degree wind direction, based on wind tunnel test.

CHAPTER 4

FULL-SCALE STUDIES

4.1 GENERAL

The unique characteristic of this project was the coupling of full-scale with wind tunnel and numerical analysis studies. In contrast to the simulated laboratory tests, full-scale tests are characterized by high cost and great difficulties. This chapter presents details about the site of the full-scale tests, the construction of the test building, the instrumentation used and finally the data acquisition and analysis procedure.

4.2 TERRAIN AND SITE CHARACTERISTICS

The full-scale test building is located in Fredericton, New Brunswick. The actual location of the facilities is at the Hugh John Fleming Forestry Centre, where the University of New Brunswick Tweeddale Center for Industrial Forest Research is also located – see Figure 4.2.1. The total area of the Center is 28 hectares and it is approximately 10 kilometers north from Fredericton's city center. The test building is

located next to the main office buildings of the Centre in a relatively open-suburban area. North and south of the building there are low-rise industrial rectangular-shape buildings of maximum height of 10 meters.

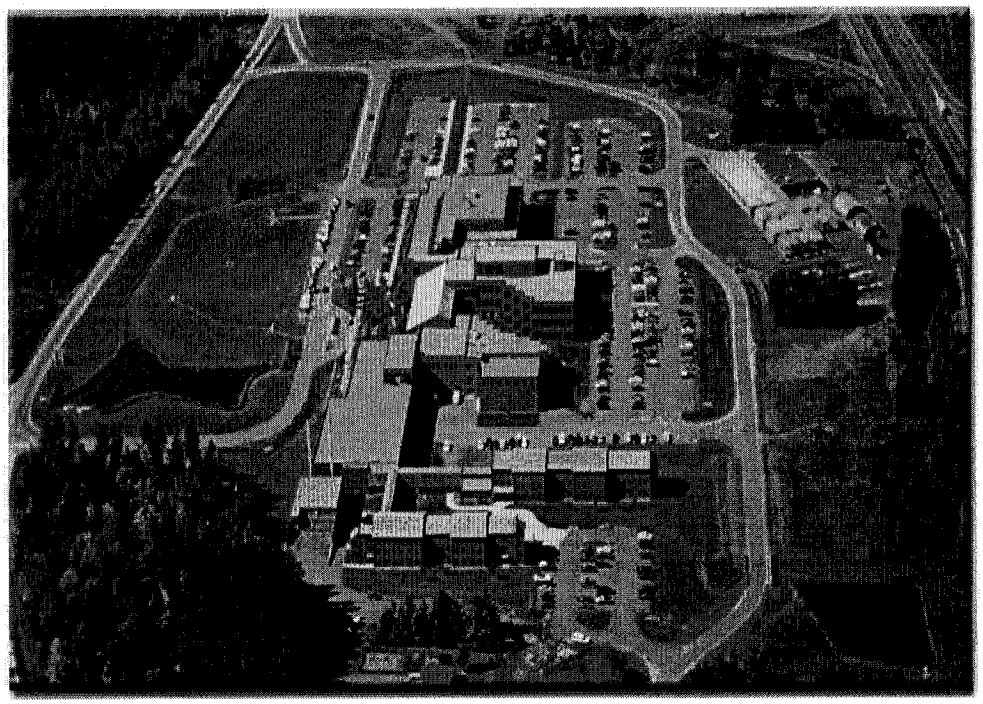

Figure 4.2.1 Aerial view of the Hugh John Fleming Forestry Centre (Canadian Forest Service – NRC) located northwest of the test building

On the east side and at a distance of approximately 80 meters, dense forestry area exists. The average tree height is 10-15 meters. From the west, two main paved streets of 6-8 meters width are approaching the building area, with small buildings and relatively dense plantation covering the space between them. An aerial view of the area is shown in Figure 4.2.2.

The center is surrounded by three main highways (NB7, NB8 and NB101) with two shopping malls located next to them. In general, the proximity area can be described as a

sparsely built-up suburb with a considerable amount of forest areas. According to Environment Canada, the most frequent wind directions are south and west as indicated in Table 4.1 and Figure 4.2.3.

Figure 4.2.2 Aerial view of the testing facilities

	Jan	Feb	Mar	Apr	May	Jun	Jul	Aug	Sep	Oct	Nov	Dec
Mean Speed[1,2]	12.7	13	14.6	14.3	13.6	12	10.8	10	10.9	11.8	12.4	12.6
Most Frequent Direction	W	W	W	W	S	S	S	S	S	S	W	W
Maximum Hourly Speed[3]	64	80	64	72	64	64	48	53	65	64	67	60

[1]Wind Speed in km/h
[2]Mean Speed is computed based on a one- or two-minute mean value. Averaging period varies from one-minute to an hour
[3]Maximum Hourly Speed is the peak value recorded during an hour

Table 4.1 Climate data from Environment Canada Weather Office

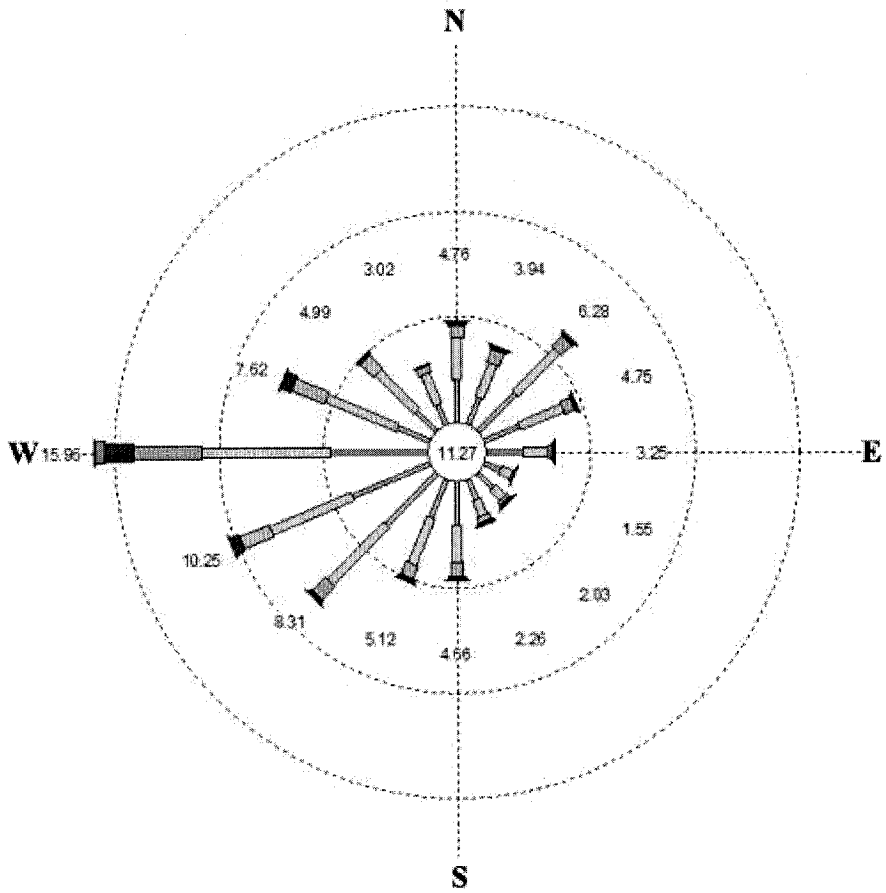

Figure 4.2.3 Wind rose for Fredericton City (source: Environment Canada Weather Office)

4.3 FACILITIES / TEST BUILDING

The main advantage of this study is that the test building was constructed according to the needs of the particular research project. In this section, a detailed description of the construction technique and the structural and mechanical properties of the building is presented.

The test building is a single storey typical North-American residential house. It has a rectangular layout with external dimensions of 8.5x16.8 m and a duo-pitch roof of 4/12 slope – see Figures 4.3.1 and 4.3.2. The house is resting on a concrete foundation wall 0.225 m thick and 1.225 m deep.

The floor system of the test building consists from 43 I-joists directed along the small side of the structure. The I-joists (JSI 40) have a total height of 508 mm. The chords are 38x89 mm and the web is oriented strand board (OSB) of 9.5 mm thickness. The I-joists are spaced at 406 mm (centre-to-centre distance). On the top of the I-joists, 15 mm thick OSB panels 1.22x2.44 m have been nailed so as to create a solid diaphragm on the floor.

The wall system consists of wall frames, sheathing and siding panels. The wall frames are assembled from 38x89 mm studs spaced at 600 mm. The studs are made by spruce-pin-fir lumber (S-P-F). Studs are also used for bottom (1 stud 38x89 mm) and top (2 studs 38x89 mm) plates in order to form the framing wall system. On the exterior side of the wall, OSB panels of 9.5 mm thickness are used to cover the framing. A final layer of stained wood is used as siding and is shown in Figure 4.3.3.

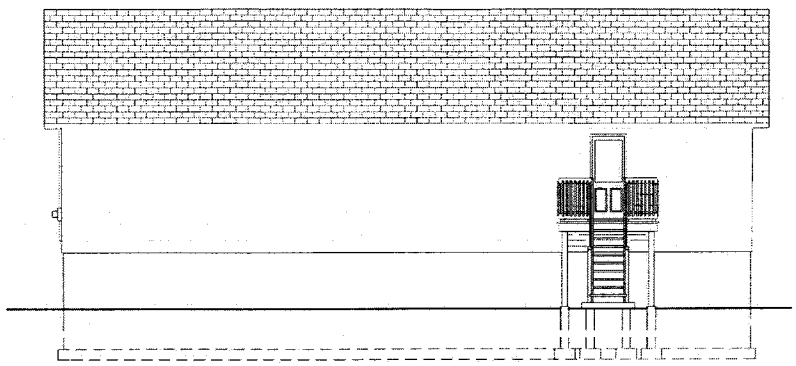

East Elevation Sketch

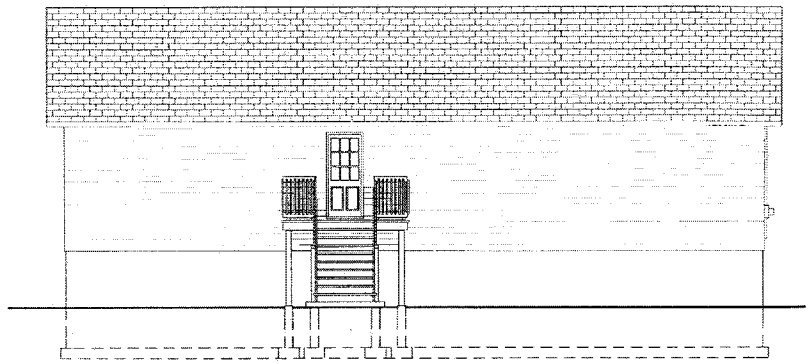

West Elevation Sketch

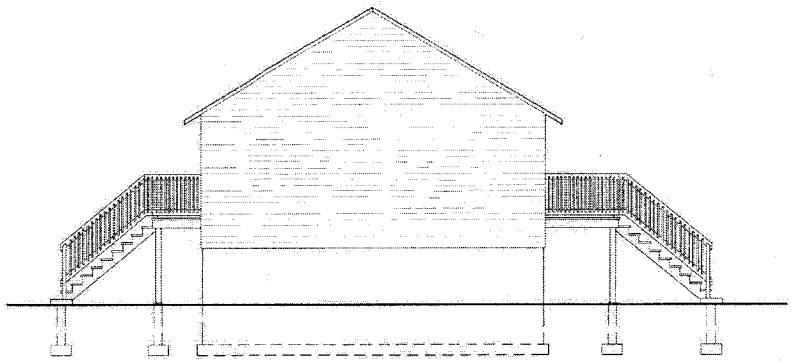

South Elevation Sketch

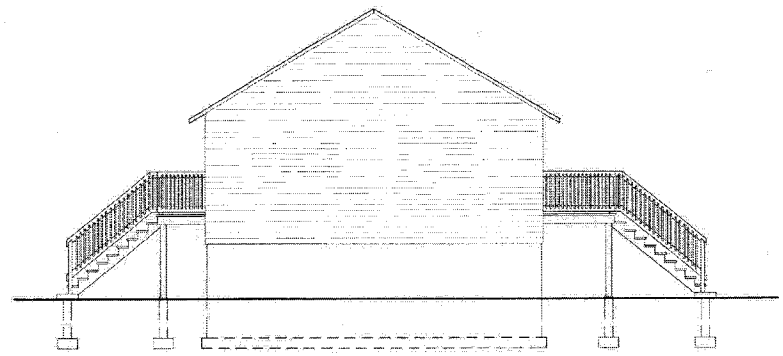

North Elevation Sketch

Figure 4.3.1 Test building elevation sketches

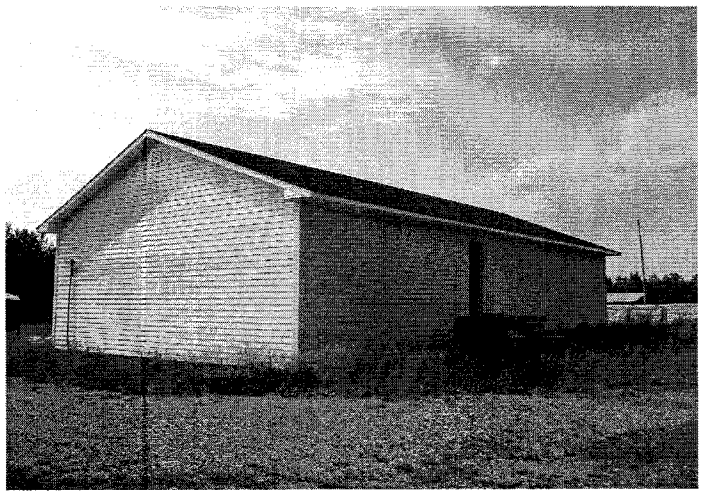

North-West View

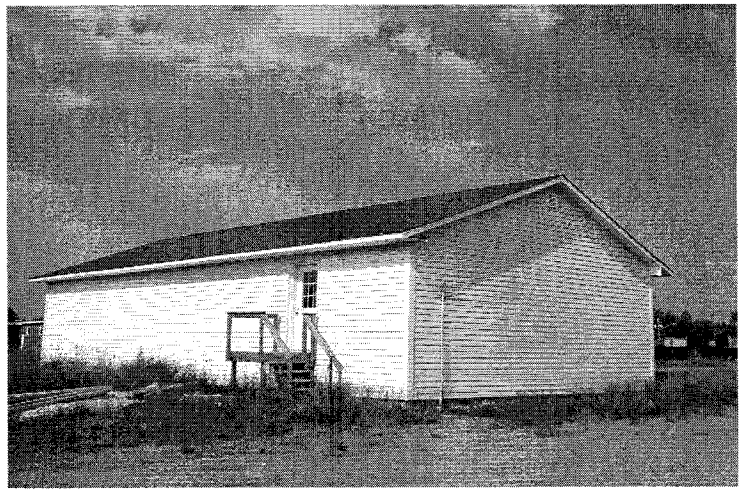

North-East View

South-East View

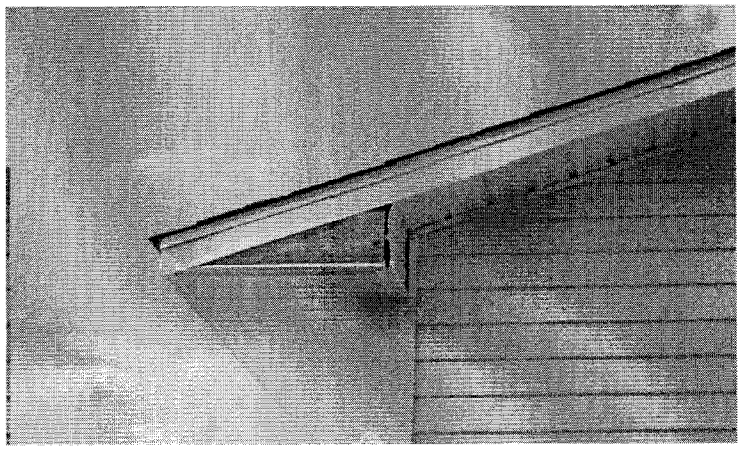

Eave Detail

Figure 4.3.2 Test building views and construction details

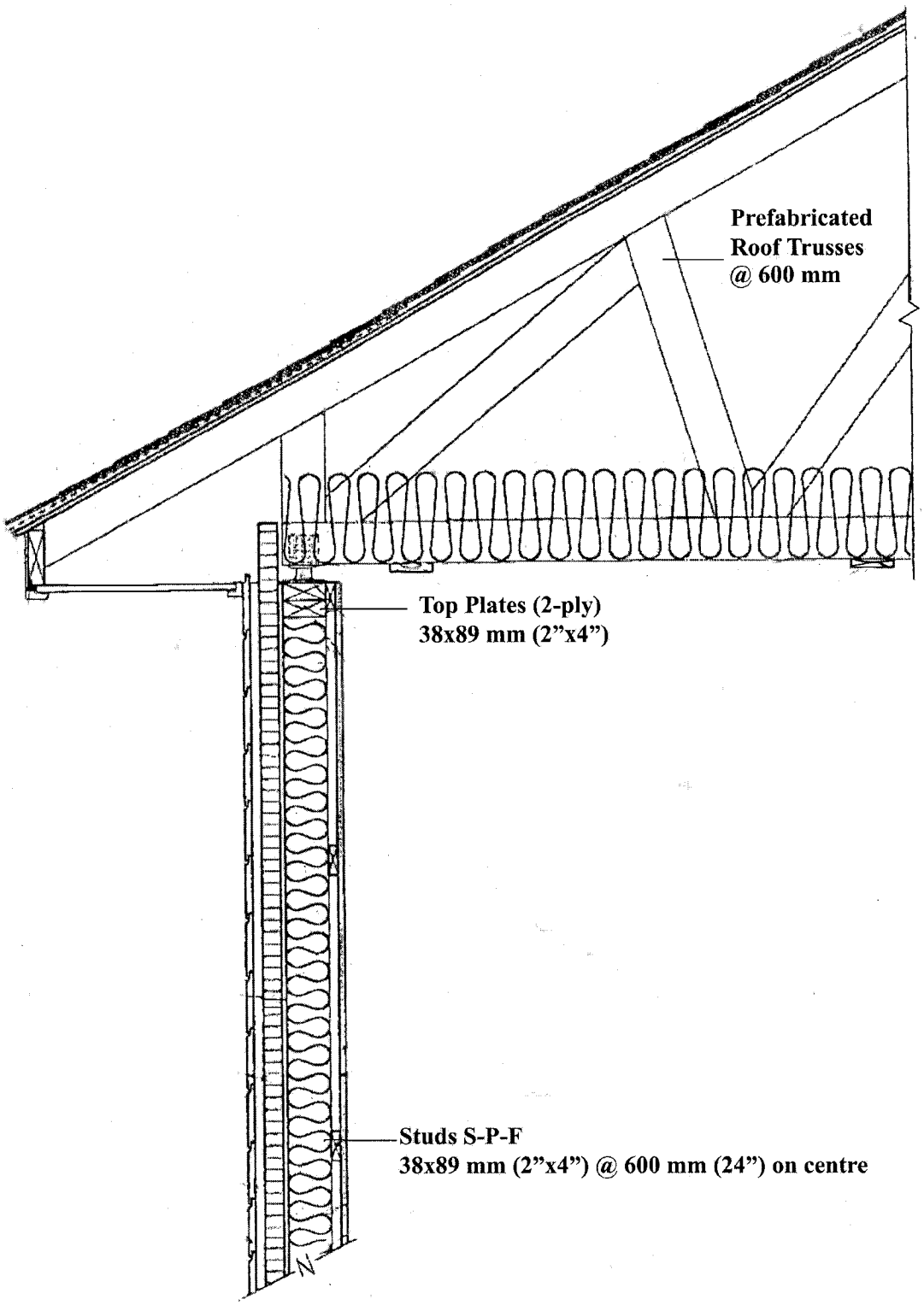

Figure 4.3.3 Wall framing system

The ceiling of the test building consists from a grid of 38x89 mm and 19x89 mm studs, which are fastened to the bottom of the roof trusses. The roof trusses finally are prefabricated fink trusses (W-trusses) spaced at 600 mm and comprised by 38x89 mm lumber elements.

At this time only two openings exist, one door on the east and one on the west wall of the building. In the near future, more openings and partitions are planned to be installed. The orientation of the building is 23 degrees right of the geometric North, as shown in Figure 3.3.4 (Chapter 3). For a radius of 15 meters around the building, only low vegetation exists (<0.3 meters) and this area is examined and is kept clean on a regular basis. More details about the construction of the test house can be found in Doudak (2005c).

4.4 INSTRUMENTATION

The main scope of this study is the structural monitoring of a wooden structure subjected to wind loads. For this reason, special, state-of-the-art equipment was installed and used, including meteorological instrumentation, pressure scanning, load cells and data acquisition systems.

One of the most important parts of a full-scale wind monitoring is the meteorological tower (Figure 4.4.1) placed on the west side of the building at a distance of approximately 20 meters. Special attention was given to avoid placing the tower close to obstructions in order to avoid contaminating the wind regime by eddies generated from

adjacent structures or trees. Two propeller anemometers were mounted on the tower, one of them at 5.5 meters (roof height), the second at 10.0 meters height - see Figure 4.4.2. Both anemometers are Young (model 0.5103V) and can measure the horizontal wind speed (0-60 m/sec range) and direction (0-360 degrees). These instruments are corrosion resistant and combine light weight with high accuracy. The anemometers were fully calibrated before shipment, but for accuracy reasons, were also checked after the final installation.

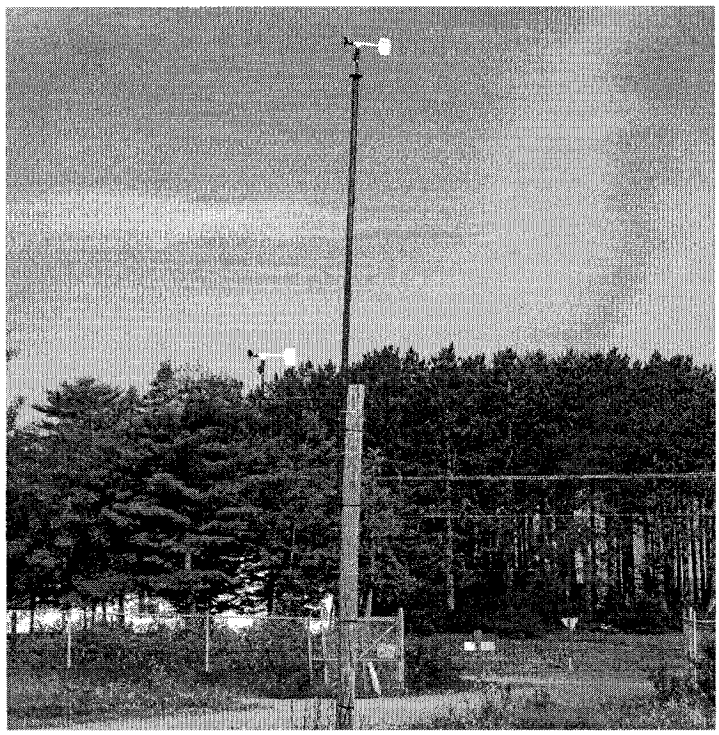

Figure 4.4.1 Meteorological tower

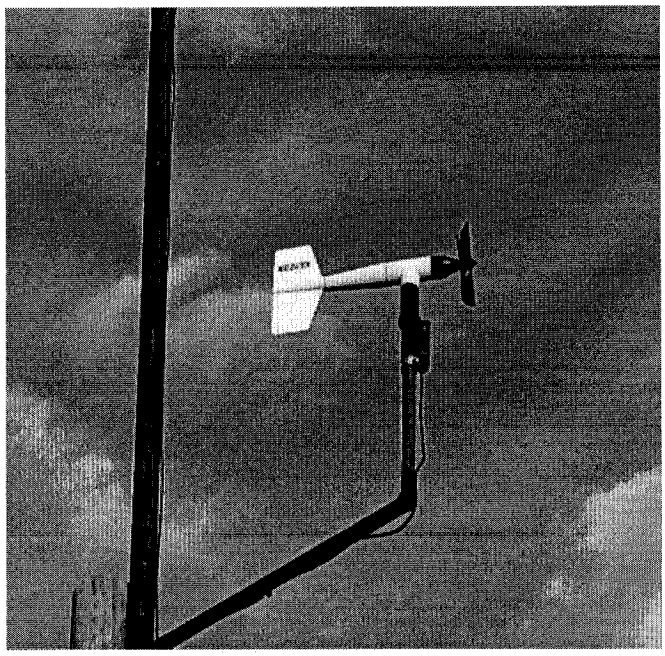

Figure 4.4.2 Propeller anemometer

In addition to monitoring wind speed and direction, a barometric pressure sensor monitoring the ambient atmospheric pressure was also used. As mentioned in Chapter 2, full-scale pressure measurements are highly affected by the way of measuring the reference atmospheric pressure. In fact, it is essential to measure the ambient atmospheric pressure accurately without any wake and eddy effects from adjacent buildings. For this reason a special barometric pressure system was obtained from Young – see Figure 4.4.3. The combination of a regular pressure sensor (model 61202) housed in a waterproof molded case and a pressure port (model 61002) was able to minimize significantly the dynamic pressure errors due to wind.

Figure 4.4.3 Barometric pressure system

The third type of instrumentation used is the pressure scanning system. The test building is equipped with 27 pressure taps, 9 of them on the wall and 18 on the roof, presented in Figure 4.4.4. The research team decided to place more pressure sensors on the south side of the roof, since this is the side exposed to the most frequent strong wind. The pressure scanning system consists of 4.8 mm inside diameter plastic tubes which have mounted on the wall and roof surface. These tubes are connected to differential pressure transducers (Micro Switch 160PC). These transducers use as reference pressure the ambient atmospheric pressure which is provided by the barometric pressure scanning system. Special attention was given to the protection of the tubing from humidity, condensation, dust and section obstruction. For this reason, special techniques were used for the roof pressure taps so as to drain the rain water from them and protect also the transducers. For the wall pressure taps a wire netting was placed at the end of the tubing so as to block the entrance to small bugs and particles – see Figure 4.4.5.

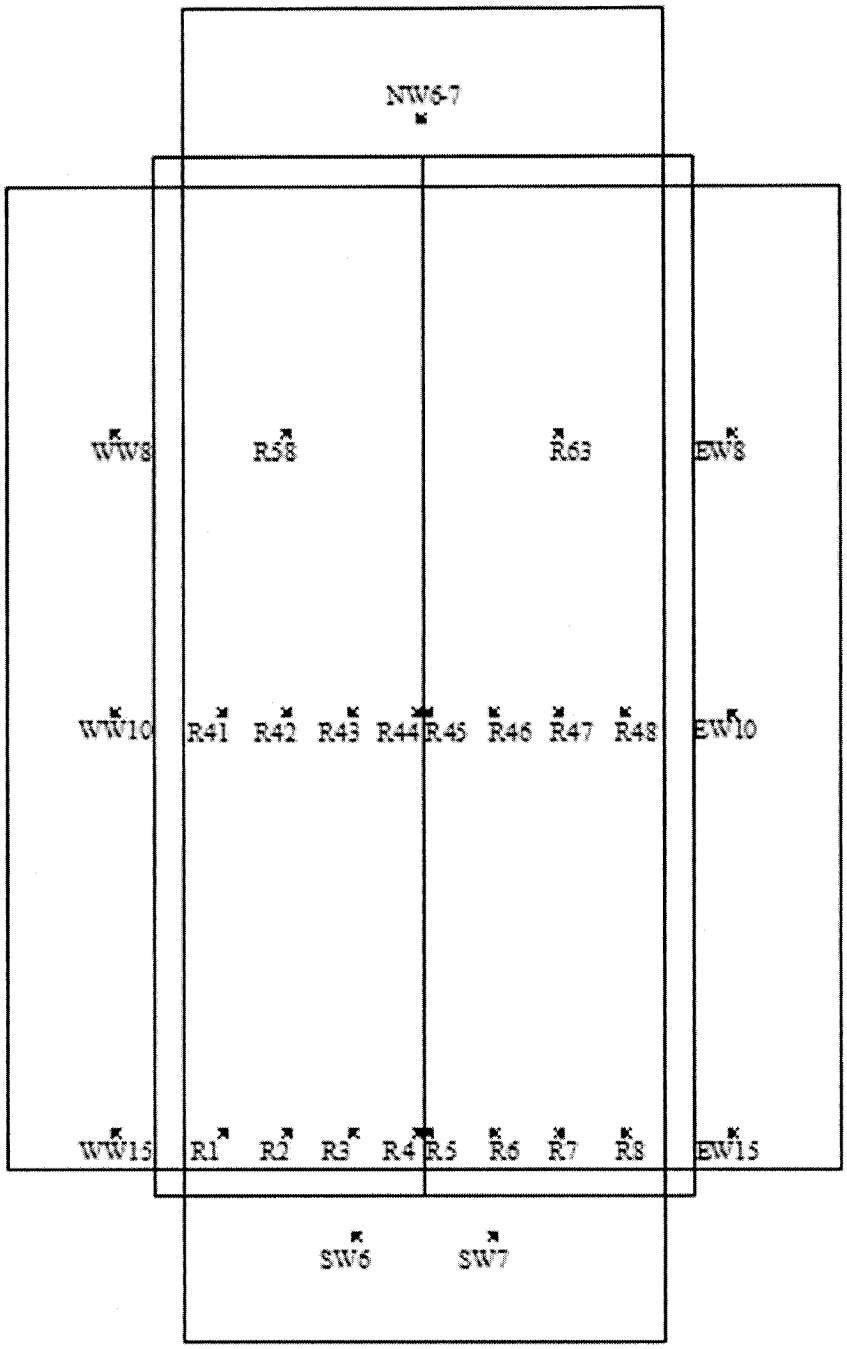

Figure 4.4.4 Test building pressure tap location and notation

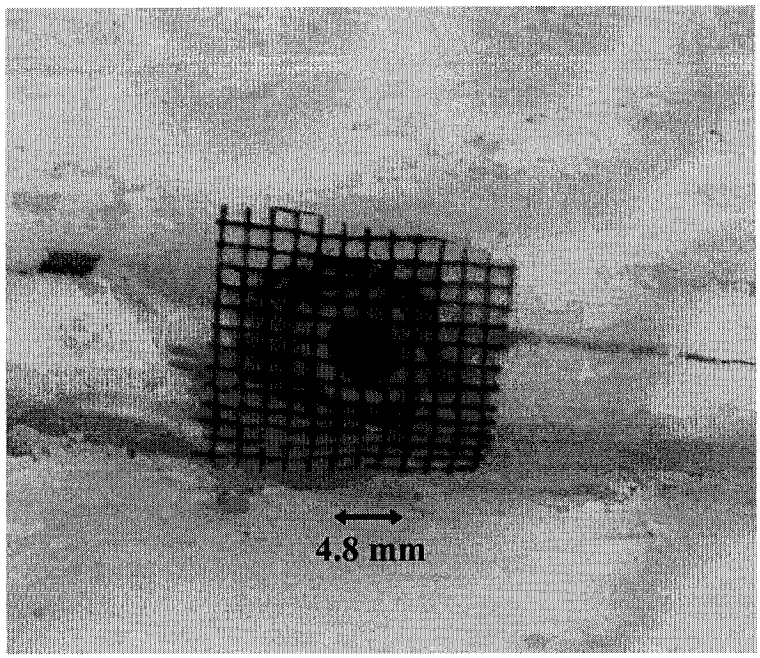

Figure 4.4.5 Wall pressure tap detail

The load cells system is an innovative part of this study. Three different types of load cells were designed and analyzed by Doudak (2005c) and placed at key points inside the structural system – see Figures 4.4.6 for location and 4.4.7 for placement details. The most important aspect of the load cells installation was the maintenance of the original structural properties of the building. In order to realistically assess the response of the building and try to define the load paths within the structure, the stiffness should remain unaltered. A total number of 6 1-D and 3-D load cells were placed between the wall and the roof. Another 27 3-D load cells were also installed around the perimeter of the building at the wall-to-foundation interface.

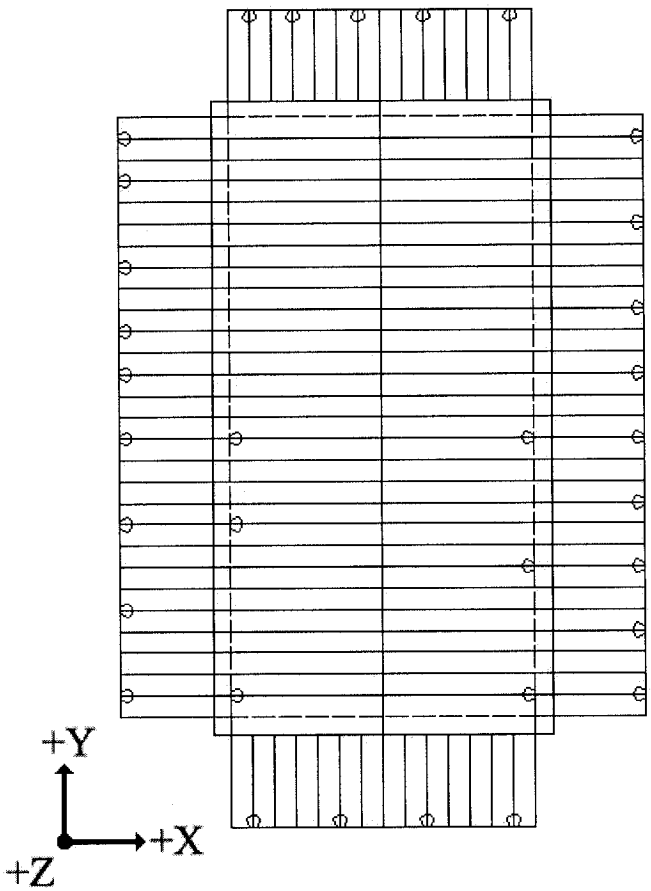

Figure 4.4.6 Roof and foundation load cell location

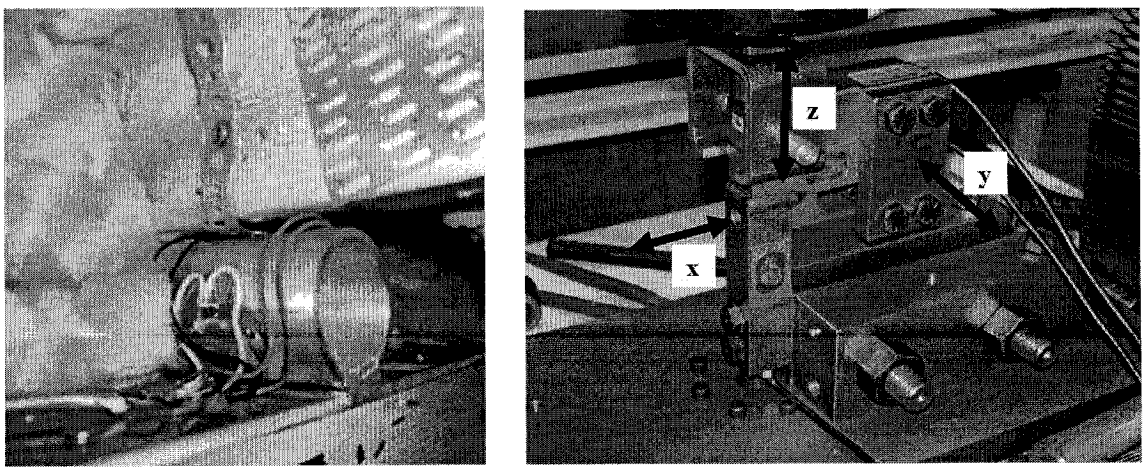

Figure 4.4.7 Roof and foundation load cell details (after Doudak 2005)

It should be mentioned that the building is completely isolated from the foundation and the only points of contact are the 3-D load cells – see Figure 4.4.8. This construction detail assures the transfer of the applied load to the foundation only through the load cells. All the load cells were custom-made for the specific study. Each of the load cells was calibrated in the laboratory and checked before and after the in-situ installation for possible drift effects.

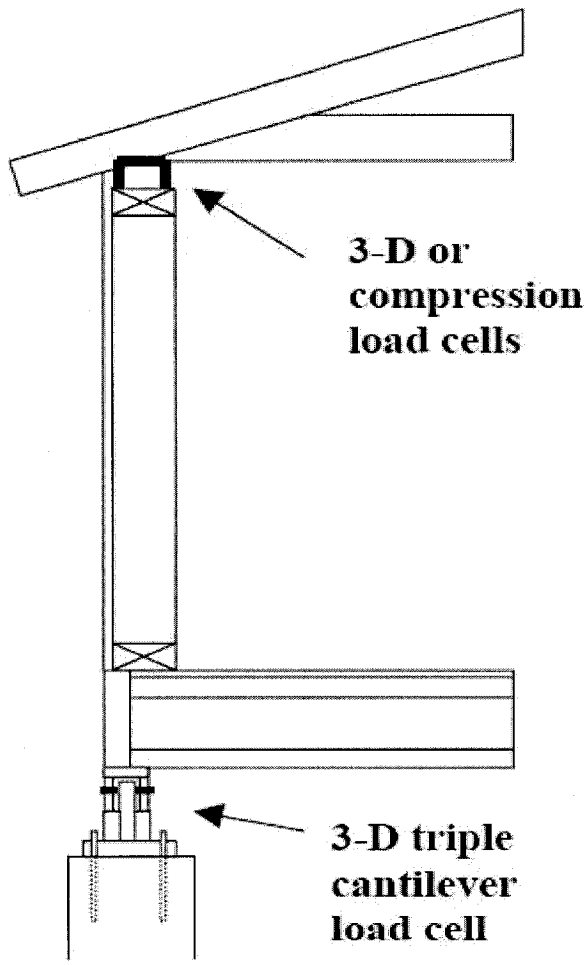

Figure 4.4.8 Wall cross-section and load cell installation detail (after Doudak 2005)

Finally, the System 5000 (Vishay System Model 5000, Intertechnology) was used for the acquisition and reduction – see Figure 4.4.9. This stress analysis data system is able to accept simple strain gauges (load cells), linear variable deformation transducers (LVDT's) and high frequency sensors (pressure tap transducers). The system is operated by sophisticated software (Strainsmart Software) provided by the same company. This Windows-based software can export the acquired data in different formats (ASCII, EXCEL, ACCESS database).

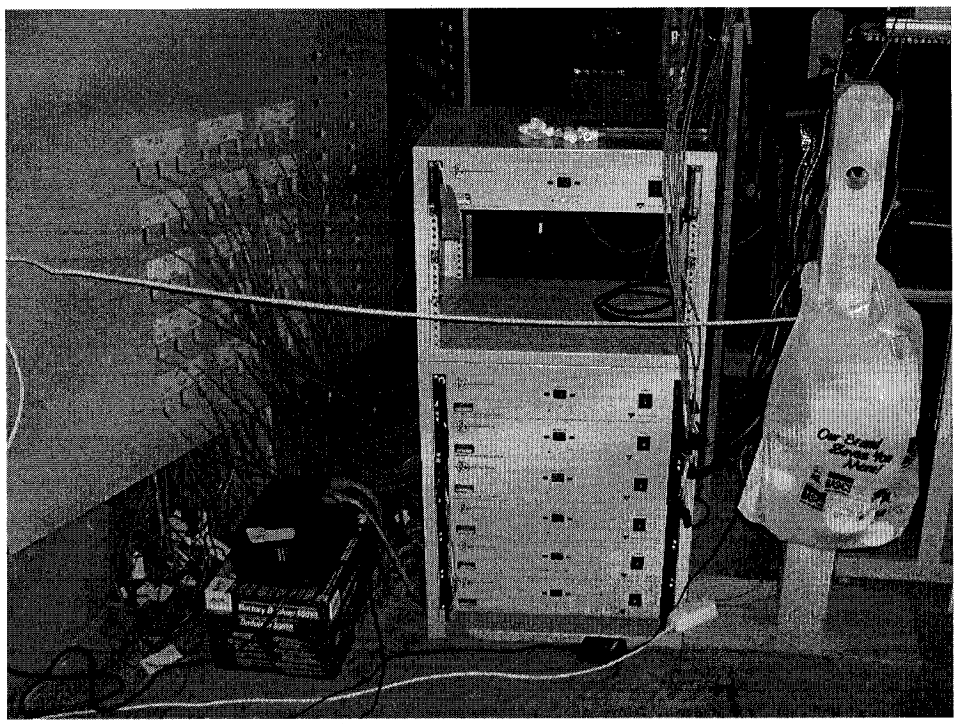

Figure 4.4.9 Data acquisition system

4.5 DATA ANALYSIS AND INTERPRETATION

As in most full-scale monitoring studies, data acquisition is a difficult task. For instance, although the data logger was operational since the spring of 2006, very few data sets were useful for further analysis. Rain, low wind speed and high fluctuations in the wind direction are some of the reasons that made the most of these records not useful.

The software used to operate the DAS has the ability to be triggered automatically and monitor the wind speed whenever it is below or above a pre-specified limit. Taking into consideration the available hard disk storage capacity and a minimum suggested wind speed, the limits were set at below 1 and above 20 km/h. Having this double limit was useful for monitoring not only the behavior of the building during high wind speed effects but also for computing the drift of the sensors during very low (almost zero) wind speed periods. After triggering, the system was recording continuously for 10 minutes. If the wind speed was still below or above the limit, then the system was re-triggered for another 10 minutes. The sampling rate was set to 10 readings per second (10 Hz). All records were in ASCII test format and saved every 2 weeks in an external storage unit.

The analysis of the recorded data was performed in two main steps. The first was the validation and the second was the detailed analysis. During the first examination, the mean and standard deviation values of the wind speed and direction were computed. The low speed and high fluctuating direction sets of data were removed from the record prior to the detailed analysis. For each of the 120 sensors, mean, minimum and maximum peak and rms values of the pressure and load records were calculated according to the equations 2.11-2.13.

For the load measurements the mean force coefficients were computed according to the formula:

- Mean Force Coefficient: $c_{f.x} = \frac{R_{x,mean}}{q \times L_x \times H}$ (4.1)

where: $q = \frac{1}{2} \times \rho \times V^2$, the dynamic velocity pressure (kPa)

R_x : the reaction at x direction (kN)

L_x : the length of the wall (m)

H : the height of the wall (m)

4.6 RESULTS

The full-scale pressure tap and load cell measurements are presented in detail in Chapter 6, where they are compared with the wind tunnel and finite element analysis results.

For the specific study, only mean pressure and force coefficients were evaluated. Unfortunately, due to measurements errors, the peak values of pressure and force coefficients appear to be contaminated with noise. Therefore, full-scale results used in the present thesis consist only of mean values of pressure and force coefficients. It should be also mentioned that analysis and evaluation of the peak response is part of future work.

CHAPTER 5

FINITE ELEMENT ANALYSIS

5.1 INTRODUCTION

The third part of this study is the finite element modeling and analysis of the test building. Computer-based structural analysis of low-rise buildings is assumed to be accurate and straightforward. Very few studies though, were able to verify this accuracy with full-scale and model scale measurements when it comes to environmental loads such as wind. The number of finite element based software today allow structural engineers to easily "built" any kind of structural form. Unfortunately, in many cases the application of load function and process of analysis are not very well described, with the result to usually over- and sometimes under-estimate the structural design. The scope of this Chapter is to create a finite element model and perform the analysis in order to compare the results of this analysis with the measurement data taken from the load cells in the test building.

5.2 FINITE ELEMENT ANALYSIS SOFTWARE AND MODELING

The numerical modeling of the test building was also essential for this study. Having obtained some full-scale and wind tunnel results, the computer based analysis provided the opportunity to compare and assess the accuracy of each individual approach. The commercial software SAP 2000 Nonlinear Version 7.11 (Computers and Structures, Inc. – CSI, 1997) was used for the finite element modeling of the test building.

A 3-D finite element model was created simulating on the actual wooden building located in Fredericton, New Brunswick. Joint, frame and area objects were used to form the structural skeleton and components of the building. All the material properties of the individual members were based on previous studies (Doudak 2005), standards and code references.

In more detail, linear frame elements were used to model the foundation, wall framing and truss members (studs and I-Joints). Shell elements (membrane types) were also used to model the panels (OSB floor, wall and roof sheathing). A three-dimensional, beam to column formulation was used to model the frame element, which includes the effects of bi-axial bending, torsion, axial deformation and bi-axial shear deformation. The shell elements with membrane type behavior are using an isotropic four-node formulation that includes translational in-plane stiffness components and a rotational stiffness component in the direction normal to the plane of the element. A plate bending behavior was also examined in order to include the out-of-plane stiffness components without significant changes in the analysis results. A small difference was expected, due to the relatively small applied load, which minimizes the effect of the out-of plane stiffness contribution.

Since the test building was specially constructed to be structurally isolated, with load cells being the only points of contact, 27 joint objects on the foundation level were modeled with restrained degrees of freedom. The three translational components (x, y, and z) of the support points assumed to be restrained and the reactions for these joints were computed during the analysis. The material, frame and shell properties used for the analysis are presented in Appendix B. Details of the finite element model are shown in Figures 5.2.1, 5.2.2 and 5.2.3.

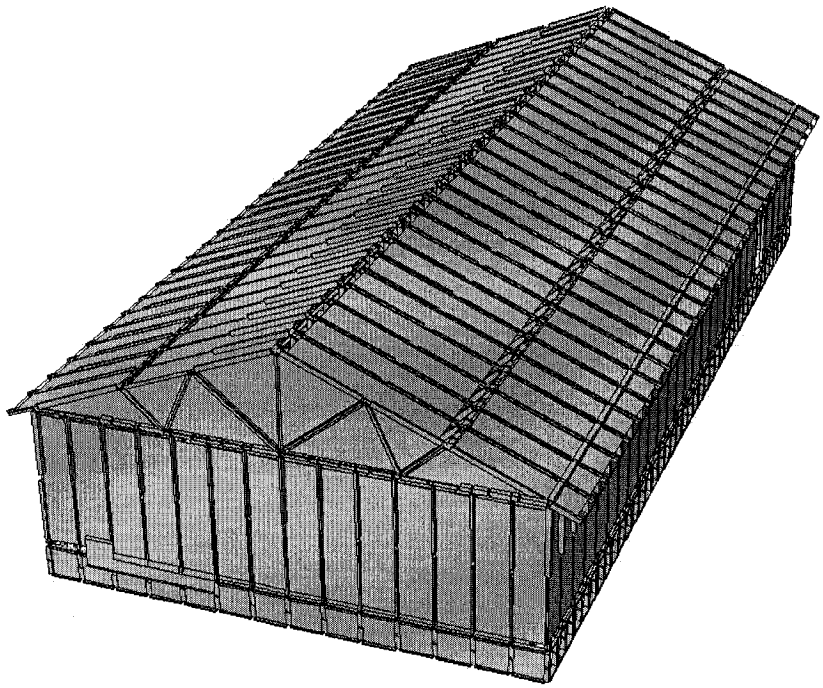

Figure 5.2.1 3-D finite element model (frame and shell elements)

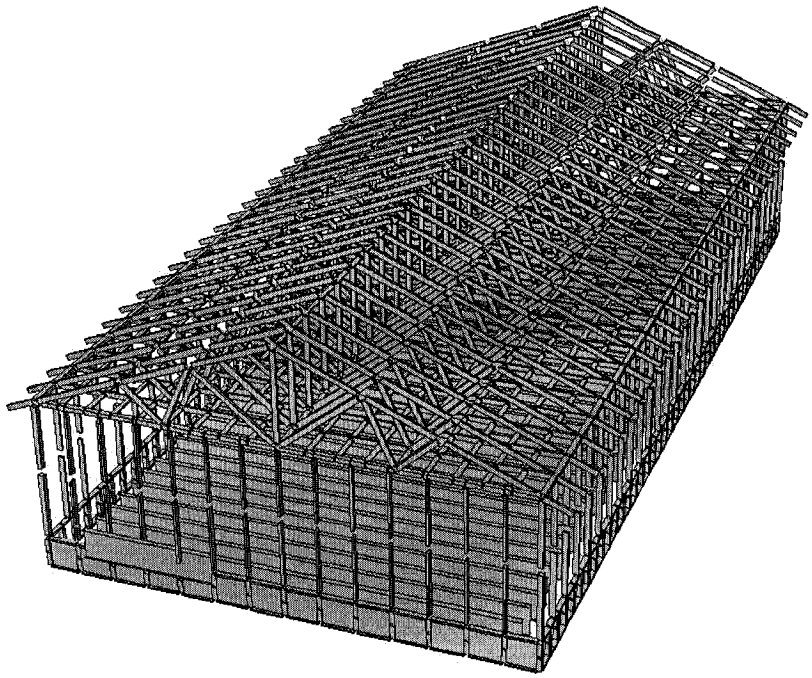

Figure 5.2.2 3-D finite element model (frame elements)

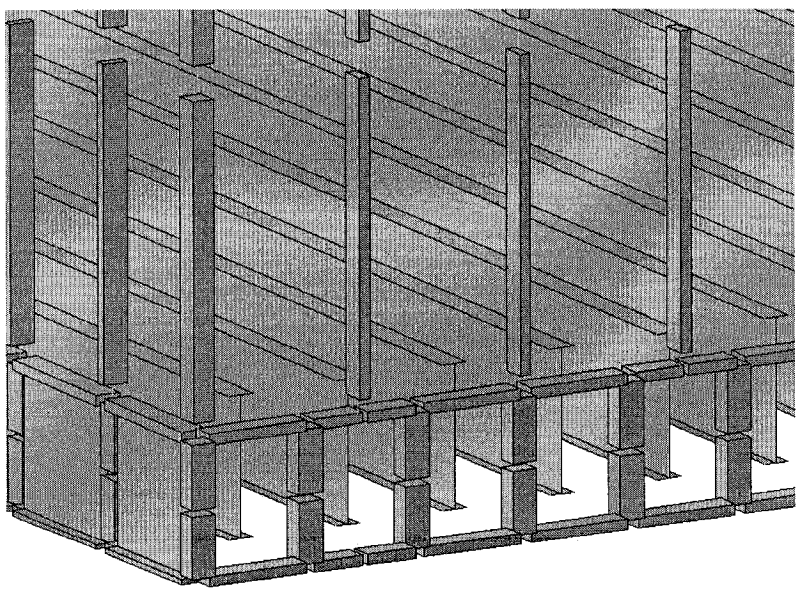

Figure 5.2.3 Finite element model floor system (studs and I-Joists elements)

At this particular stage of the study, a linear finite element model was decided to be used. A more sophisticated and detailed model is going to be created in the future. The reason for considering a linear model was mainly the low wind loads used for the analysis. Such loads generally correspond to small and linear deformations of the structural members.

5.3 LOAD INPUT DATA

In order to perform the analysis of the finite element model, a detailed load scheme should first be defined. As mentioned previously, the specific research project couples full-scale, wind tunnel and numerical modeling studies with the scope to evaluate the response of a wooden building subjected to environmental loads. Both full-scale monitoring and wind tunnel tests have been used to define the surface pressure distribution on the walls and roof of the building. Due to the small number of pressure taps on the full-scale building, only the wind tunnel data were used to compute the actual applied load on the building. Full-scale pressure measurements were used for verification and comparison with wind tunnel results so as to be confident that the simulated model scale results were accurate and comparable to the real full-scale measurements.

The area-averaged method was used to transform the point readings of the 124 pressure taps into area loads, for each of the 15 examined directions. The surface of the structure was divided into smaller areas according to the variation of the pressure coefficients. Smaller areas were used close to the wall and roof edges in order to represent, in the most

accurate way, the pressure distribution. An exploded plan view of the building with the selected areas used for the averaging method is shown in Figure 5.3.1. The instantaneous values of the fluctuating pressures for each group of pressure taps were averaged and the mean and peak values of area-pressure coefficients were calculated. Using the appropriate wind speed, these coefficients were transformed into actual pressure (or suction) which was applied to each tributary area. The finite element analysis was performed for 15 wind directions and results are presented in detail in the next section.

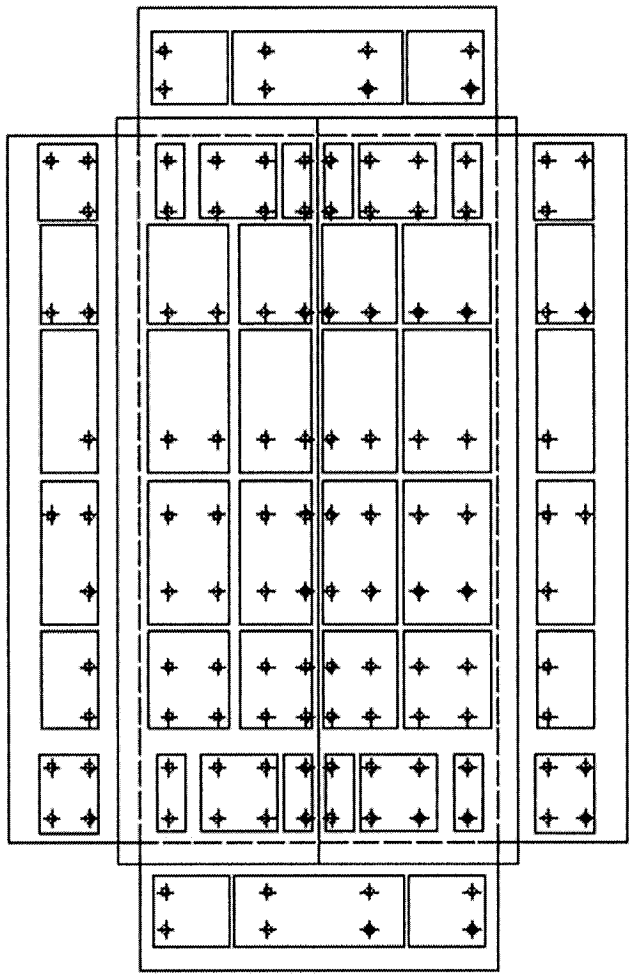

Figure 5.3.1 Exploded building plan view with area-averaged pressure tap groups

5.4 RESULTS

In order to better compare the results of the finite element analysis and the full-scale measurements, the dimensionless force coefficient Cf,x introduced in equation (4.1) was used. The force coefficients in the y and z direction are defined in the same manner.

The load cell location and the direction of the orthogonal axes are presented in Figure 5.4.1 and the examined wind angles of attack in Figure 3.6.1 (Chapter 3).

Three sets of results are presented in this section. First all x, y and z mean force coefficients for 0^{o} azimuth are shown in the building plan view, next to the load cell they represent (see Figure 5.4.2). As expected, for this specific angle of attack, pressure dominates on the north wall and suction on the rest of the walls (see Figure 3.8.1 for wind tunnel contour graphs for 0^{o}). The positive y-direction force coefficients justify the expected behavior and show that the building resists the wind coming from this direction. The z-direction results show a general uplift behavior. The x-direction force coefficients prove also that the building resists the north-west applied wind pressure.

The second set of results summarizes the variation of the individual load cell force coefficients as a function of wind direction. Results from four representative load cells are shown in Figure 5.4.3. For instance, for the load cell NW3 in the center of the wall, the x-direction force coefficient is positive for wind directions where pressure is applied on the east wall, the y-direction force coefficient is positive for the wind directions where pressure is applied on north wall and z-direction force coefficient is negative for all wind directions where an uplift wind pressure (suction) is applied on the roof. The rest of the results for all other load cells are included in Appendix C.

Finally Figure 5.4.4 shows the integrated force coefficients for each wall (the sum of the individual load cell force coefficients) and Figure 5.4.5 the total x, y and z force coefficient variation over wind direction for the entire building. In Figures 5.4.4 the contribution of each wall to the resistance of the entire building can be evaluated. Clearly the response of the walls as well as that of the entire building is directly affected by the wind direction. For example, north wall x-direction force coefficient is positive for the range of 30 to 180 degrees; on the other hand, the y-direction north wall force coefficient is only positive for the 0 to 80 degrees wind direction, where the north wall is windward. The z-direction north wall coefficient is negative for all wind directions which shows an uplift behavior for the specific wall.

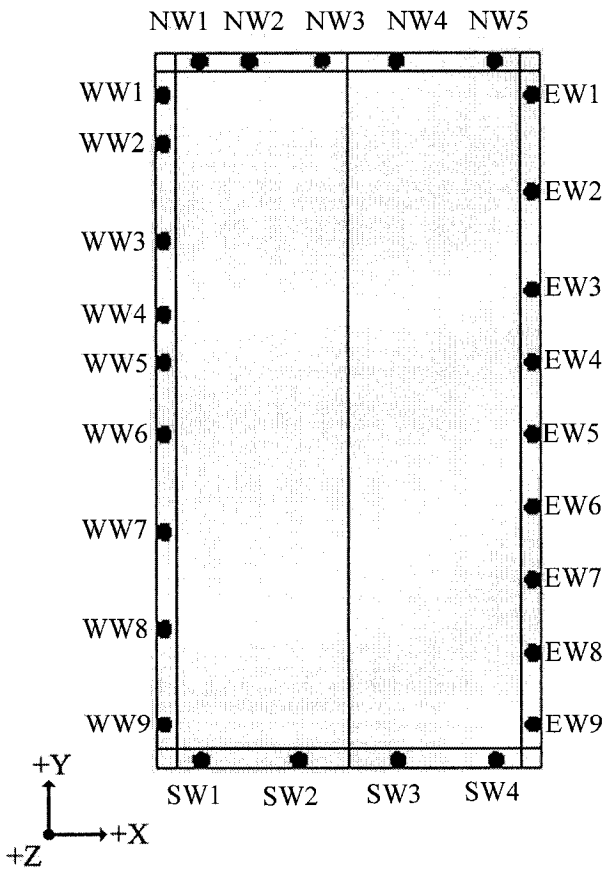

Figure 5.4.1 Load cell notation and direction of orthogonal axes

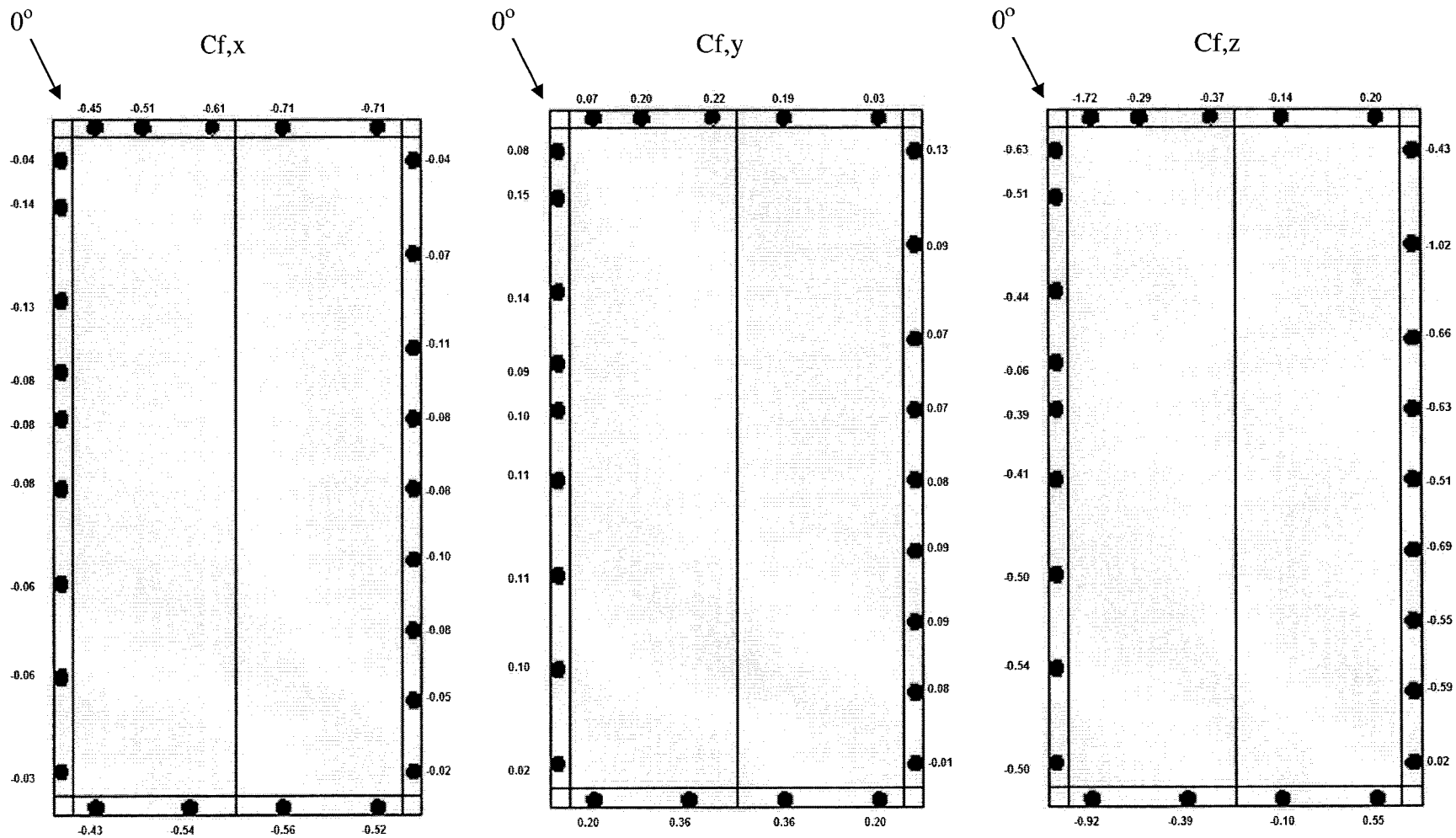

Figure 5.4.2 Mean force coefficients for 0-degree wind direction, based on F-E analysis

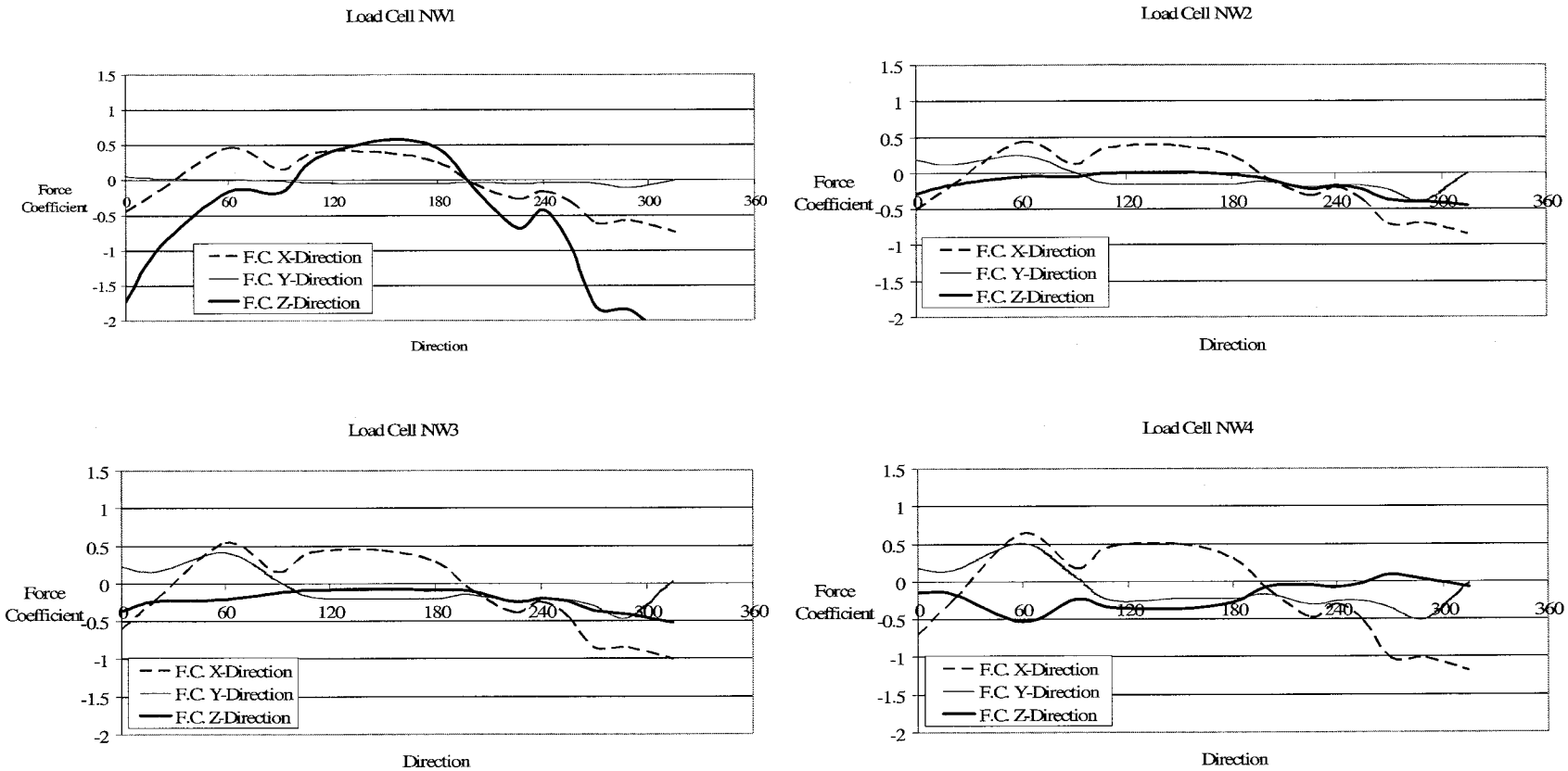

Figure 5.4.3 Individual load cell force coefficient variation over direction (based on F-E analysis)

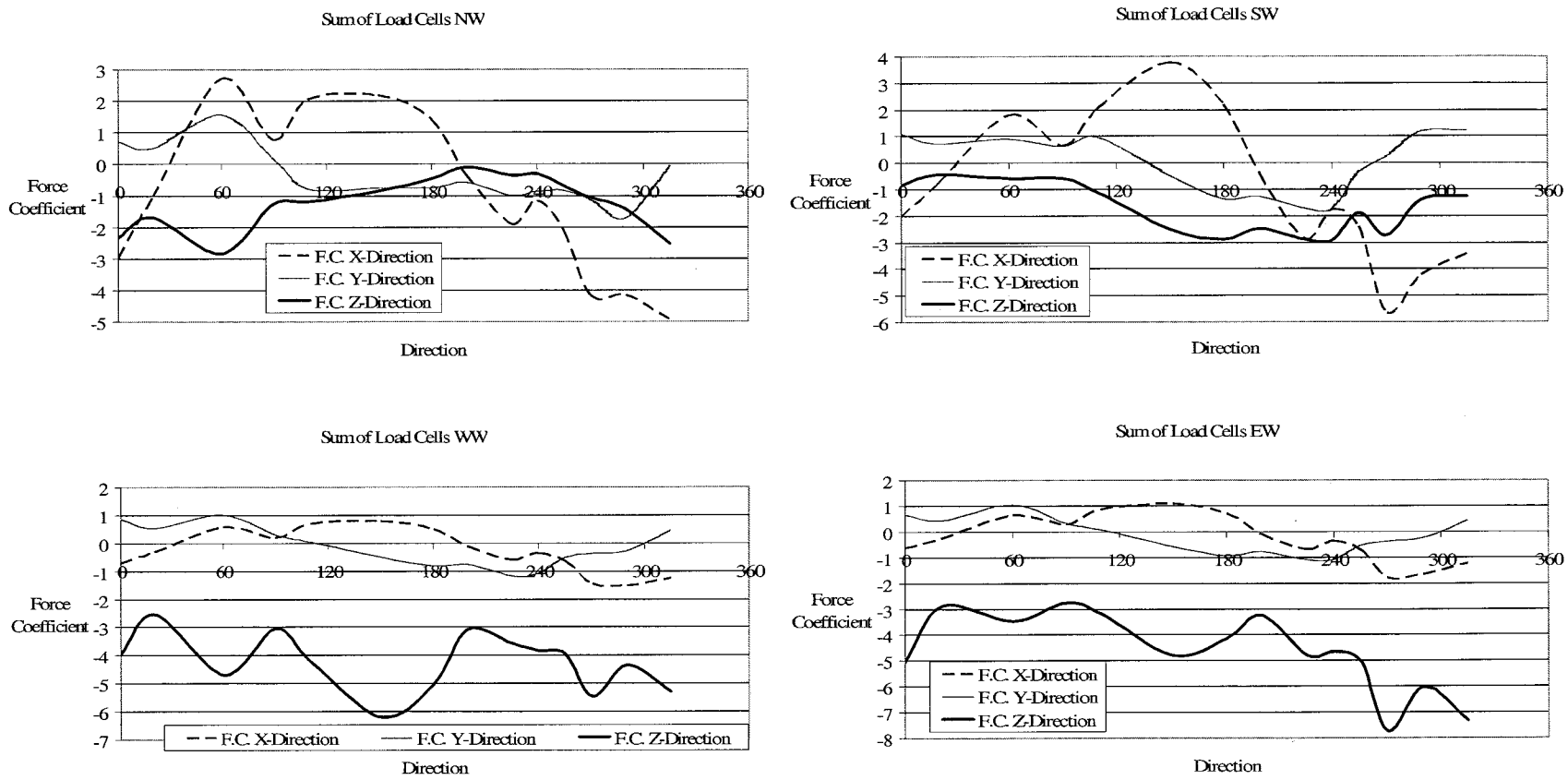

Figure 5.4.4 Integrated wall force coefficient variation with direction (based on F-E analysis)

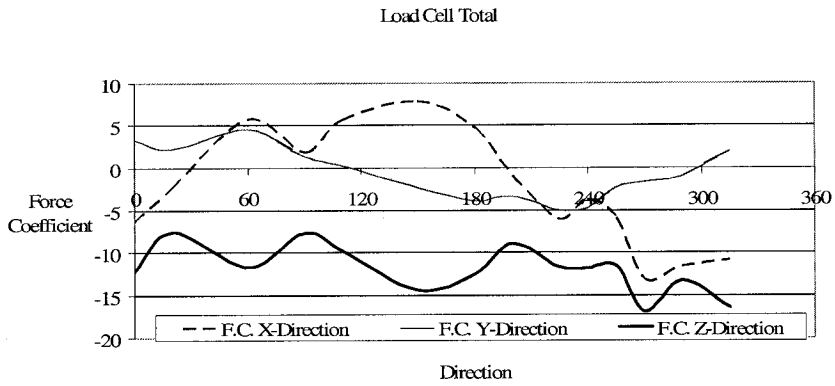

Figure 5.4.5 Total building force coefficient variation with direction (based on F-E analysis)

CHAPTER 6

RESULTS: COMPARISON AND DISCUSSION

6.1 GENERAL

This chapter presents four main categories of results and comparisons. The first section presents weather data measured at the test building and compares them with Environment Canada Weather Office archives. A two-dimensional structural analysis response is included in the second section, where the response of a single frame is assessed. In the third section, pressure data measured in the wind tunnel and the field are compared. Finally, in the last section the full-scale load cell measurements are presented along with the finite element analysis results.

6.2 CLIMATE DATA COMPARISON

The meteorological tower, located next to the test building (Figure 6.2.1), was continuously recording wind speed and direction data during the monitoring of the response of the building. For verification purposes these data were compared with the archives from Environment's Canada Weather Office. Past climate data are available

through Environment Canada portal (http://www.climate.weatheroffice.ec.gc.ca) for major cities across Canada. For this particular comparison, the CDA CS meteorological station was selected. The geographical coordinates for this specific station, located approximately 4 km east from the test building, are 45°55' - latitude, 66°36' - longitude and 35.10 m – elevation.

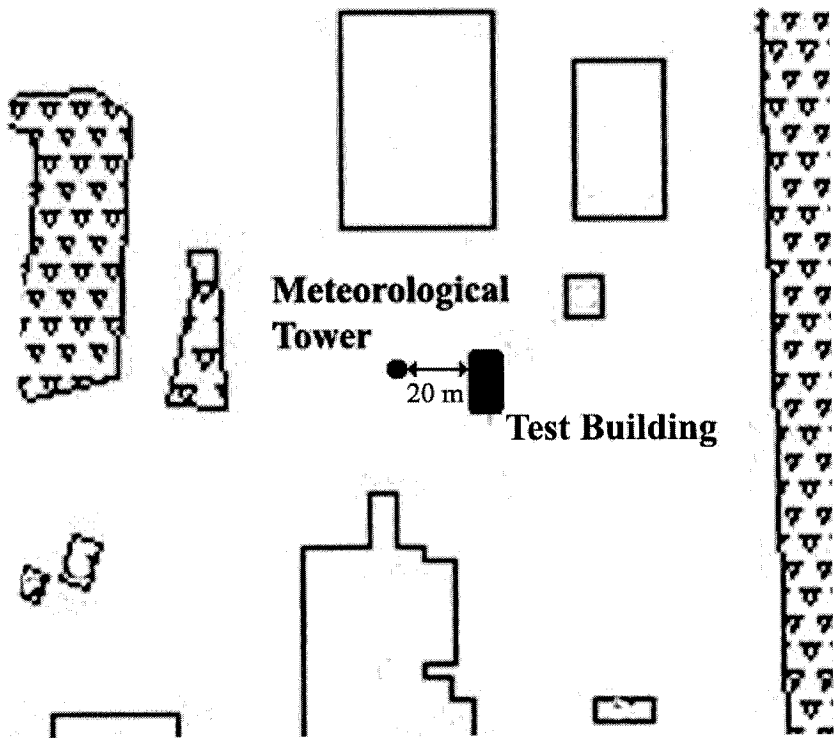

Figure 6.2.1 Test building and meteorological tower location

In order to be able to compare the recorded data with those from the station, appropriate transformation for the wind speed was made, using the power law velocity profile, as indicated in Figure 6.2.2. This transformation takes into consideration the upstream

terrain and the height difference of the two anemometers (5.5 and 10.0 meters for the meteorological tower and the weather station respectively).

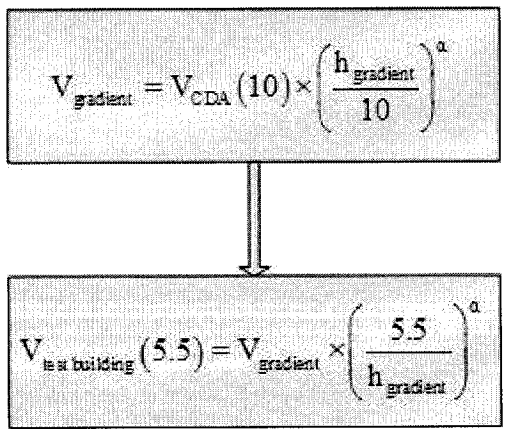

Figure 6.2.2 Transformation procedure schematic

Two of the measured records are shown in Figures 6.2.3 and 6.2.4. The first one is a 24-hour record and the second is a 12-hour record. The presented charts show good agreement, between the measured and meteorological station data. The trends are similar with only few periods of small discrepancy. Considering the distance between the two stations and the topography of the area, these results are better than expected. Thus, the results assure high accuracy wind measurements in the location of the building and increase confidence in the findings of this thesis.

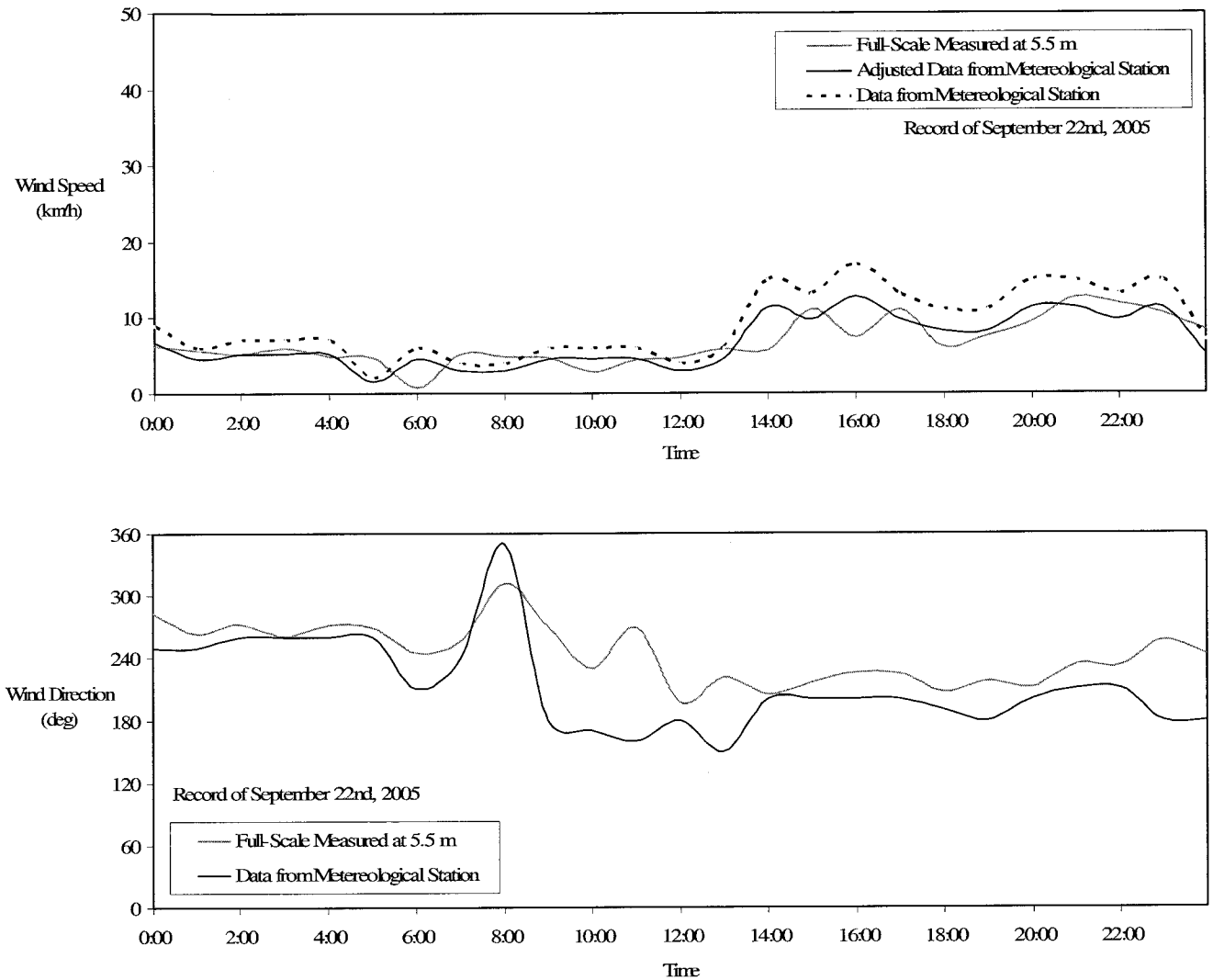

Figure 6.2.3 Wind speed and direction records for September 22nd, 2005

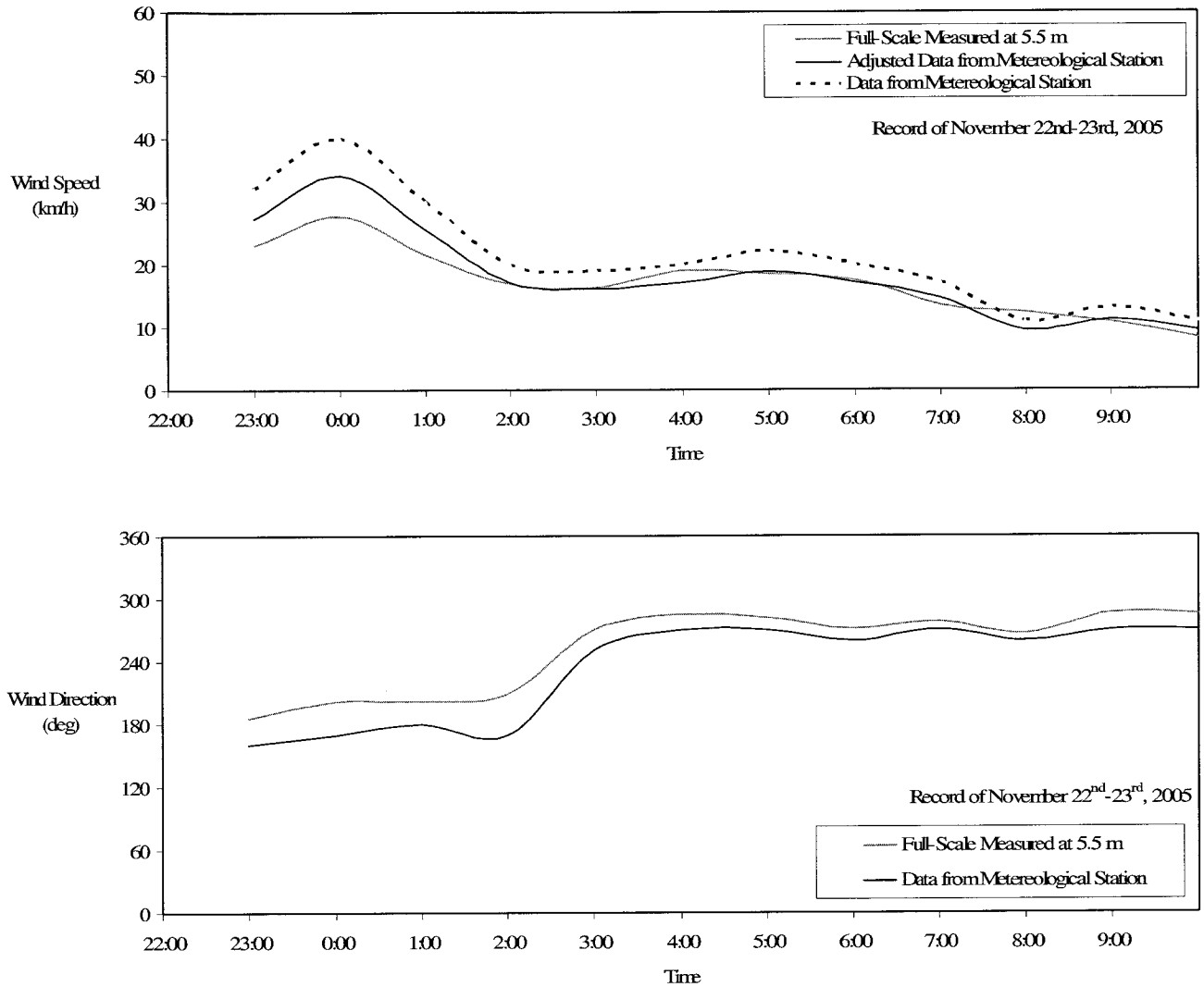

Figure 6.2.4 Wind speed and direction records for November 22nd-23rd, 2005

6.3 SINGLE FRAME RESPONSE

Prior to the consideration of the entire structural system of the building, two main frames of the structural system were isolated in order to perform a two-dimensional structural analysis. These two frames (#2 and #14) were selected according to the full-scale pressure tap location – see Figure 6.3.1 - so as to be able to know the pressure distribution on them.

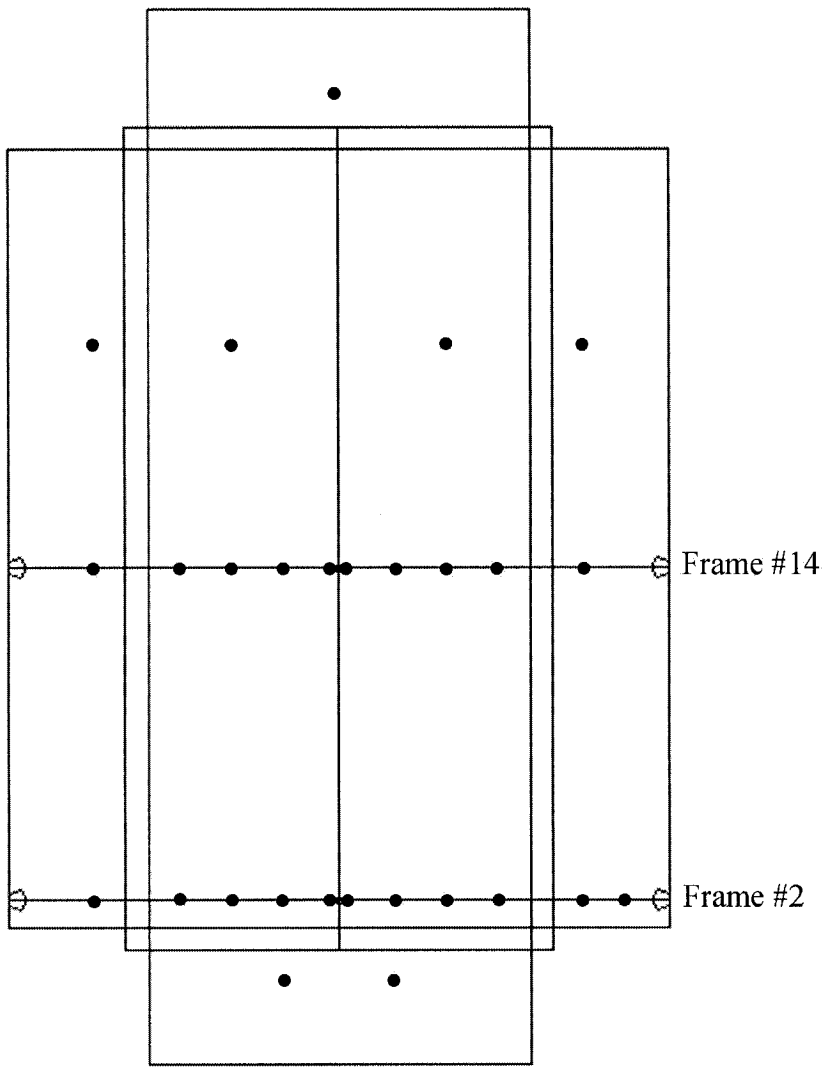

Figure 6.3.1 Frame #2 and #14 location

For each frame the individual roof pressure records were added so as to take the total vertical pressure applied to the frame. Using the tributary area for each frame and making appropriate unit conversions, the total expected reaction due to the applied wind pressure was computed. In the same manner the readings from the two load cells located in the base of each frame, were added and the actual reaction reading from the load cells was computed. The two different resulting records are compared in Figures 6.3.2 (frame #2) and 6.3.3 (frame #14), in terms of actual forces in kN. Data were collected on April 12th 2006 for a wind speed of 25 km/h and 200^{o} direction.

The comparison between the sum of reactions measured directly (load cells) and those computed on the basis of measured pressures shows good agreement in the trend. The mean values show also excellent agreement. However a significantly more fluctuating signal with much higher peaks is resulting from the pressure measurement approach. Two comments can be made at this point in order to justify this difference. The first is related to the frequency response of the two different types of sensors. As mentioned in Chapter 3, the pressure tap transducers are high frequency sensitive sensors, whereas load cell sensors are custom made strain gages, which are not able to reach the same frequency response as the pressure transducers. The second outcome, which is the most important and should be further investigated, is the attenuation effect due to structural and material damping of the building components which result to lower than computed reactions and stresses. This should be examined in detail, by taking a considerable amount of recorded data and analyzing them. In addition, the response of the two sensors should be examined and defined to fully describe their actual behavior.

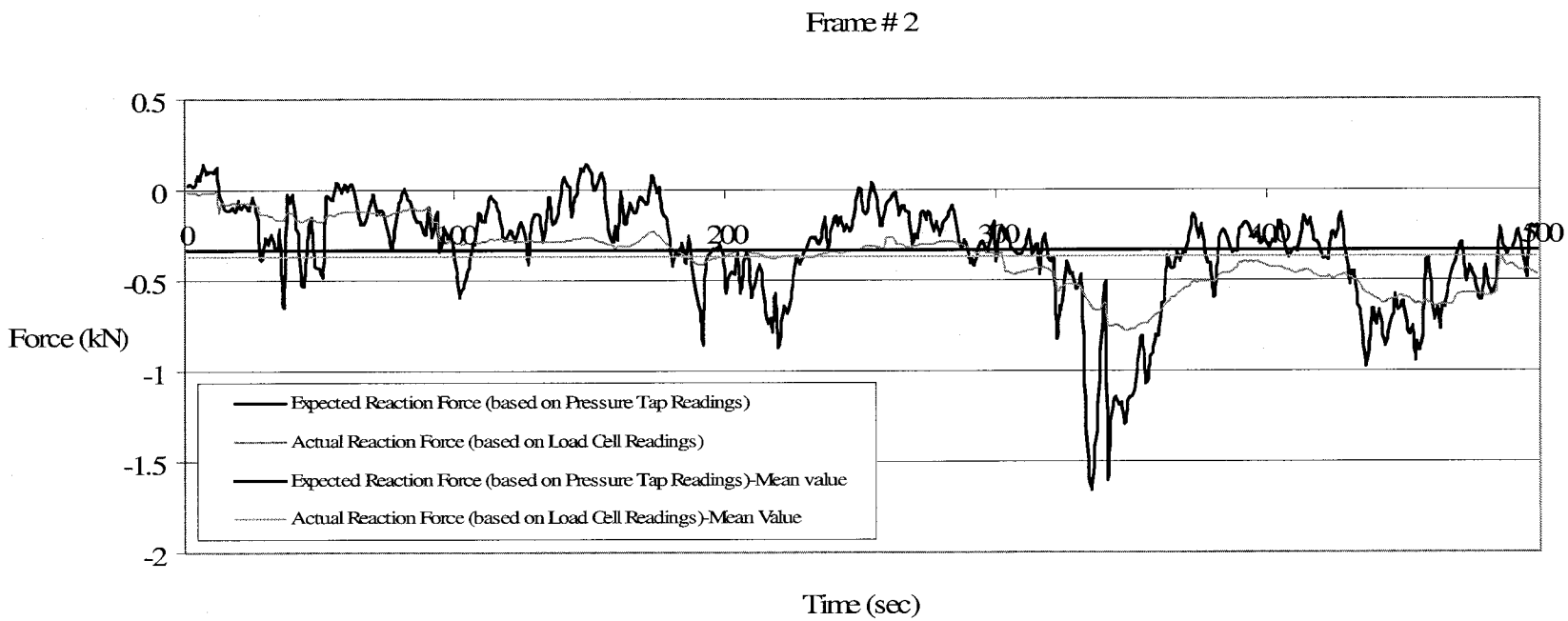

Figure 6.3.2 Frame #2 response record

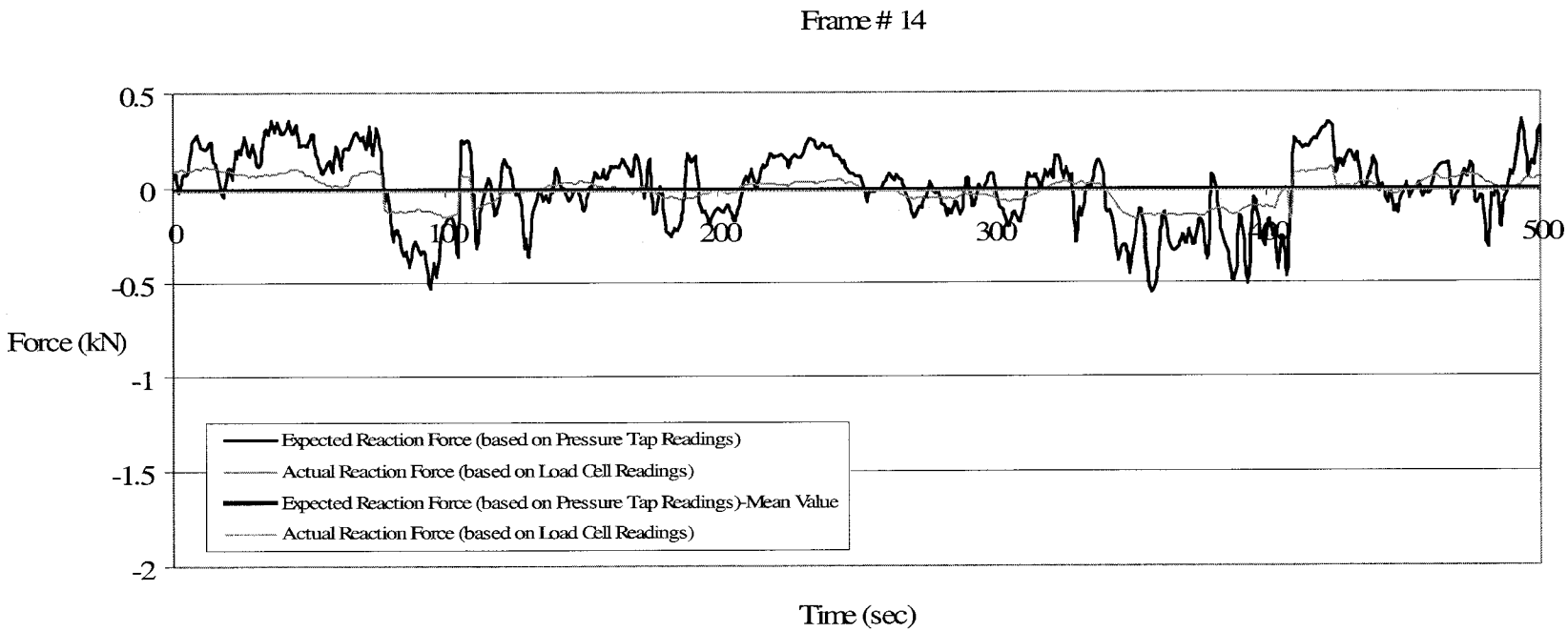

Figure 6.3.3 Frame #14 response record

6.4 WIND TUNNEL AND FULL-SCALE PRESSURE MEASUREMENTS

The role of the wind tunnel studies in this project was the calculation of the pressure distribution on the surface of the building. The verification of these results was the scope of the full-scale pressure measurements. For the model-scale experiments it was quite simple and straightforward to examine any possible angle of wind attack. For the full-scale measurements though, only a small amount of useful data was recorded and these were for specific wind directions, usually the dominant ones according to the statistics. The full-scale records are measurements taken from spring to fall 2006, with most of them measured during summer 2006. The mean wind speed is in most cases greater than 20 km/h and the standard deviation for the wind direction lower than 15 degrees.

Mean pressure coefficient comparison results are presented in two sets. The first shows the variation of the wind tunnel mean pressure coefficient as function of wind direction for typical pressure taps (see Figure 4.4.4 – Chapter 4). The single points indicate full-scale mean pressure coefficients, see Figures 6.4.1 and 6.4.2. The charts correspond to specific pressure taps, located both on the wall and the roof surface. The second set, uses scatter plots to compare the mean pressure coefficient results (Figure 6.4.3). In these scatter plots the x-axis represents the wind tunnel results and the y-axis represents the full-scale results. In these plots all the wall and roof pressure taps are included and results for four different direction are compared.

Both types of plots show good agreement for the mean pressure coefficient measured in the model and full-scale test building. For the direction graphs (Figure 6.4.1 and 6.4.2), most of the full-scale measurement results are close to the wind tunnel data. The high

fluctuation in the full-scale wind direction records could be the reason for the few outlying points.

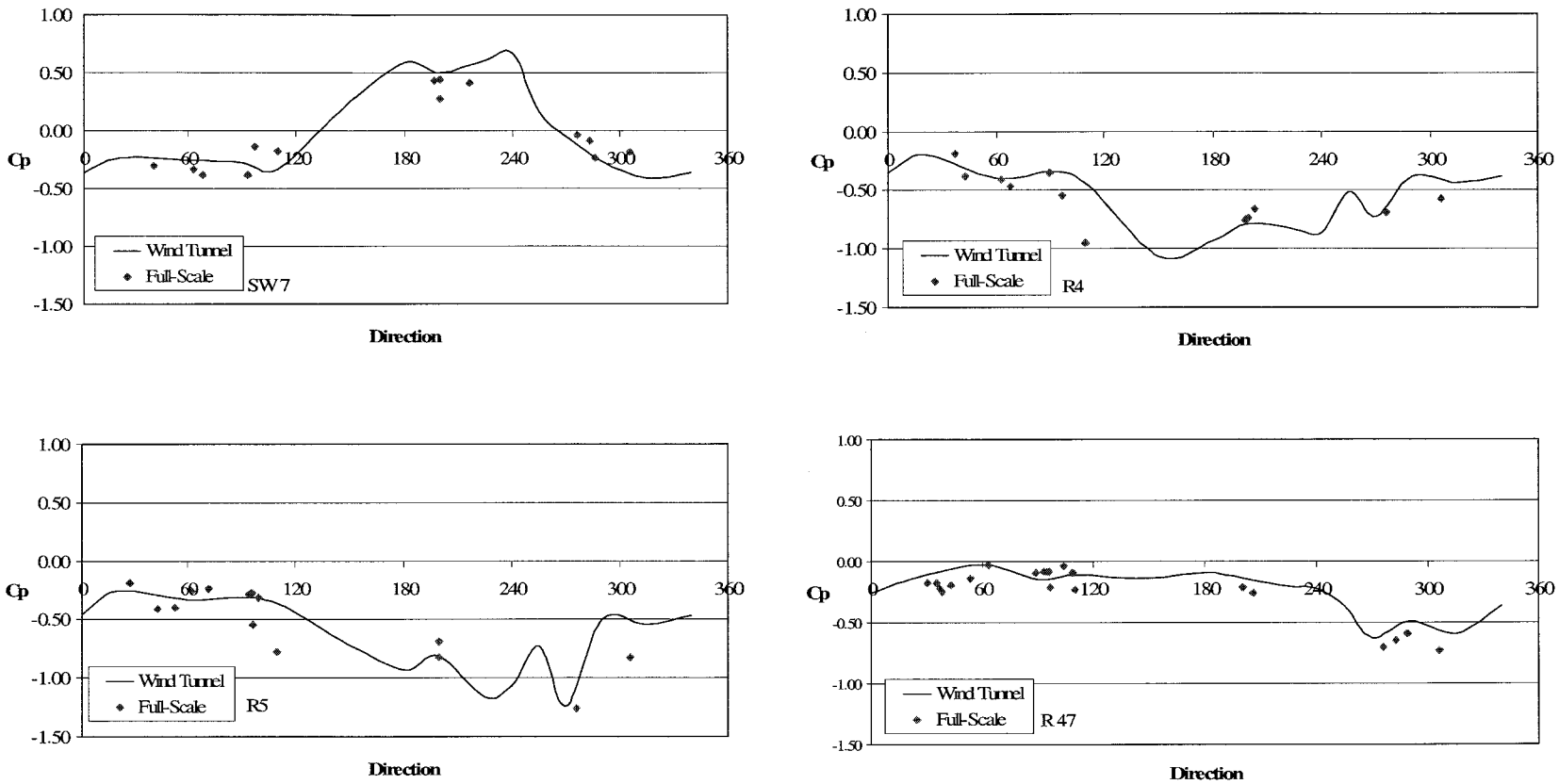

Figure 6.4.1 Variation of the wind-tunnel and full-scale mean pressure coefficient over the wind direction for pressure taps SW7, R4, R5 and R47.

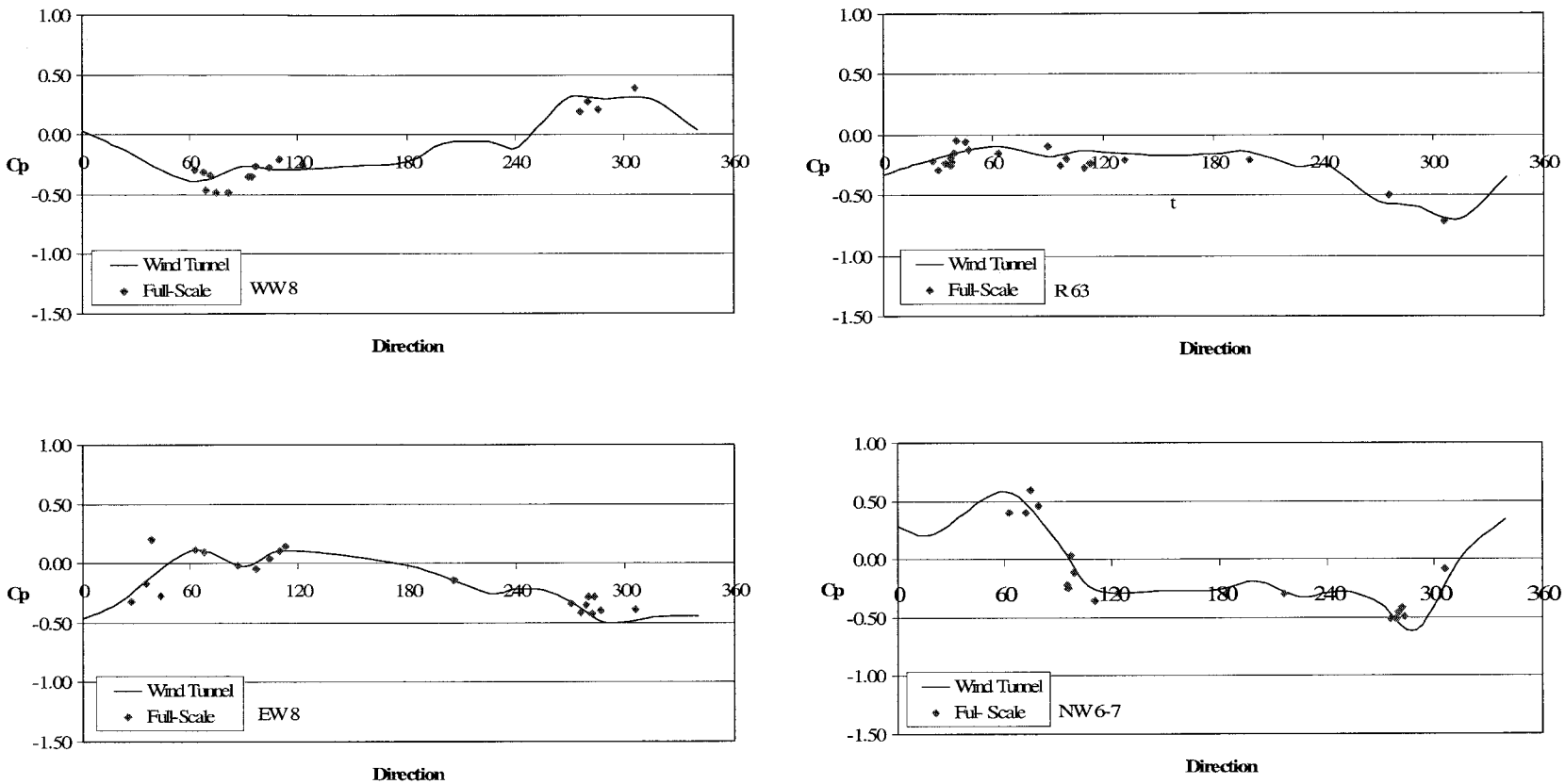

Figure 6.4.2 Variation of the wind-tunnel and full-scale mean pressure coefficient over the wind direction for pressure taps WW8, R63, EW8 and NW6-7.

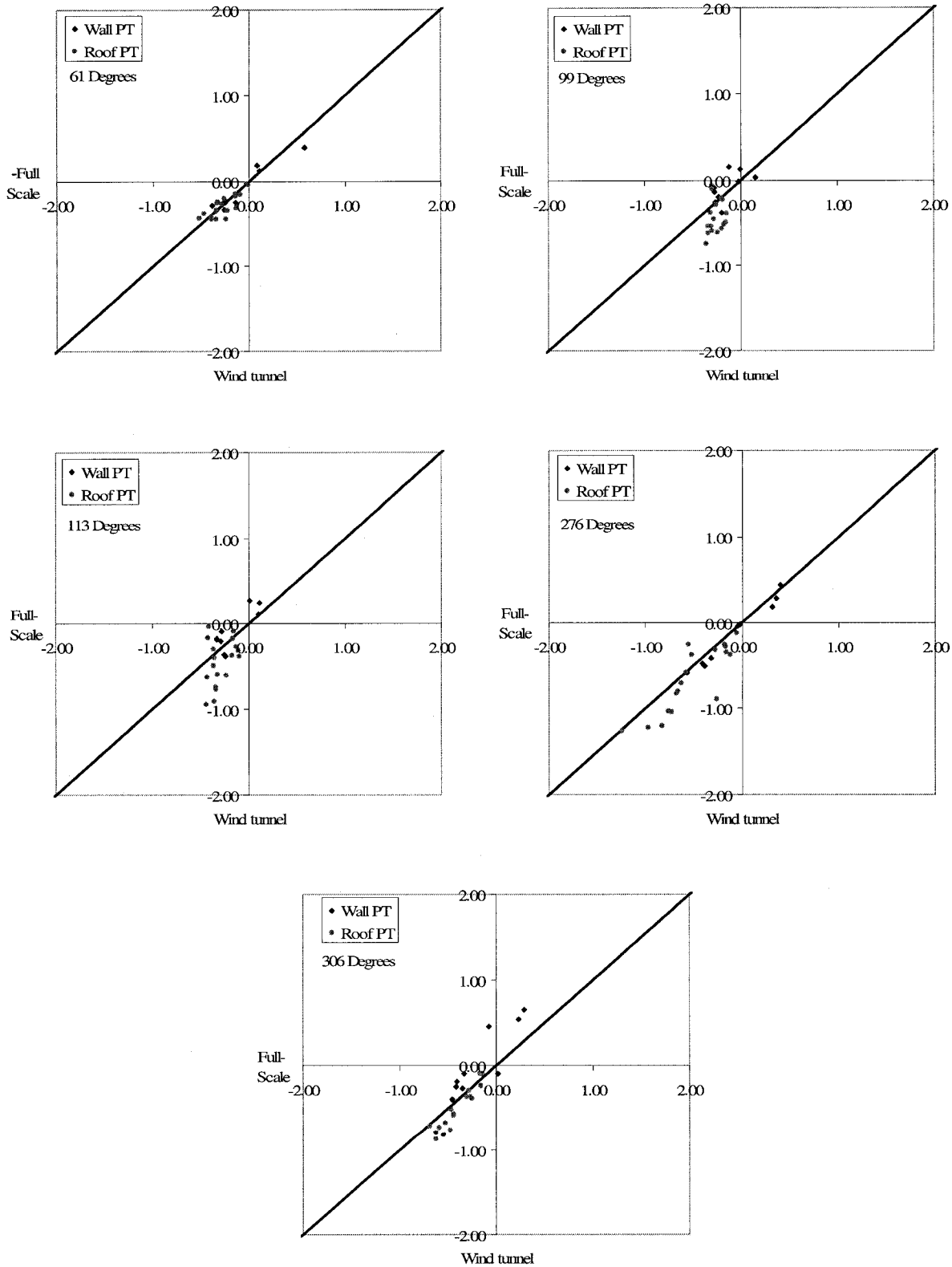

Figure 6.4.3 Wind-tunnel and full-scale mean pressure coefficient scatter plots

6.5 FULL-SCALE AND FINITE ELEMENT MODELING COMPARISON RESULTS

In this section, a comparison between the full-scale load measurements and the finite element analysis results is made. Similar to the wind tunnel tests, finite element analysis was possible for any desired load and wind direction. As mentioned in Chapter 5, through the computer-based analysis all 15 wind directions examined and a range of wind speeds were analyzed. However for full-scale measurements only a small number of records were qualified for further analysis due to the low wind speed and high wind direction fluctuations. The comparison results are presented in the form of force coefficient plots. The load cell notation and the three orthogonal axes direction are shown in Figure 5.3.2 (Chapter 5).

For the first set of graphs (Figures 6.5.1, 6.5.2 and 6.5.3) the continuous line represents the finite element analysis results and the single points the full-scale measurement data. A number of load cells from each wall was selected and the variation of the force coefficients over the direction for each axis was plotted. These plots show a good agreement. As mentioned previously, the collected full-scale data are in most cases part of a fluctuating wind record. These fluctuations make the data unstable and result to higher standard deviation values for mean force coefficients. This phenomenon is usually the reason for the discrepancy of the full-scale point force coefficients in the direction charts. However, the trend of the full-scale measurement data seems to be quite accurate following the finite element analysis results.

The second set of results is shown in Figures 6.5.4 to 6.5.7. These data consist of percentages of force distribution along the walls compared for two wind directions. In this comparison, the percentage of the total applied external load transferred in each wall is computed for both full-scale and finite element models. For both cases only two directions of the force distribution are considered, namely that along the main wind component and the vertical direction (Z-component). The force distribution along the smallest wind component is considered less important since its variation and participation is small.

For the wall participation results the following comments can be made: For the case of 60 degrees, the Y-direction distribution shows disagreement between the two approaches for the east wall. The finite element analysis provides a more balanced distribution between the west and east wall and somewhat higher between the north (windward) and south (leeward) wall. On the other hand, the full-scale results indicate a larger participation of the east wall and almost equal distribution between the windward and leeward wall. This significant difference can be partially justified by the wind angle of attack, which is approximately 40 degrees apart from the normal to the windward wall. For the Z-direction (Figure 6.5.5), results show better agreement with only exception the west wall, where the full-scale measurements indicate a higher participation than the finite element analysis. For the 290 degrees wind direction which is normal to the west wall a good agreement is found for both X and Z directions – see Figure 6.5.6 and 6.5.7. Again, the east wall has a higher participation for the full-scale X force component. For the Z direction though, the distribution has a better agreement with only a small discrepancy for the west wall.

It should be mentioned at this point, that scope of the current comparison was to verify the functionality of the load cells; i.e. the calibration and data acquisition process from these very sensitive instruments. The finite element analysis was also simplified without including nonlinearities of the wooden structure.

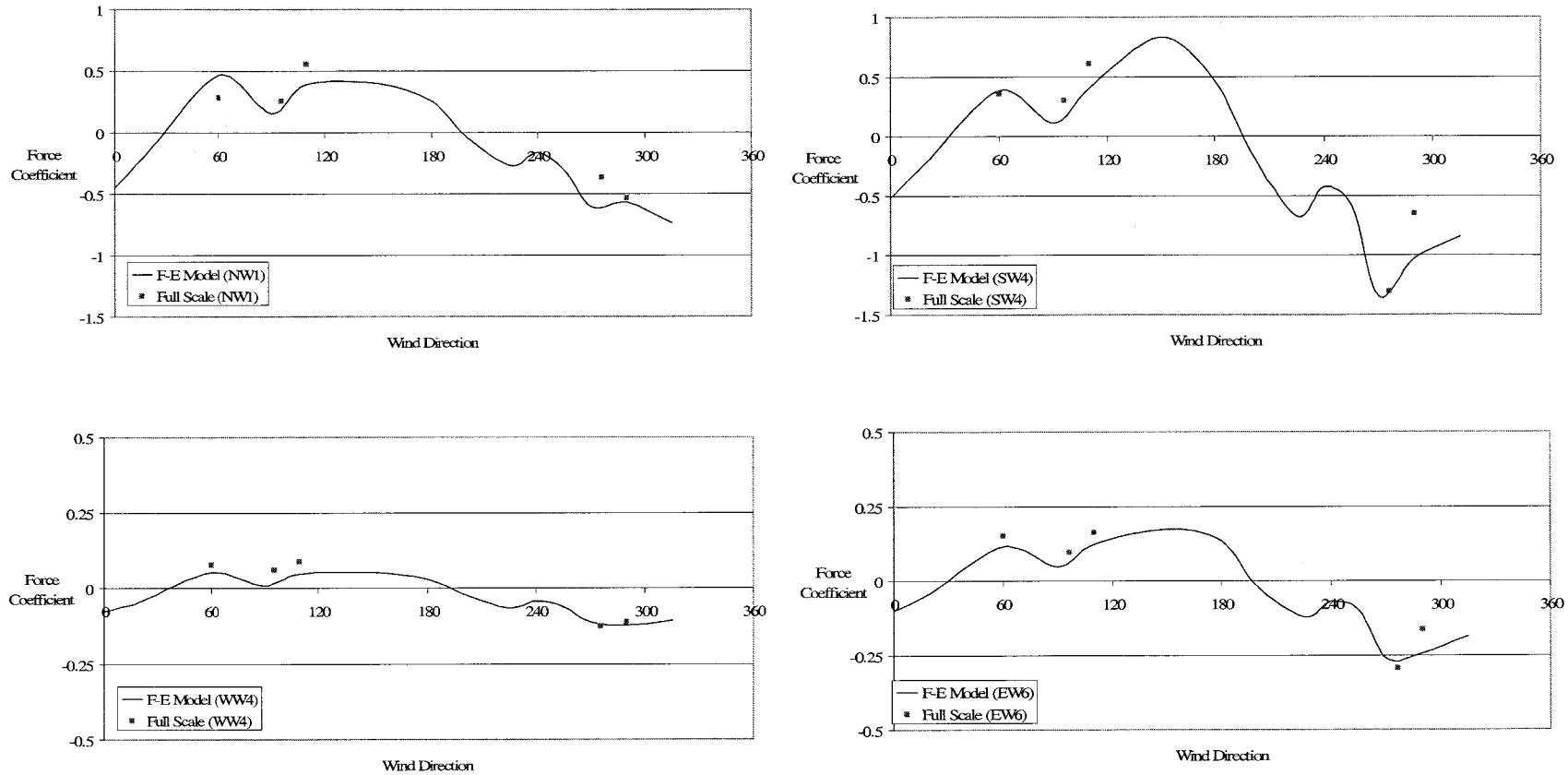

Figure 6.5.1 Variation of the wind-tunnel and full-scale X-mean force coefficient (Cf,x) over the wind direction for load cells NW1, SW4, WW4 and EW6.

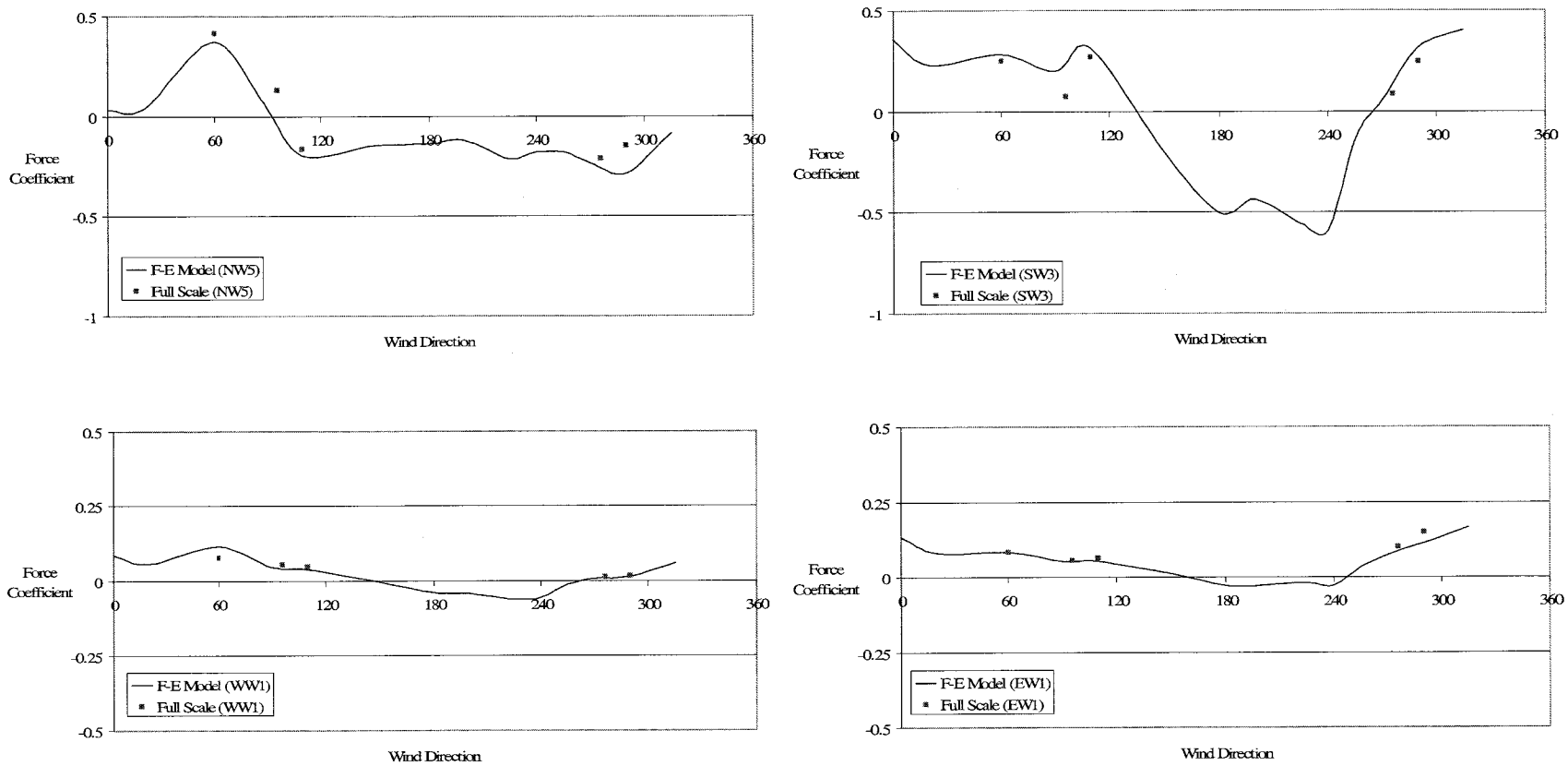

Figure 6.5.2 Variation of the wind-tunnel and full-scale Y-mean force coefficient (Cf,y) over the wind direction for load cells NW5, SW3, WW1 and EW1.

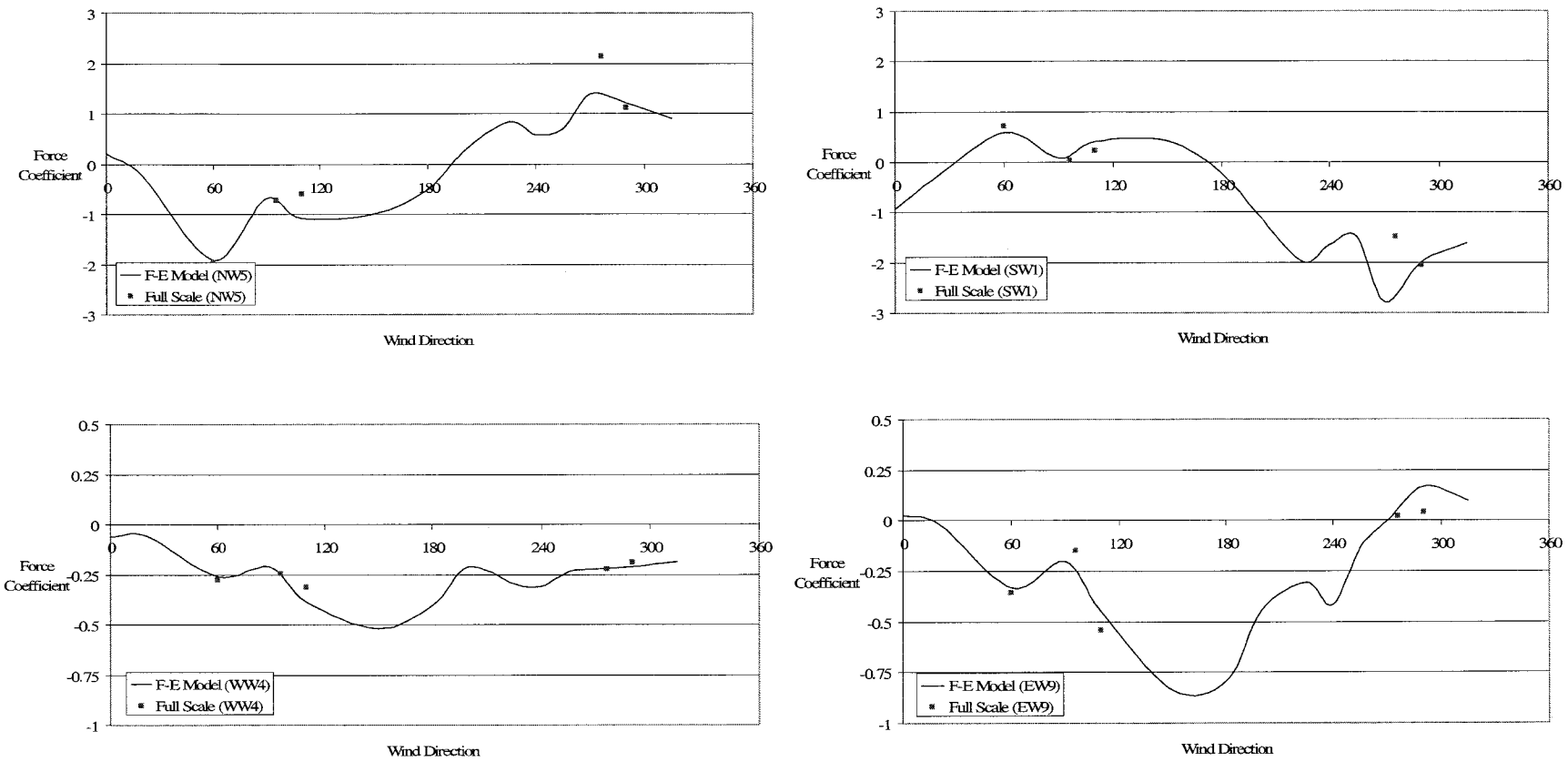

Figure 6.5.3 Variation of the wind-tunnel and full-scale Z-mean force coefficient (Cf,z) over the wind direction for load cells NW5, SW1, WW4 and EW9.

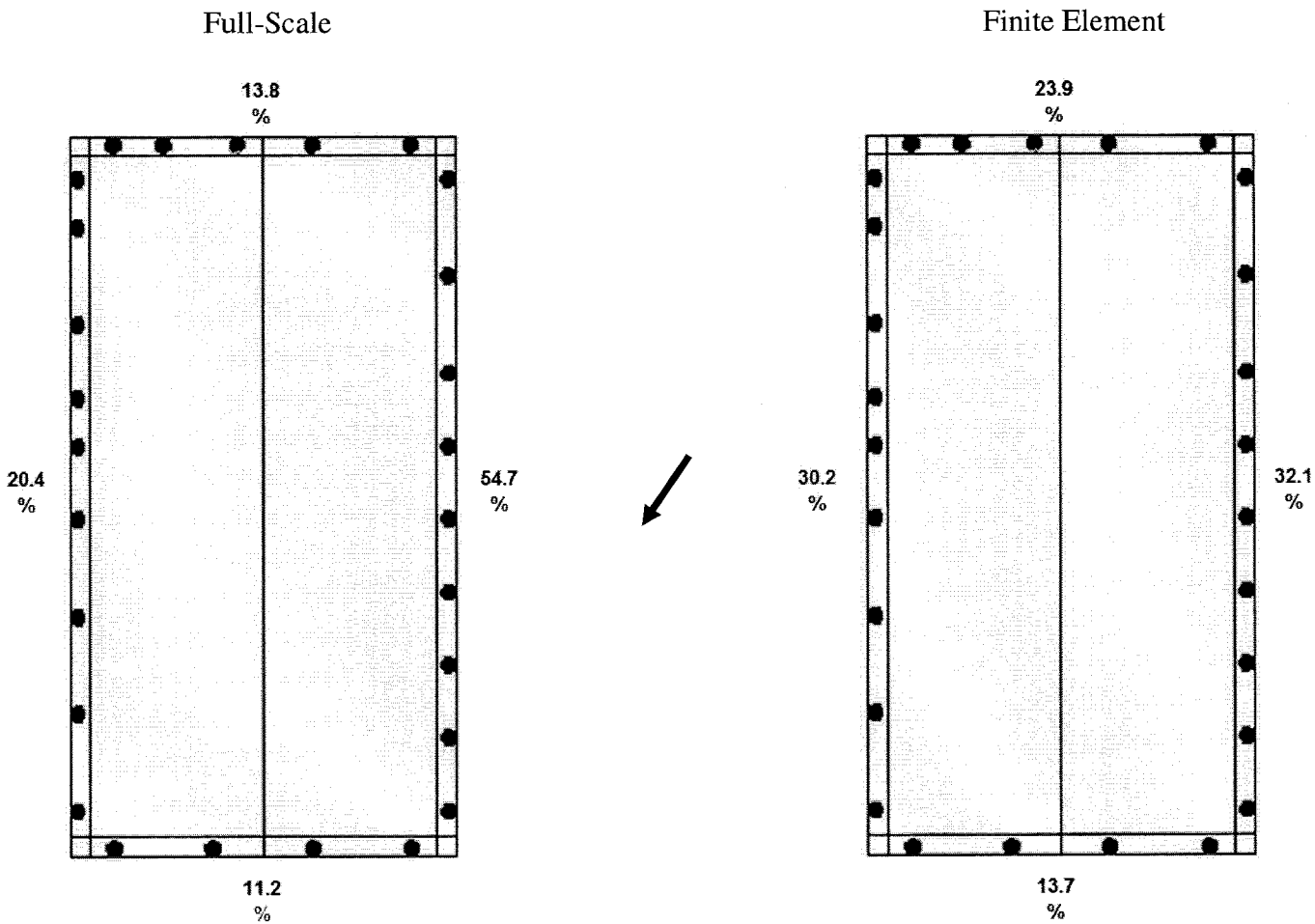

Figure 6.5.4 Distribution of total applied wind load to the walls - Case A-1: 60 degrees (Y-Direction)

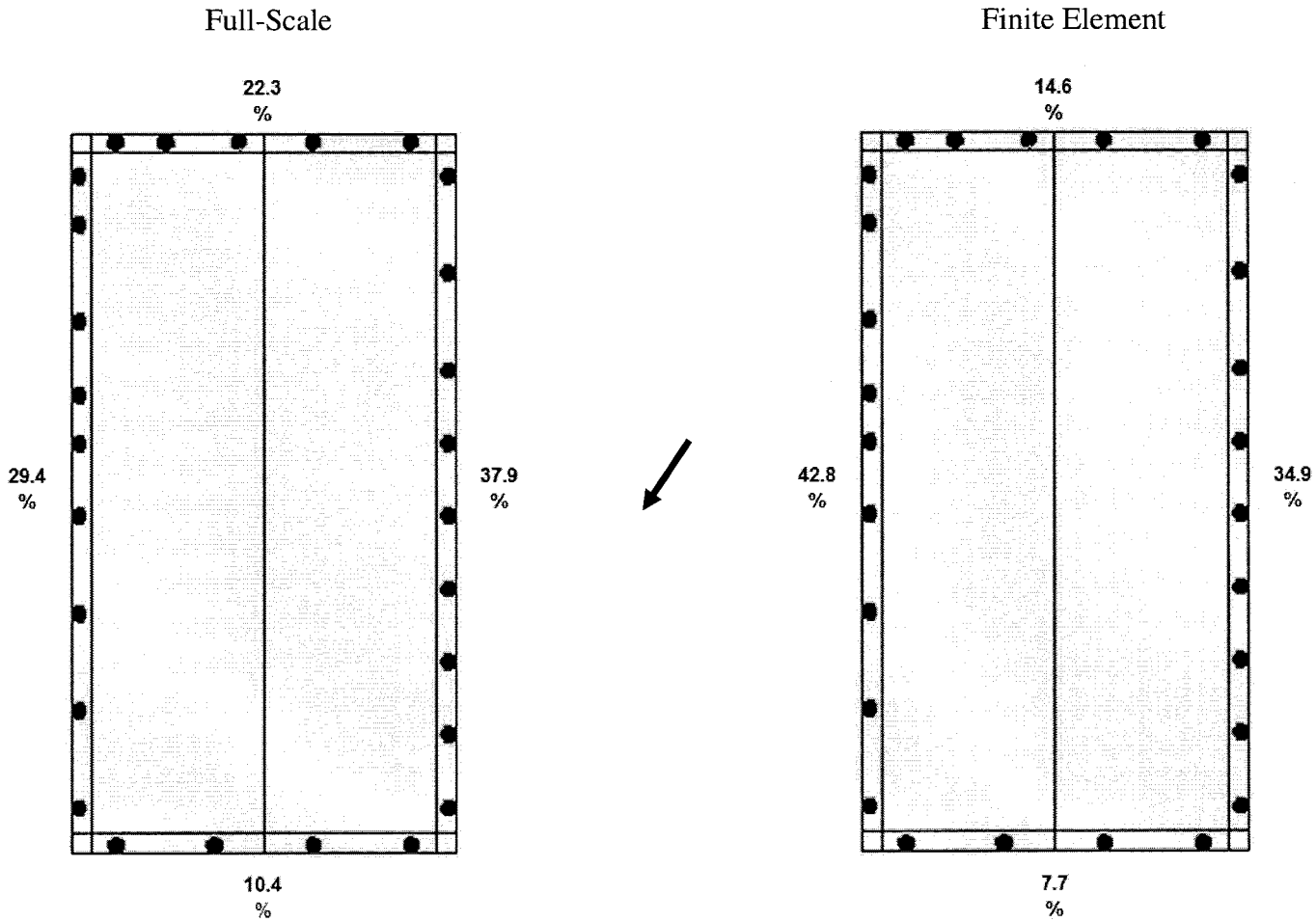

Figure 6.5.5 Distribution of total applied wind load to the walls - Case A-2: 60 degrees (Z-Direction)

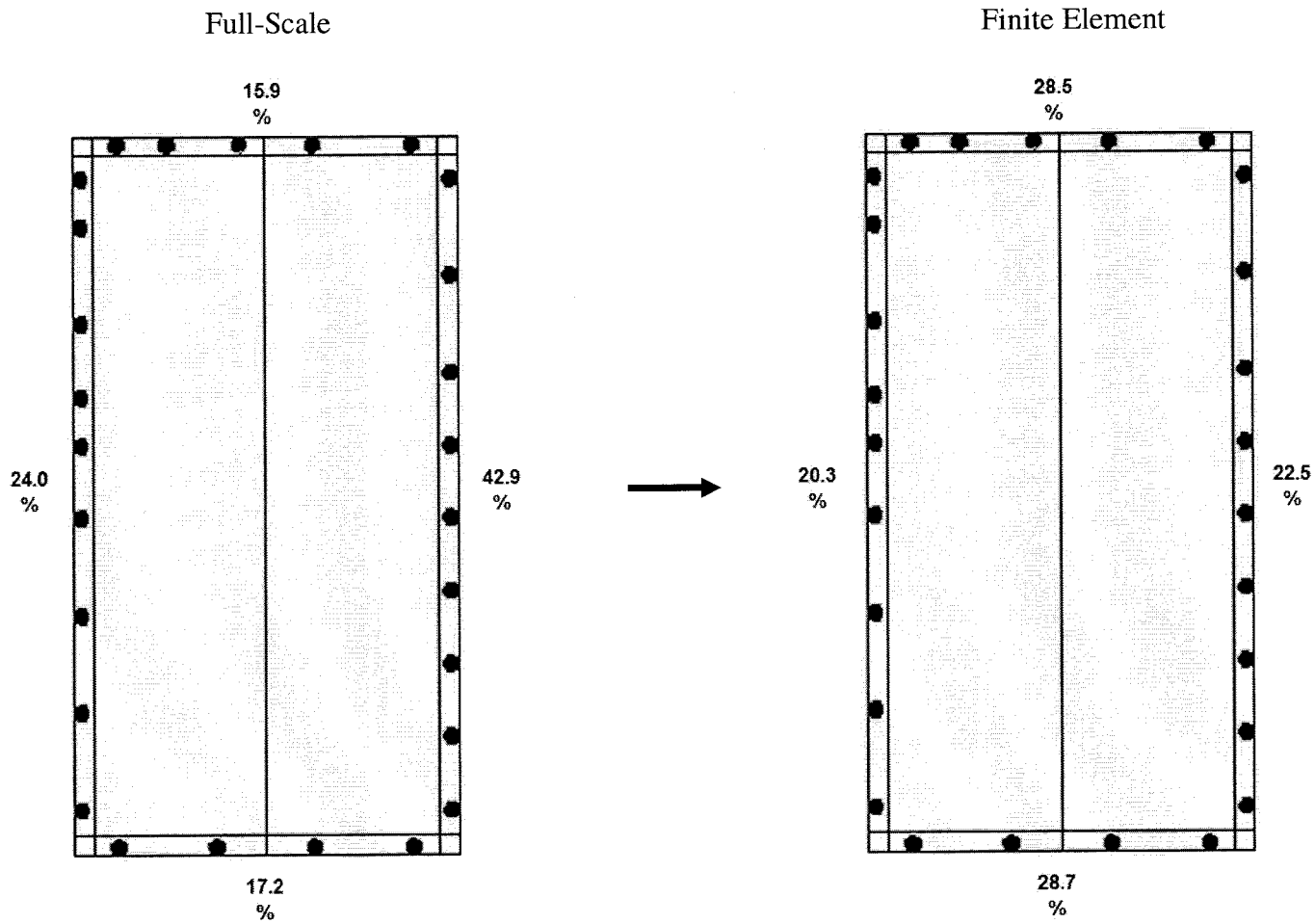

Figure 6.5.6 Distribution of total applied wind load to the walls - Case B-1: 290 degrees (X-Direction)

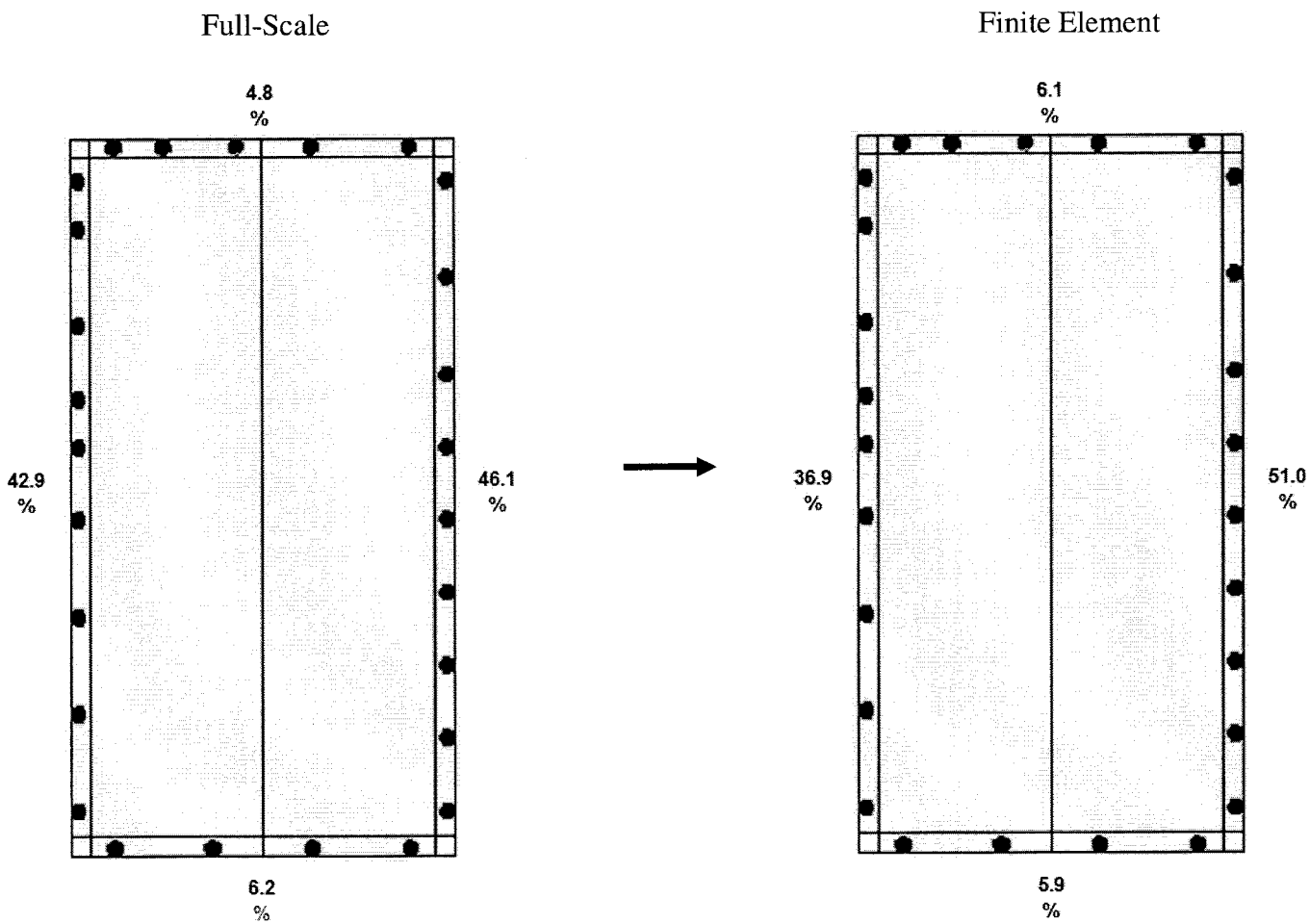

Figure 6.5.7 Distribution of total applied wind load to the walls - Case B-2: 290 degrees (Z-Direction)

CHAPTER 7

CONCLUSIONS AND RECOMMENDATIONS

7.1 SUMMARY

During this study three individual fields of application were coupled in order to better understand the phenomenon and accomplish the desired objectives. Full-scale studies, wind tunnel experiments and finite element modeling were used for the study of a wooden low-rise building subjected to wind loads.

A real-scale wooden structure was specially constructed for the scope of this project. This structure was equipped with state-of-the-art wind and stress monitoring instrumentation. The wind surface pressure distribution and the internal stresses at key points of the structural system were recorded at any time using a sophisticated data acquisition system. All data recorded were first evaluated and then analyzed and transformed into pressure and force coefficients.

In addition to the full-scale monitoring, a building model of 1:200 geometric scale was tested in the boundary layer wind tunnel of Concordia University. The model was equipped with 130 pressure taps and the analysis of the wind tunnel results gave a detailed representation of the surface pressure distribution. Pressure coefficients were also computed for the wind tunnel results and a comparison with the full-scale measurements was made.

Finally, a finite element model was created using a commercial finite element software package. Using the pressure distribution of the wind tunnel tests, as the applied loading, the model computed all internal forces for the desired key points. Having also these forces from the full-scale monitoring, a successful comparison between the two studies took was carried out.

7.2 CONCLUSIONS

The conclusions of this study can be summarized as follows:

- Wind speed and direction data from the meteorological tower of the full-scale facilities shows excellent agreement with those from the Environment Canada Weather Office archives.
- The pressure distribution comparison between the wind tunnel and the full-scale results shows good agreement. The mean pressure coefficient trends were similar and some discrepancies can be justified by the high fluctuations of the wind direction in the full-scale records.
- The wind tunnel / full-scale agreement confirmed the wind tunnel results and allowed their use for the finite element analysis.
- The comparison between the full-scale load cell readings and the base reactions computed by the finite element analysis made in the form of force coefficients shows good agreement. Discrepancies were somehow higher than those of pressure coefficients comparison but, in general, the trends were similar.

- Load cell readings data were very difficult to analyze. The lack of constant direction full-scale records was the main reason for most of the comparison differences.

7.3 RECOMMENDATIONS FOR FURTHER STUDY

The next step of this research project is to continue the full-scale monitoring and to create a more sophisticated finite element model to include possible nonlinearities of the test building. The finite element analysis, as well as the wind tunnel testing, are very powerful tools which can continuously improve. Another interesting part of the future work is the installation of partition and openings on the test building. These non structural elements can affect the behavior of the structure, without knowing at this point, the degree of this influence.

It should be also mentioned that in the near future the roof load cells will be operational to record the internal stresses in the roof to wall intersection. These recordings will provide data about the load distribution and eventually will assist to define the paths, which the external applied loads follow through the structural form in order to be transferred to the ground. The determination of these load paths will also lead to a better understanding of the response of the building and the effect of the natural damping of a wooden structure. Peak response of the structure should also be evaluated in detail. Both wind pressure and internal force distribution, need to be examined and defined during peak wind incidents. The real objective in structural design is to assess the behavior of structures during strong winds.

REFERENCES

ASCE/SEI 7-05 (2005) Minimum Design Loads for Building and Other Structures, American Society of Civil Engineers, New York, N.Y.

CAMBELL SCIENTIFIC INC, 05103, 05106 and 05305 R. M. Young Wind Monitors, Instruction Manual, Revision: 11/05

Cochran L. S. and Cermak J. E., 1992, Full- and model-scale cladding pressures on the Texas Tech University experimental building, Journal of Wind Engineering and Industrial Aerodynamics, 41-44, pp. 1589-1600

Computers and Structures, Inc. (CSI), 1997, SAP®2000, Integrated Structural Analysis and Design Software. CSI, Berkeley, CA, USA

Computers and Structures, Inc. (CSI), 1998, SAP®2000, Basic Analysis Reference, CSI, Berkeley, CA, USA

Doudak G., Ghallagher A., Kasal B., McClure G., Mohammad M., Smith I., Stathopoulos T., Zisis I., 2005a, Towards wind load paths on wood buildings, EACWE4, The Fourth European & African Conference on Wind Engineering, Prague, Paper #285

Doudak G., McClure G., Smith I., Hu L. and Stathopoulos T., 2005b, Monitoring Structural Response of a Wooden Light-Frame Industrial Shed Building to Environmental Loads, Journal of Structural Engineering, ASCE, Volume 131, No. 5, pp. 794-805

Doudak G., 2005c, Field Determination and Modelling of Load Paths in Wood Light-Frame Structures, PhD Thesis, Department of Civil Engineering and Applied Mechanics, McGill University, Montreal, Canada

Eaton K. J. and Mayne J. R., 1975, The Measurement of Wind Pressures on Two-Storey Houses at Aylesbury, Journal of Wind Engineering and Industrial Aerodynamics, Volume 1, No. 1, pp. 67-109

Eaton K. J., Mayne J. B. and Cook N. J., 1976, Wind Loads on Low-Rise Buildings - Effects of Roof Geometry, Building Research Establishment Current Paper 1/76

Environment Canada Weather Office, Natural Resources Canada (NRC)

Levitan M. L. and Mehta K. C., 1992a, Texas Tech field experiments for wind loads part 1: building and pressure measuring system, Journal of Wind Engineering and Industrial Aerodynamics, Volume 41-44, pp. 1565-1576

Levitan M. L. and Mehta K. C., 1992b, Texas Tech field experiments for wind loads part II: meteorological instrumentation and terrain parameters, Journal of Wind Engineering and Industrial Aerodynamics, Volume 41-44, pp. 1577-1588

Liu H., Wind Engineering: A Handbook for Structural Engineers, Prentice Hall, New Jersey, 1991

Okadaa H. and Hab Y. C., 1992, Comparison of Wind Tunnel and Full-Scale Pressure Measurement Tests on the Texas Tech Building, Journal of Wind Engineering and Industrial Aerodynamics, Volume 41-44, pp. 1601-1612

Richardson G.M. and Surry D., 1991,Comparisons of Wind-Tunnel and Full-Scale Surface Pressure Measurements on Low-Rise Pitched-Roof Buildings, Journal of Wind Engineering and Industrial Aerodynamics, Volume 38, pp. 249-256

Richardson G.M. and Surry D., 1992, The Silsoe Building: A Comparison of Pressure Coefficients and Spectra at Model and Full-Scale, Journal of Wind Engineering and Industrial Aerodynamics, Volume 41-44, pp. 1653-1664

Richardson G.M. and Surry D., 1994, The Silsoe Structures Building: Comparison between Full-Scale and Wind-Tunnel Data, Journal of Wind Engineering and Industrial Aerodynamics, Volume 51, pp. 157-176

Richardson G.M. and Blackmore P.A., 1995, The Silsoe Structures Building: Comparison of 1:100 Model-Scale Data with Full-Scale Data, Journal of Wind Engineering and Industrial Aerodynamics, Volume 57, pp. 191-201

Richardson G.M., Hoxey R.P., Robertson A.P., Short J.L., 1997, The Silsoe Structures Building: Comparisons of Pressures Measured at Full-Scale and in two Wind Tunnels, Journal of Wind Engineering and Industrial Aerodynamics, Volume 72, pp. 187-197

Rofeil, A.W., 1995, Full-Scale / Model Scale Comparisons of Wind Pressures on the TTU Building, 9th International Conference on Wind Engineering (ICWE), New Delhi, India

R. M. YOUNG COMPANY, 05103Model 61202L Barometric pressure Sensor, Instruction Manual, October 2001

Scanivalve Corporation, ZOC 33/64Px – Electronic Pressure Scanning Module, Instruction and Service Manual

Scanivalve Corporation, DSMLINK V2.90, Installation and Operation Manual

Scanivalve Corporation, DSM 3000 – Digital Service Module, Instruction and Service Manual

Sill, B.L., Cook N.J. and Blackmore P.A., 1989, IAWE Aylesbury Comparative Experiment - Preliminary Results of Wind Tunnel Comparisons, Journal of Wind Engineering and Industrial Aerodynamics, Volume 32, pp. 285-302

Sill B.L., Cook N.J. and Fang C., 1992, The Aylesbury Comparative Experiment: A Final Report, Journal of Wind Engineering and Industrial Aerodynamics, Volume 41-44, pp. 1553-1564

Simiu E. and Scanlan R. H., 1996, Wind Effects on Structures: Fundamentals and Applications to Design, John Wiley & Sons, New York

Stathopoulos T., 1984, Design and Fabrication of a Wind Tunnel for Building Aerodynamics, Journal of Wind Engineering and Industrial Aerodynamics, Volume 16, pp. 361-376

Tieleman H.W., Surry D., Mehta K.C., 1996, Full/model-scale comparison of surface pressures on the Texas Tech experimental building, Journal of Wind Engineering and Industrial Aerodynamics, Volume 61, pp. 1-23

Tieleman H.W., Hajj M.R., Reinhold T.A., 1998, Wind Tunnel Simulation Requirements to assess wind loads on low-rise buildings, Journal of Wind Engineering and Industrial Aerodynamics, Volume 74-76, pp. 675-685

VISHAY, StrainSmart Software Specification/Features Version 3.1, Bulletin 256S, Vishay Measurements Group

VISHAY, System 5000 Hardware Specifications, Bulletin 257H, Vishay Measurements Group

BIBLIOGRAPHY AND OTHER SOURCES

Apperley L., Surry D., Stathopoulos T. and Davenport A. G., 1978, Comparative Measurements of Wind Pressure on a Model of the Full-Scale Experimental House at Aylesbury, England, Journal of Wind Engineering and Industrial Aerodynamics, Volume 4, pp. 207-228

ASCE 7-95 (1995) Minimum Design Loads for Building and Other Structures, American Society of Civil Engineers, New York, N.Y.

Chopra A., Dynamics of Structures: Theory and Applications to Earthquake Engineering, Prentice Hall, New York, 2000

CMHC-SCHL, Canadian Wood-Frame House Construction, Canadian Mortgage and Housing Corporation, 2003

National Building Code of Canada 1995. National Research Council of Canada, Ottawa

Smith I., Mohammad M., and Dick K., 2004, Structural monitoring of timber buildings: overview of work in Canada, 8th World Conference on Timber Engineering, Lahti, Finland

Stathopoulos T., 1985, Wind Loads on Low-Rise Buildings: A Review of the State of the Art, Engineering Structures, Volume 6, No. 2, pp. 119-135

Surry D., and Stathopoulos T., 1978, An Experimental Approach to the Economical Measurement of Spatially-Averaged Wind Loads, Journal of Wind Engineering and Industrial Aerodynamics, Volume 2, pp.385-397

Surry D., 1992, Wind Tunnel Simulation of the Texas Tech Building, Journal of Wind Engineering and Industrial Aerodynamics, Volume 41-44, pp. 1613-1614

Vickery P. J. and Surry D., 1983, The Aylesbury Experiments Revisited -Further Wind Tunnel Tests and Comparisons, England, Journal of Wind Engineering and Industrial Aerodynamics, Volume 11, pp. 39-62

APPENDIX A

Appendix A includes:

- Mean, minimum and maximum pressure coefficient results based on wind tunnel model test. The examined wind directions are: 20°, 60°, 90°, 110°, 150°, 180°, 200°, 225°, 240°, 255°, 270°, 290°, 315° and 340° are shown in Figure A.1.

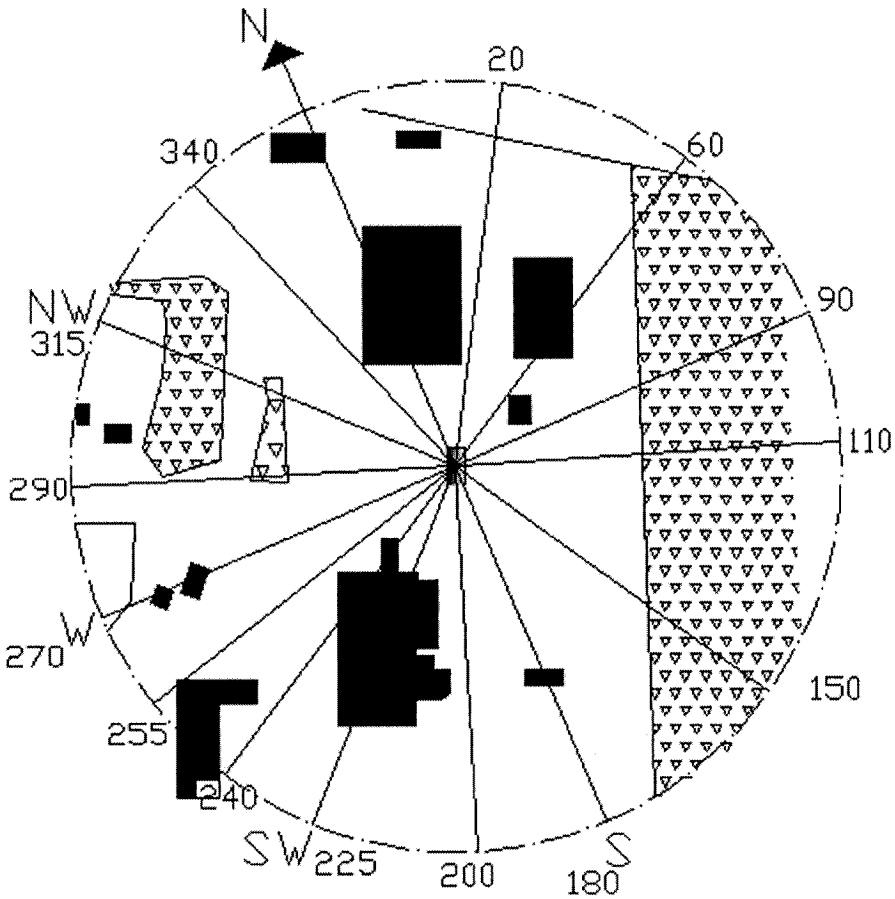

Figure A.1 Wind tunnel directions used in the study

20 DEGREES

Mean Pressure Coefficient

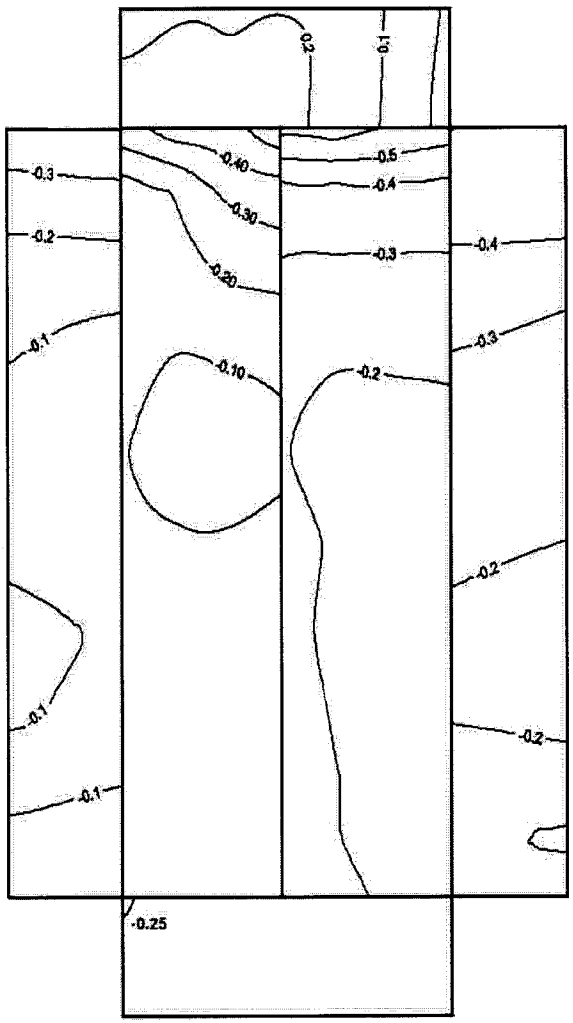

Minimum Pressure Coefficient

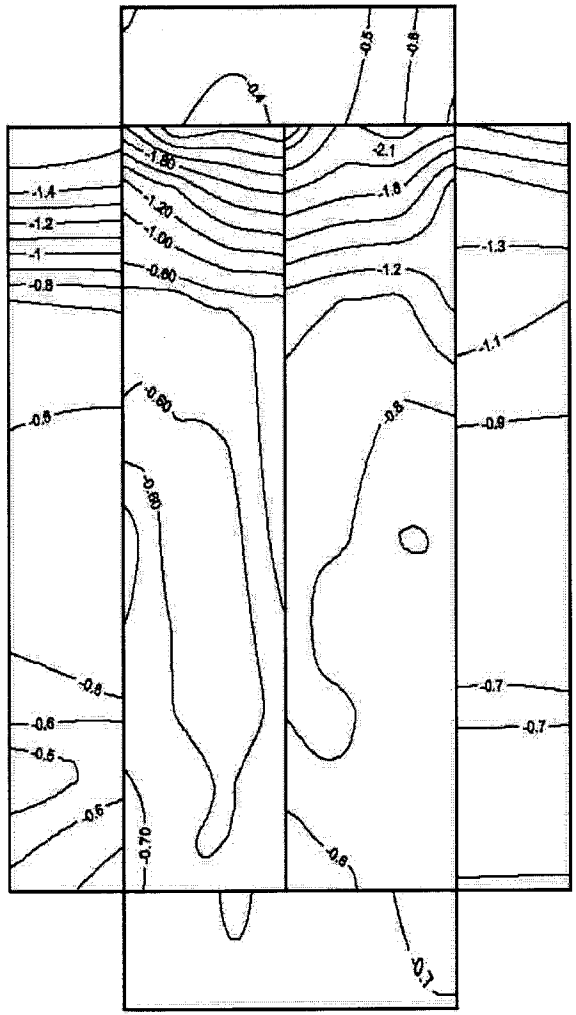

Maximum Pressure Coefficient

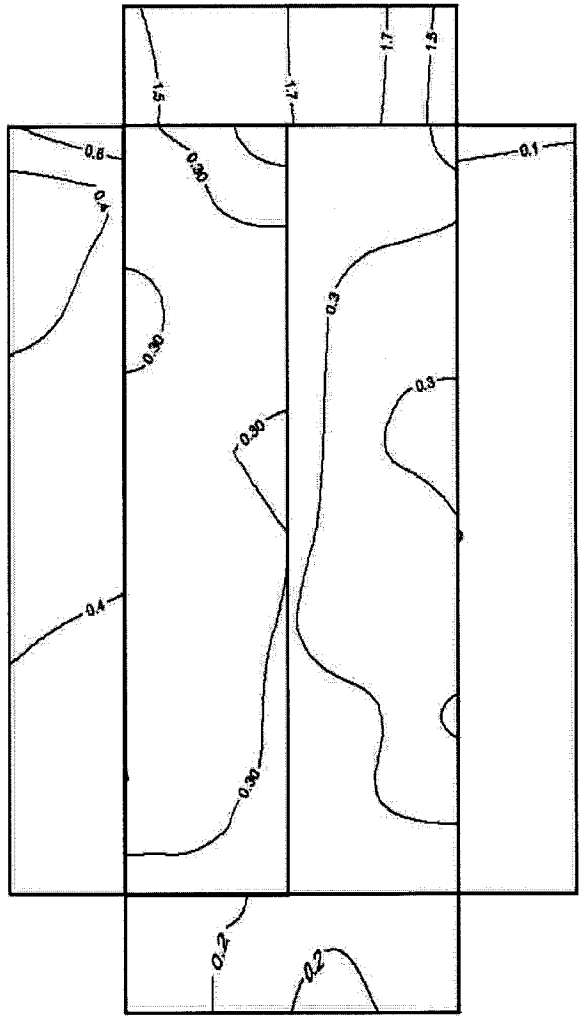

60 DEGREES

Mean Pressure Coefficient

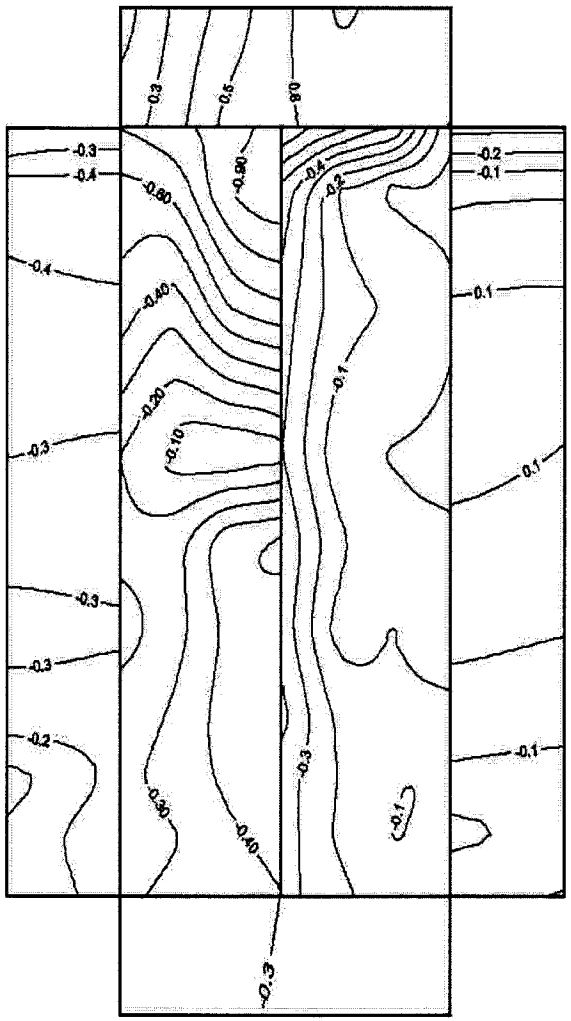

Minimum Pressure Coefficient

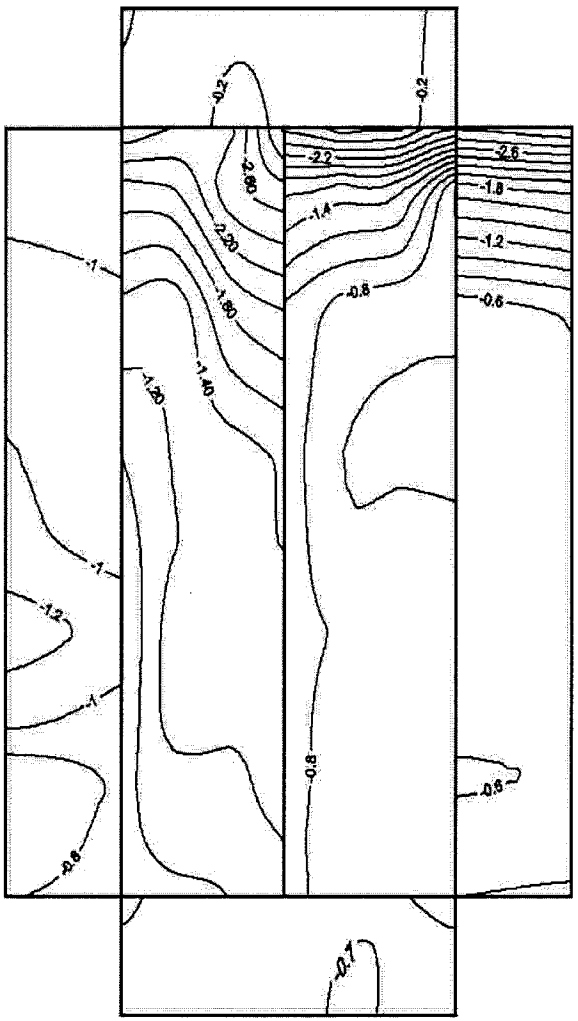

Maximum Pressure Coefficient

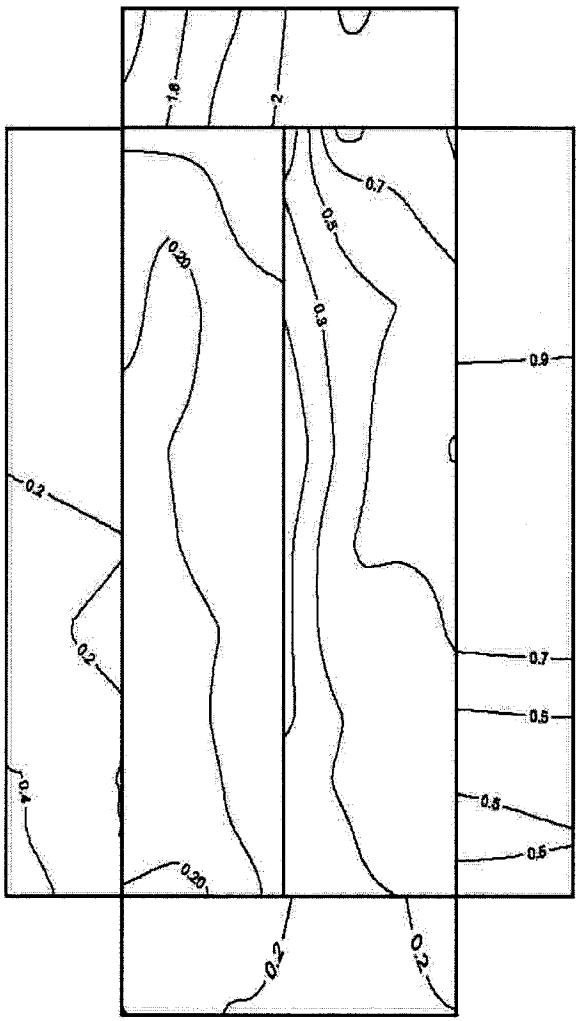

90 DEGREES

Mean Pressure Coefficient

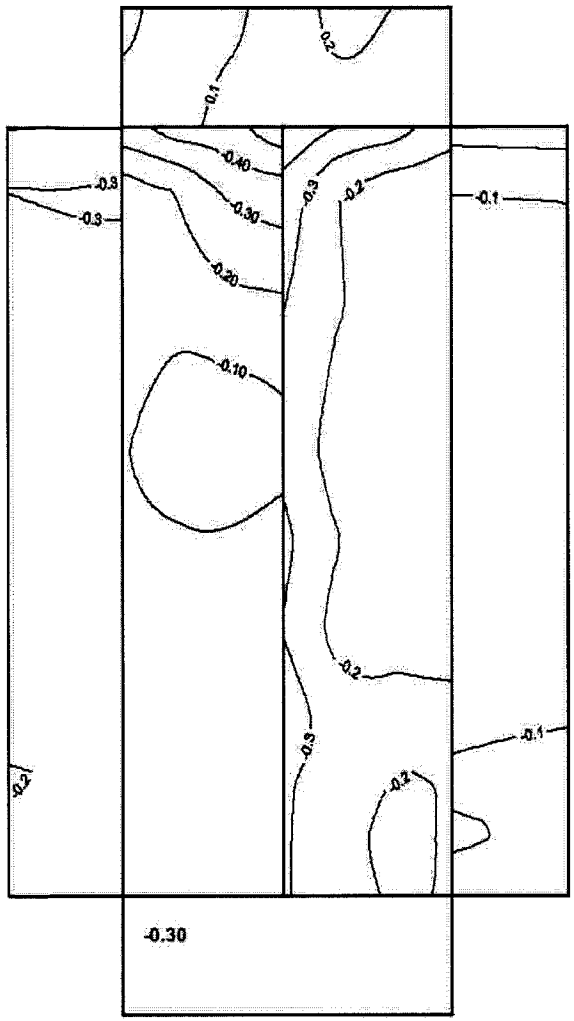

Minimum Pressure Coefficient

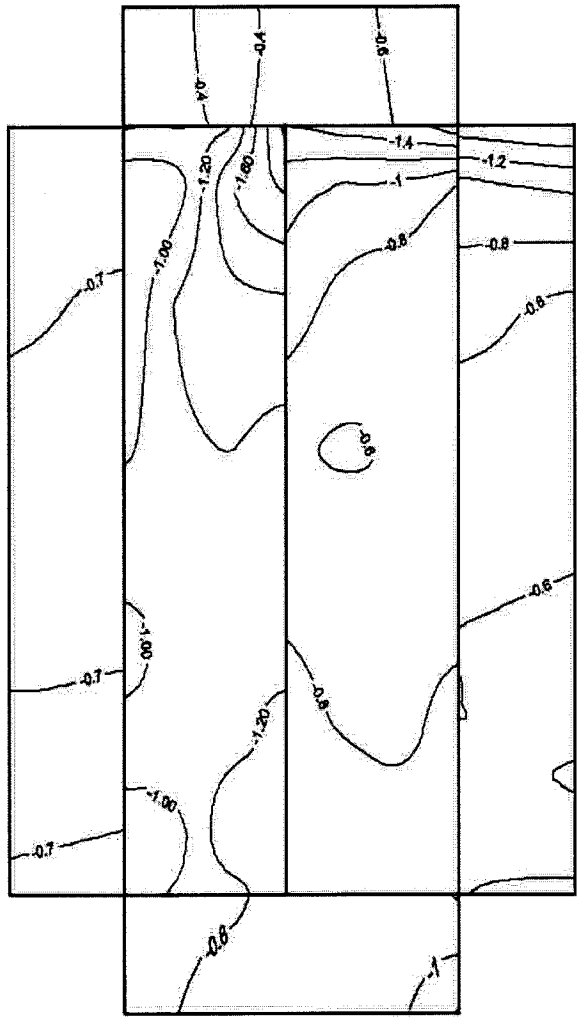

Maximum Pressure Coefficient

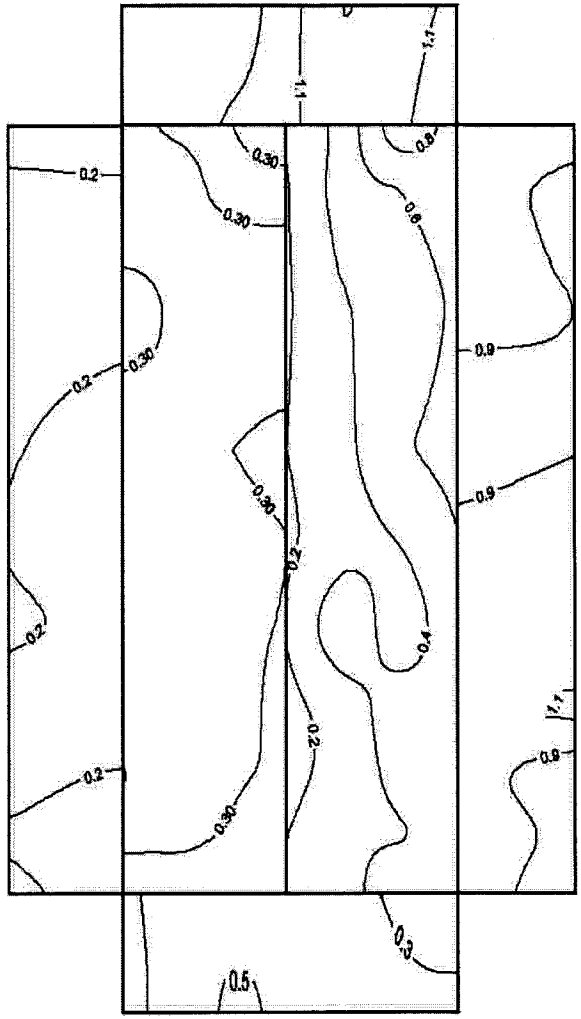

110 DEGREES

Mean Pressure Coefficient

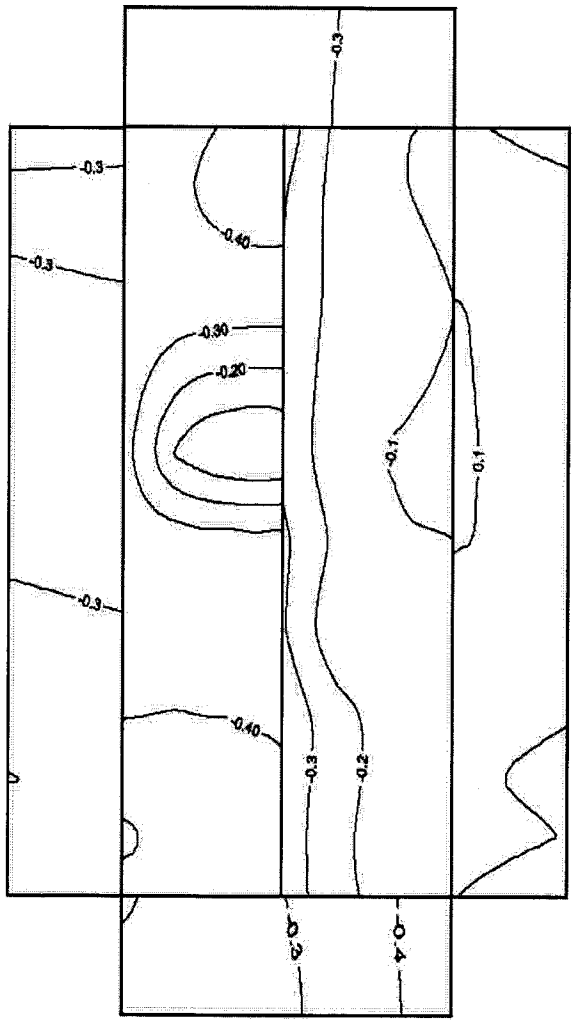

Minimum Pressure Coefficient

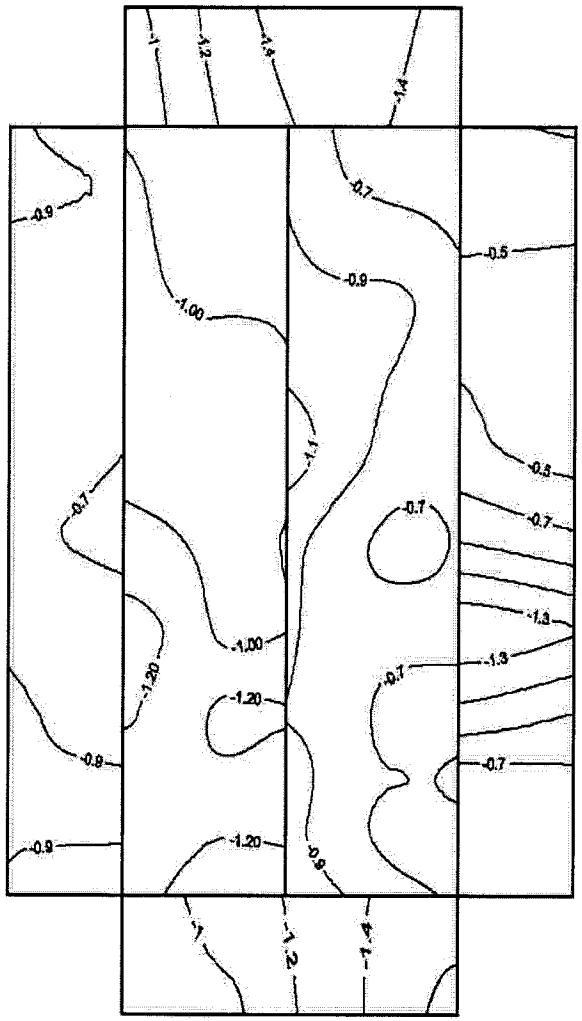

Maximum Pressure Coefficient

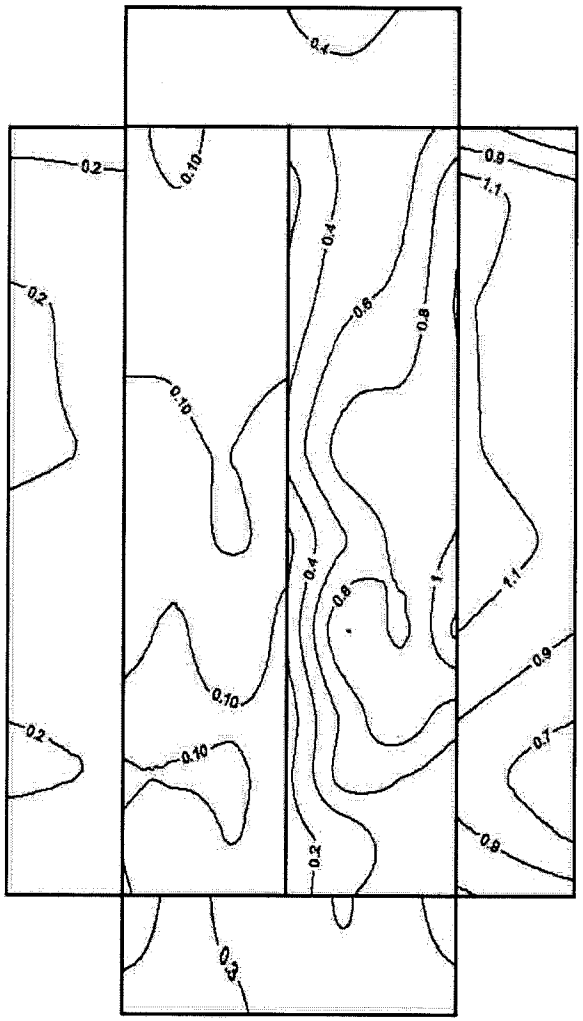

150 DEGREES

Mean Pressure Coefficient

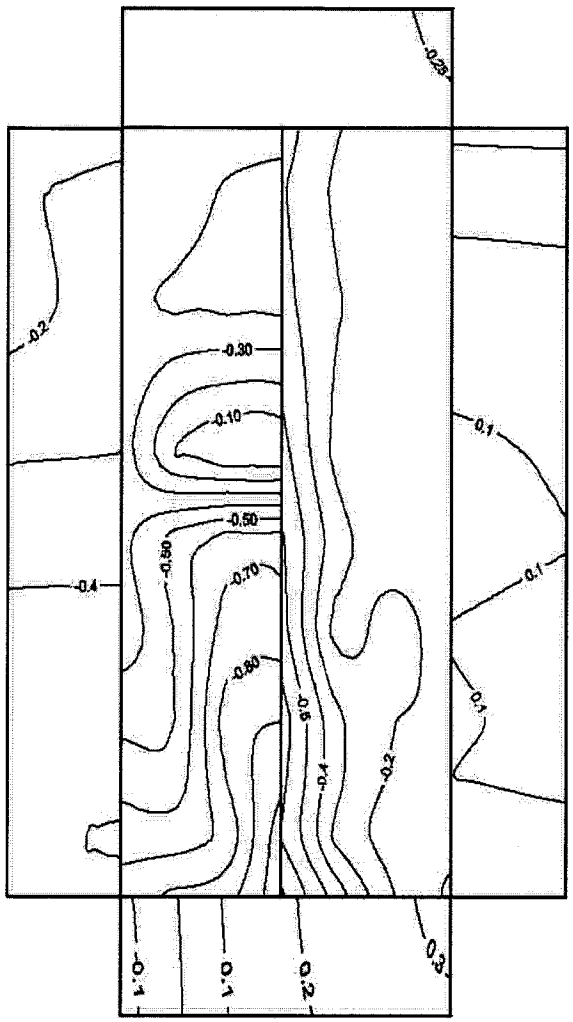

Minimum Pressure Coefficient

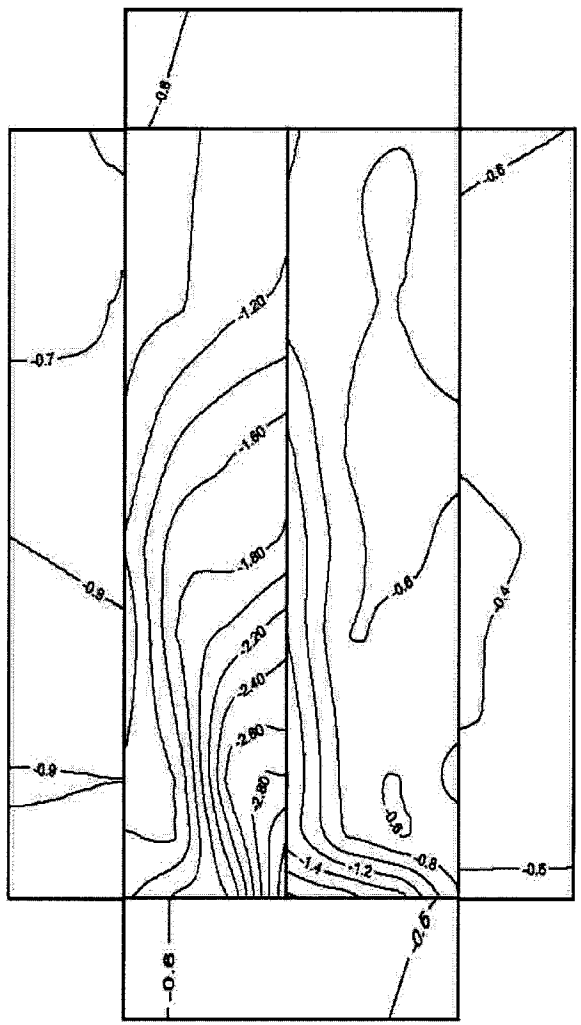

Maximum Pressure Coefficient

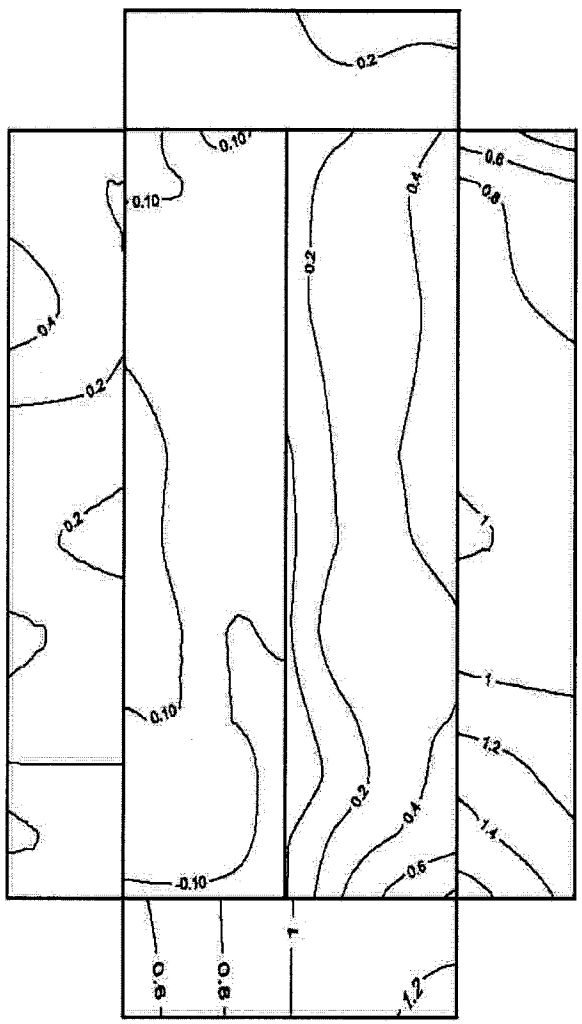

180 DEGREES

Mean Pressure Coefficient

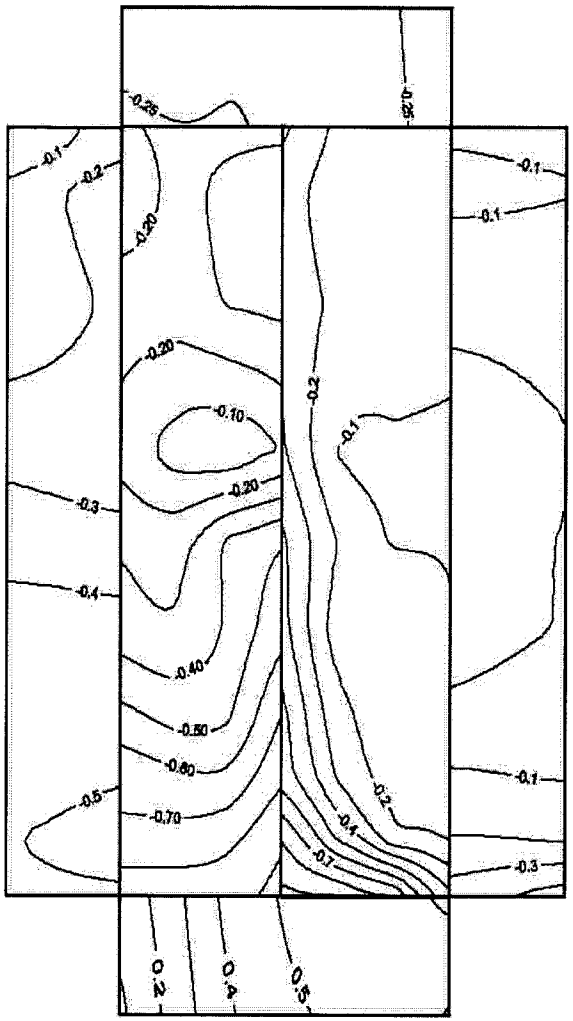

Minimum Pressure Coefficient

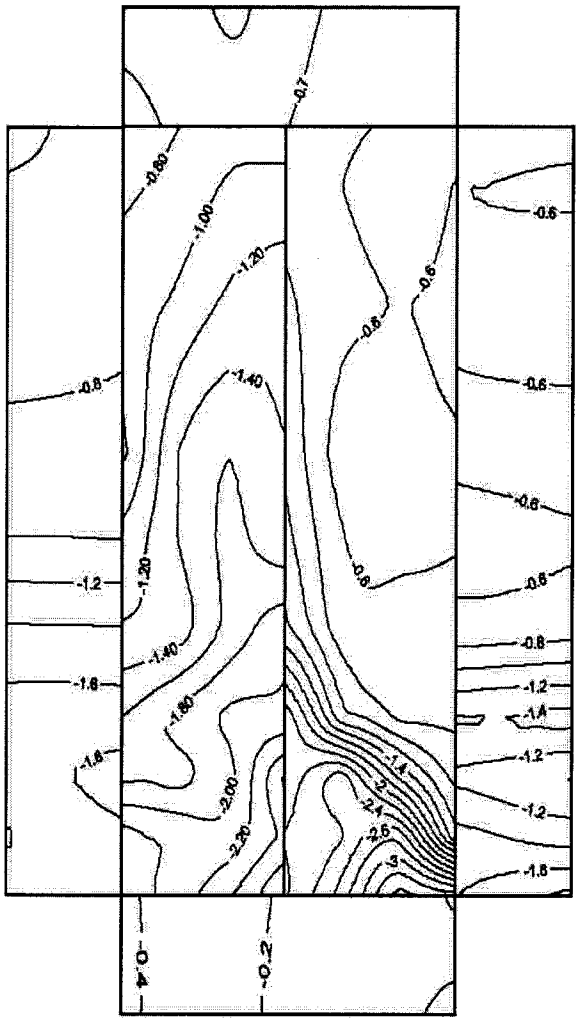

Maximum Pressure Coefficient

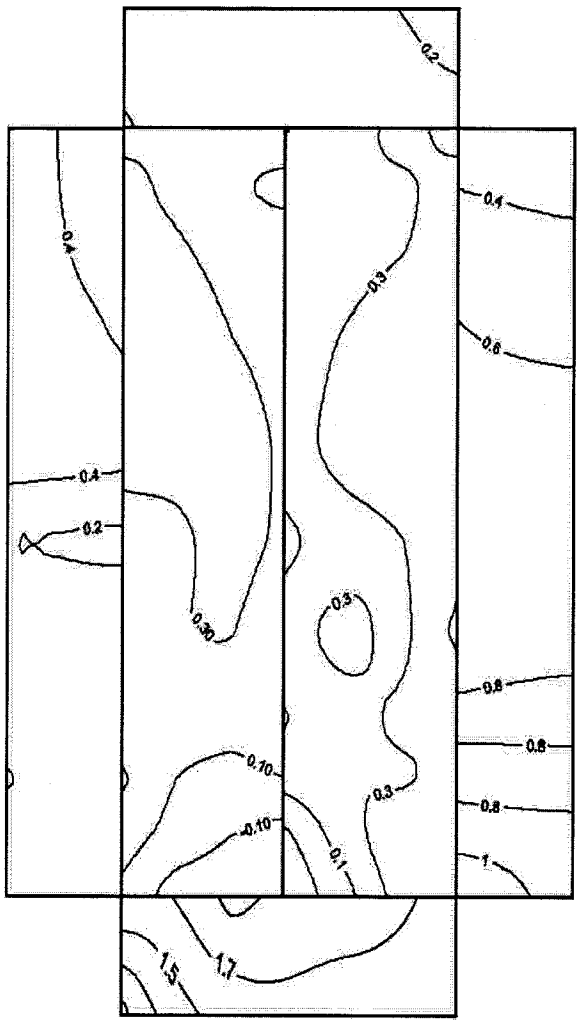

200 DEGREES

Mean Pressure Coefficient

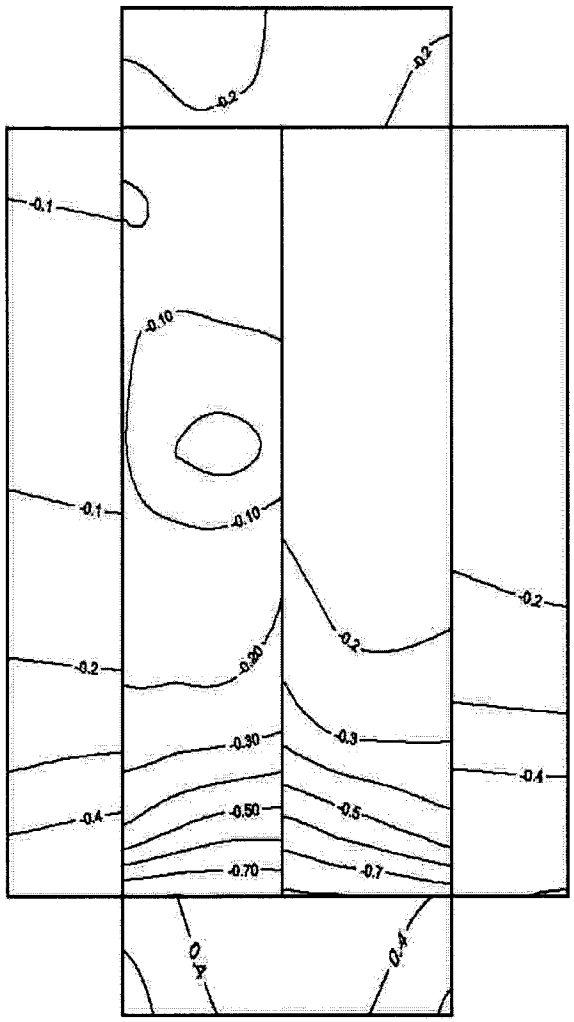

Minimum Pressure Coefficient

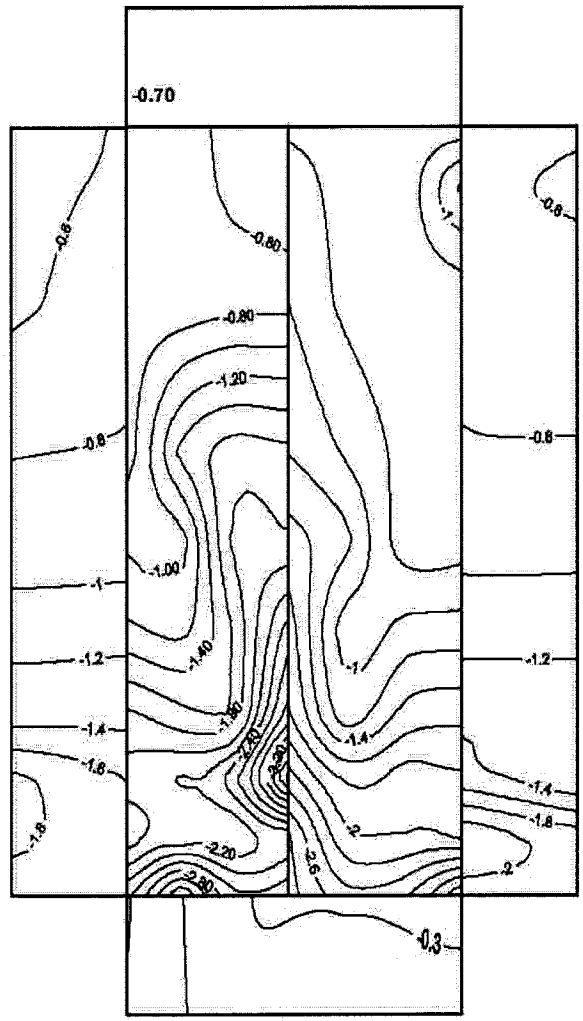

Maximum Pressure Coefficient

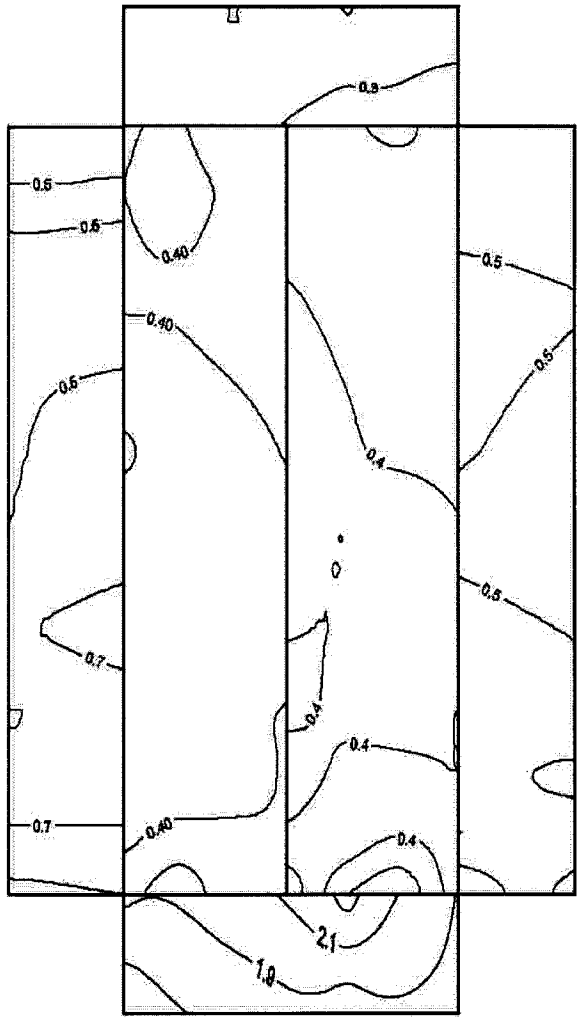

225 DEGREES

Mean Pressure Coefficient

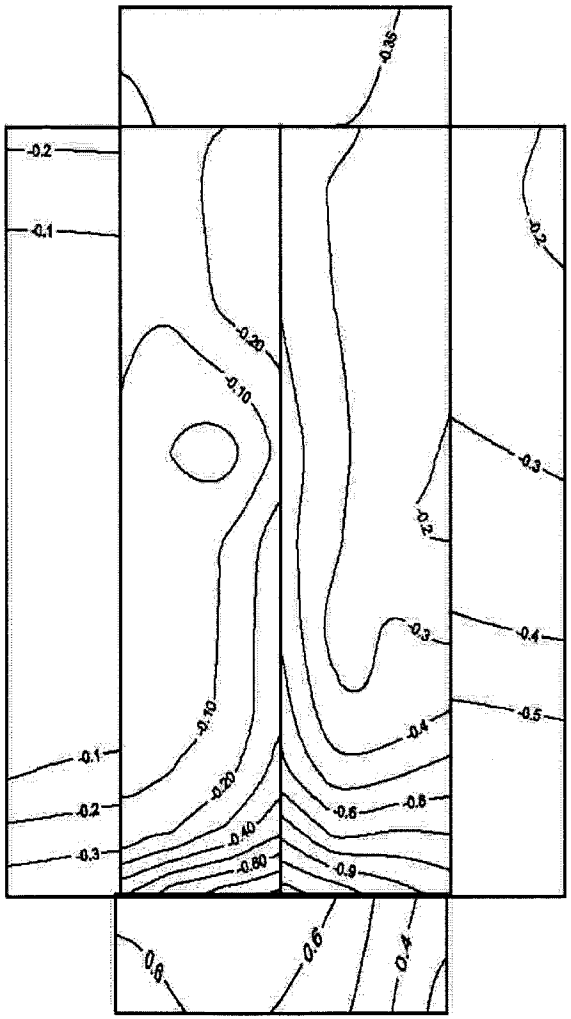

Minimum Pressure Coefficient

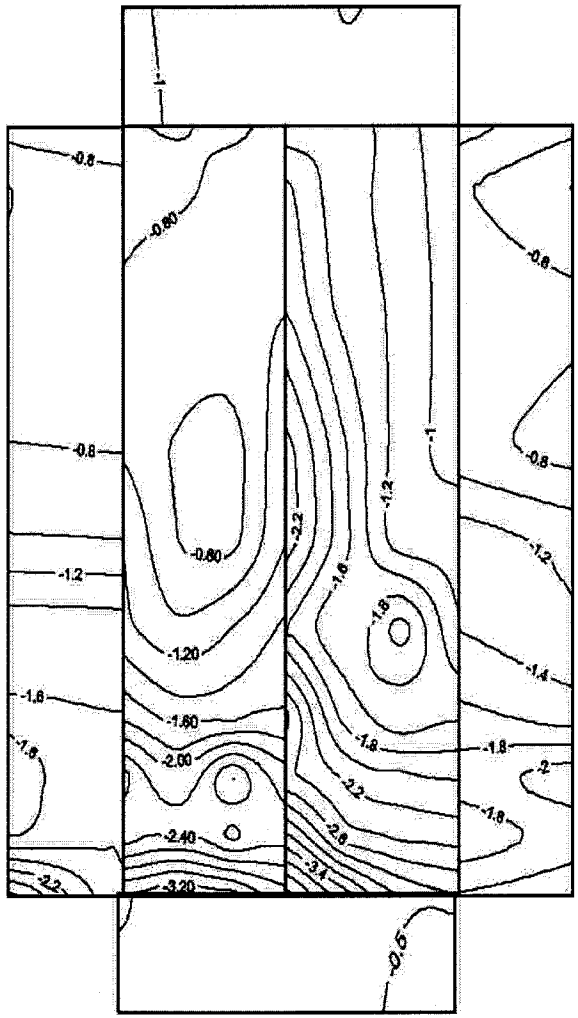

Maximum Pressure Coefficient

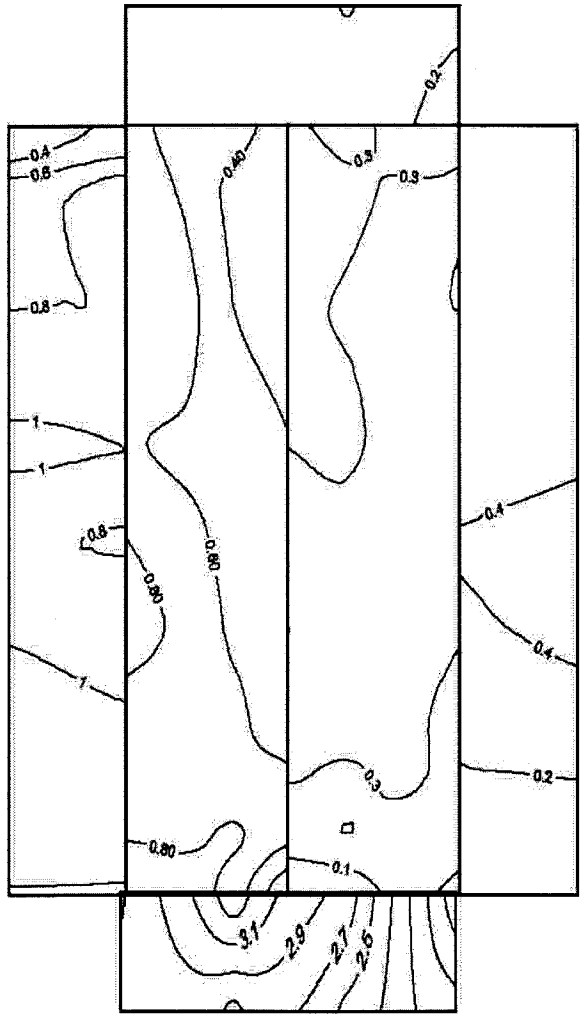

240 DEGREES

Mean Pressure Coefficient

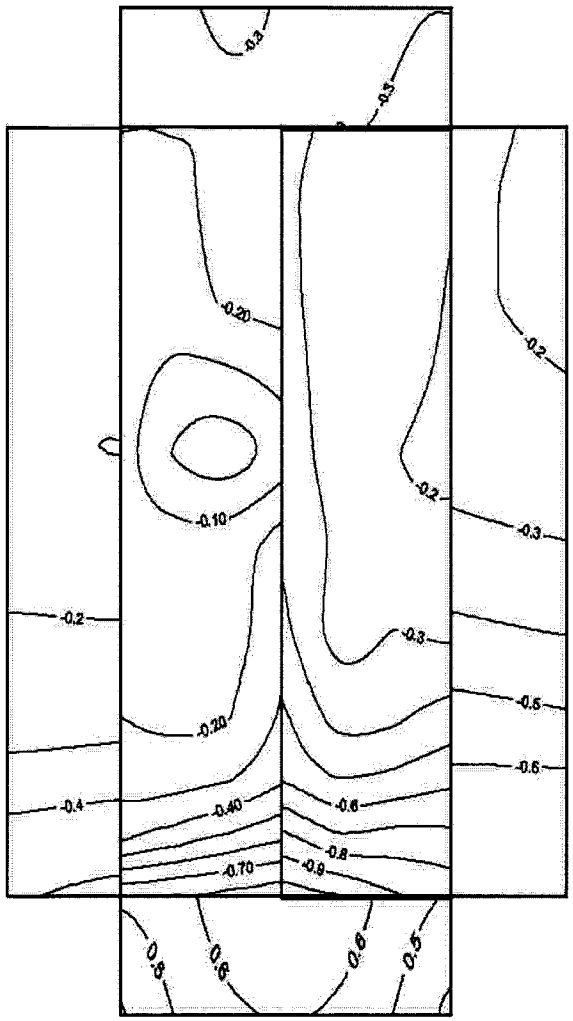

Minimum Pressure Coefficient

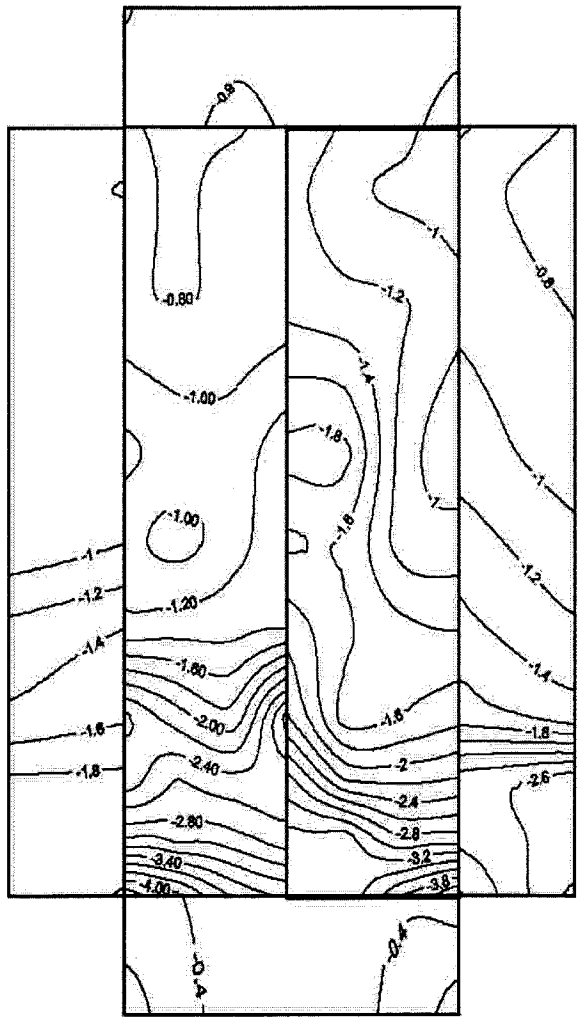

Maximum Pressure Coefficient

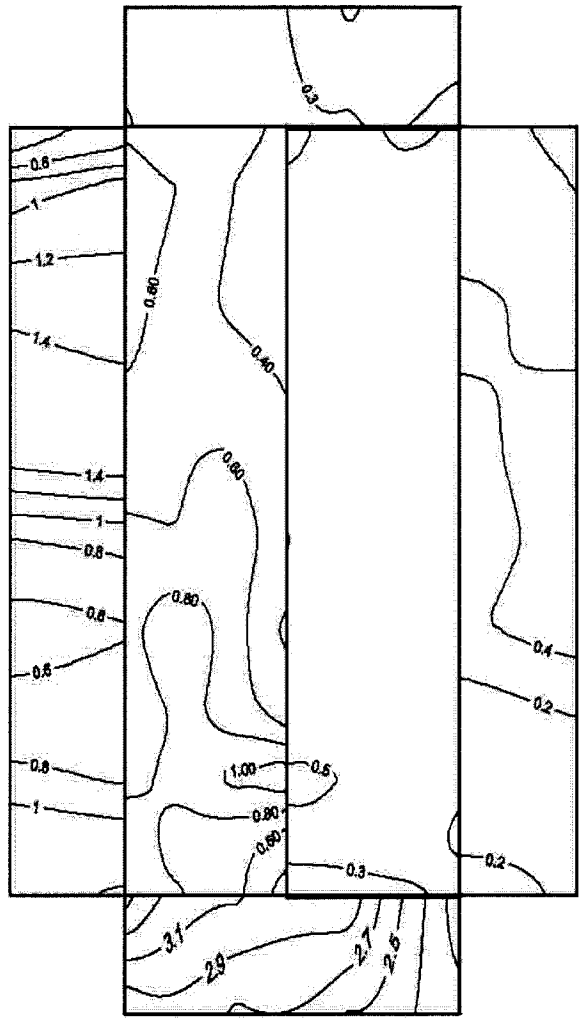

255 DEGREES

Mean Pressure Coefficient

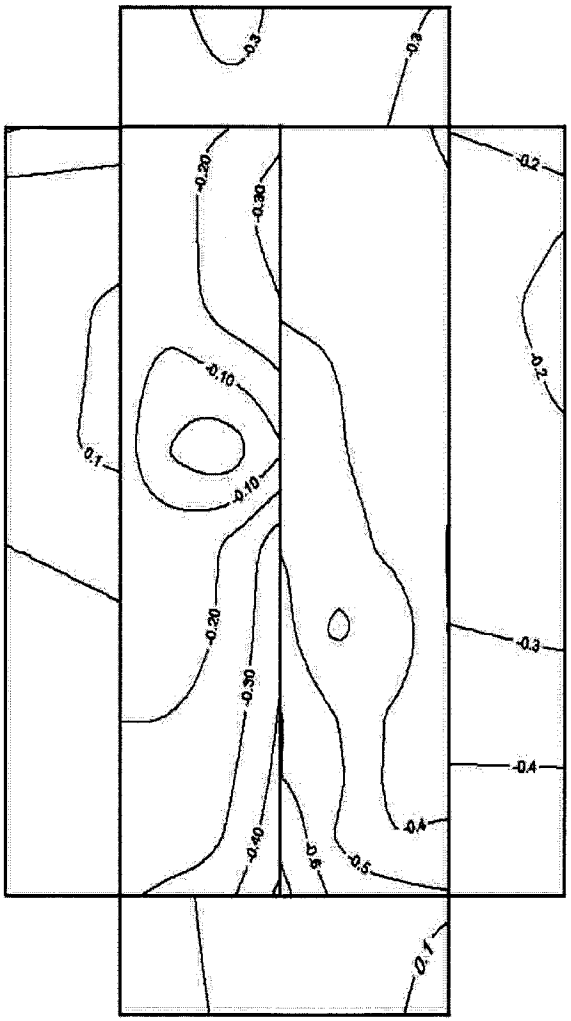

Minimum Pressure Coefficient

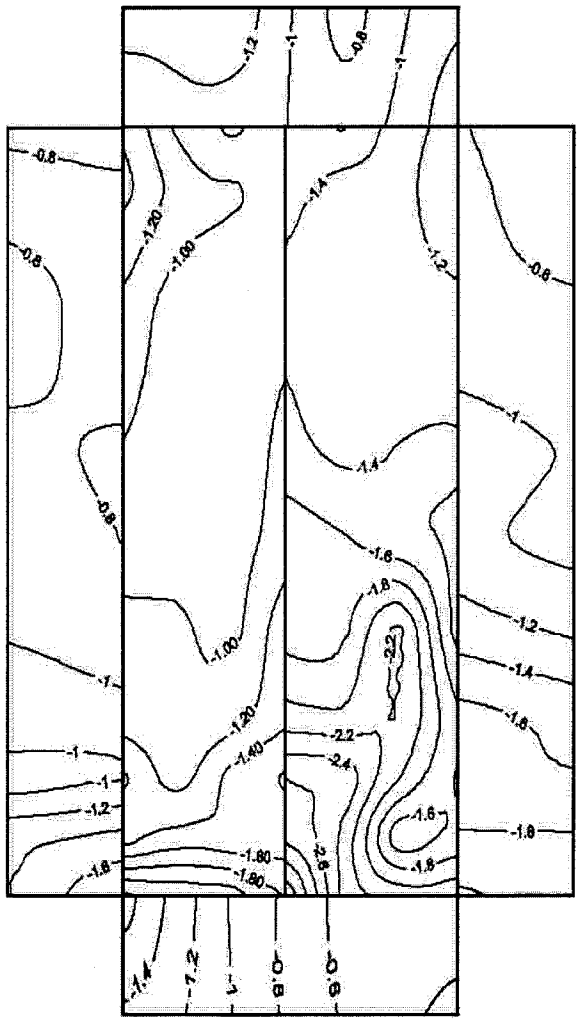

Maximum Pressure Coefficient

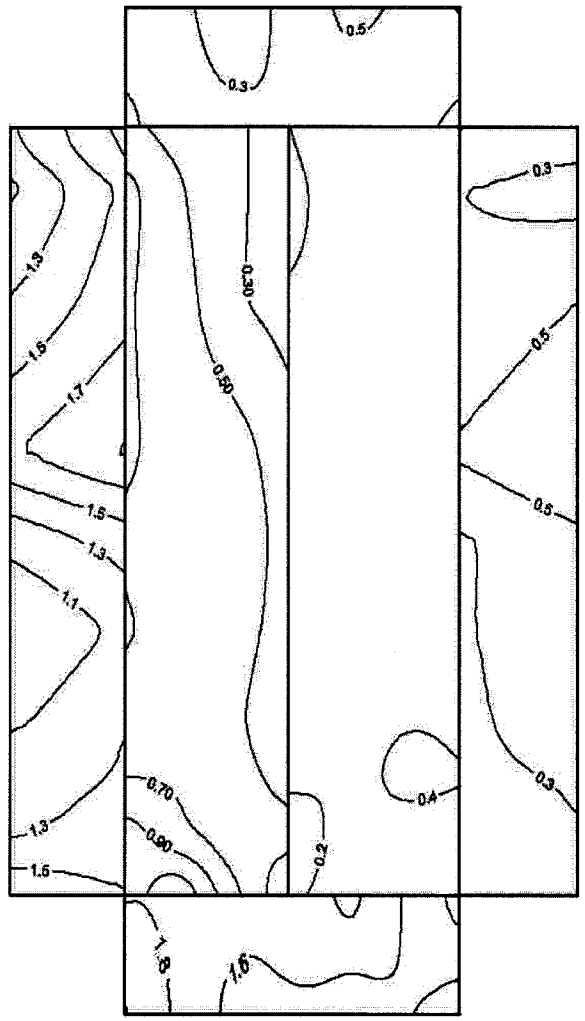

270 DEGREES

Mean Pressure Coefficient

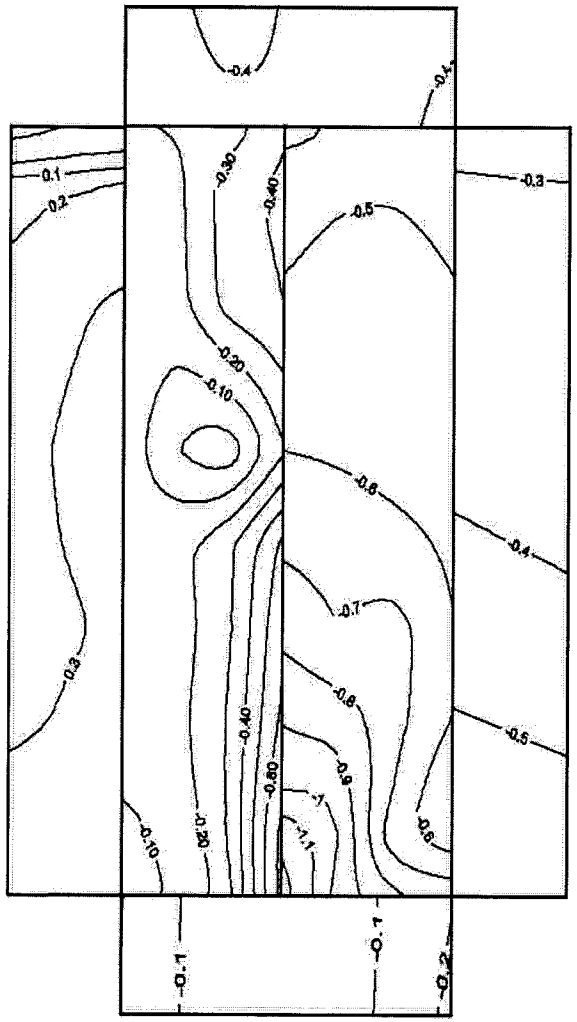

Minimum Pressure Coefficient

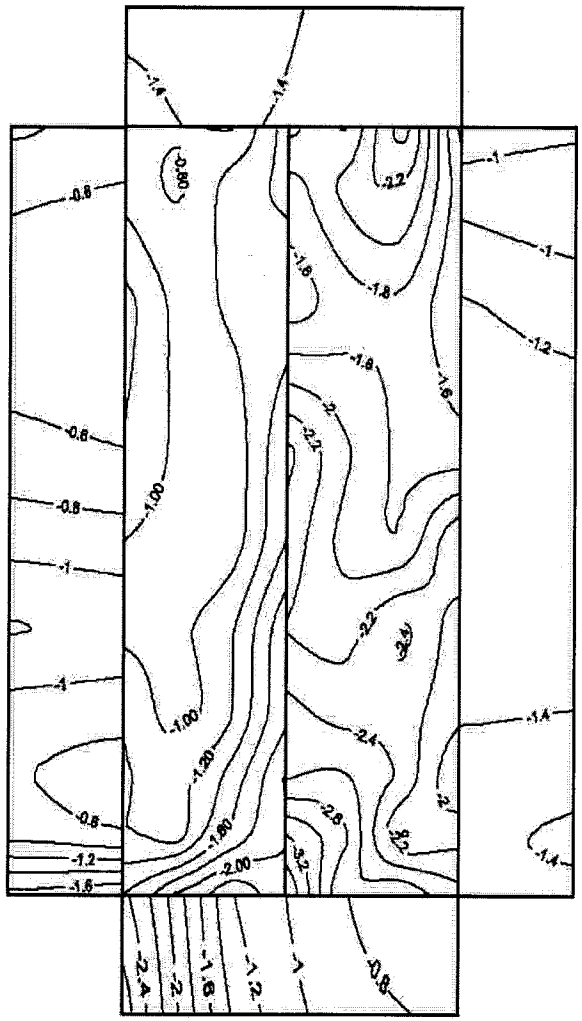

Maximum Pressure Coefficient

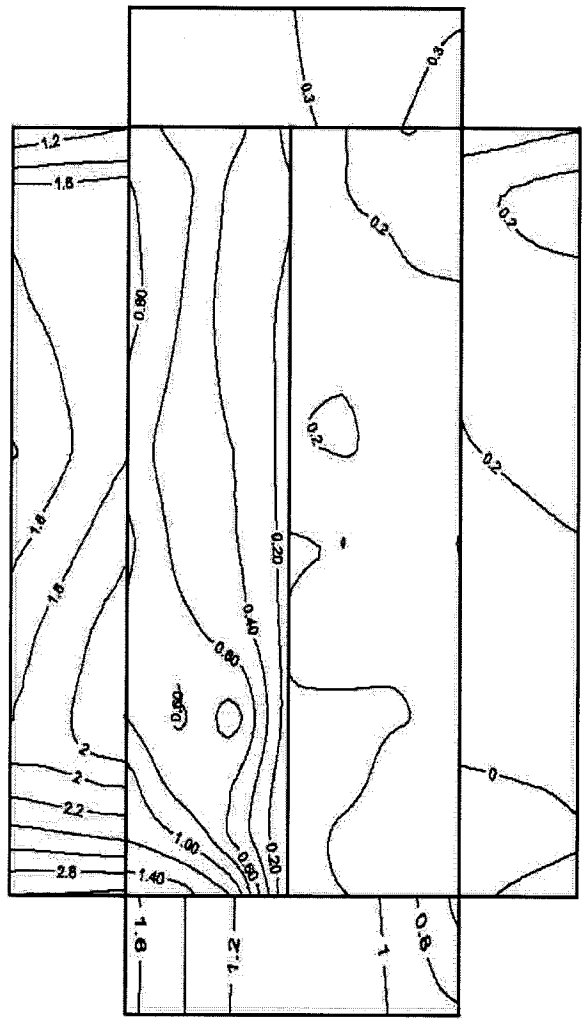

290 DEGREES

Mean Pressure Coefficient

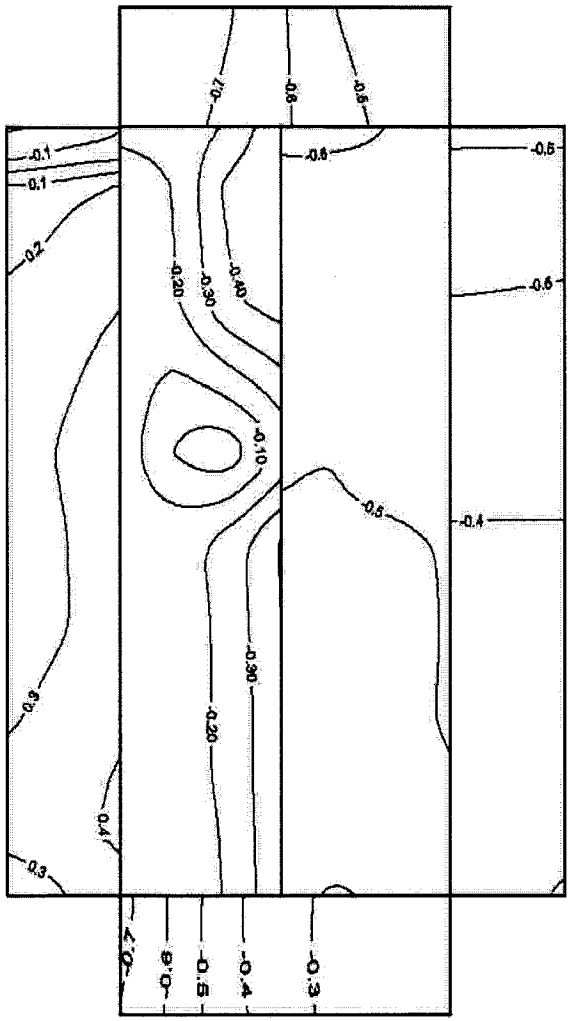

Minimum Pressure Coefficient

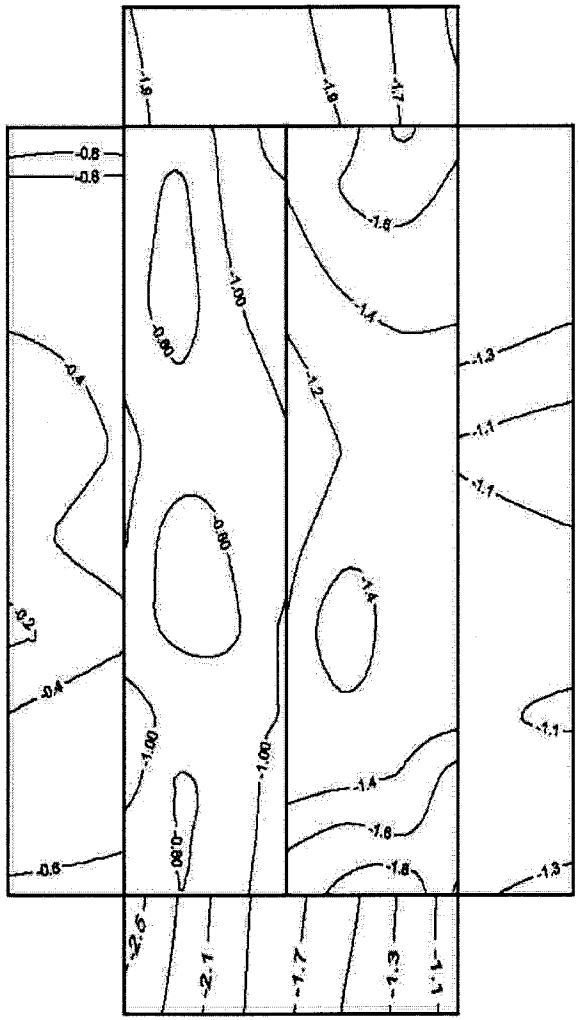

Maximum Pressure Coefficient

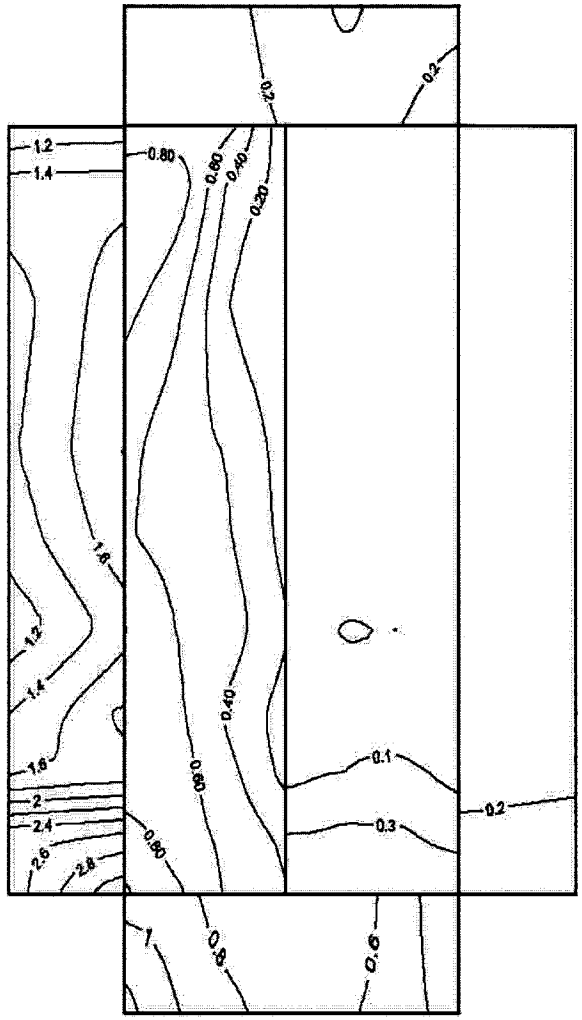

315 DEGREES

Mean Pressure Coefficient

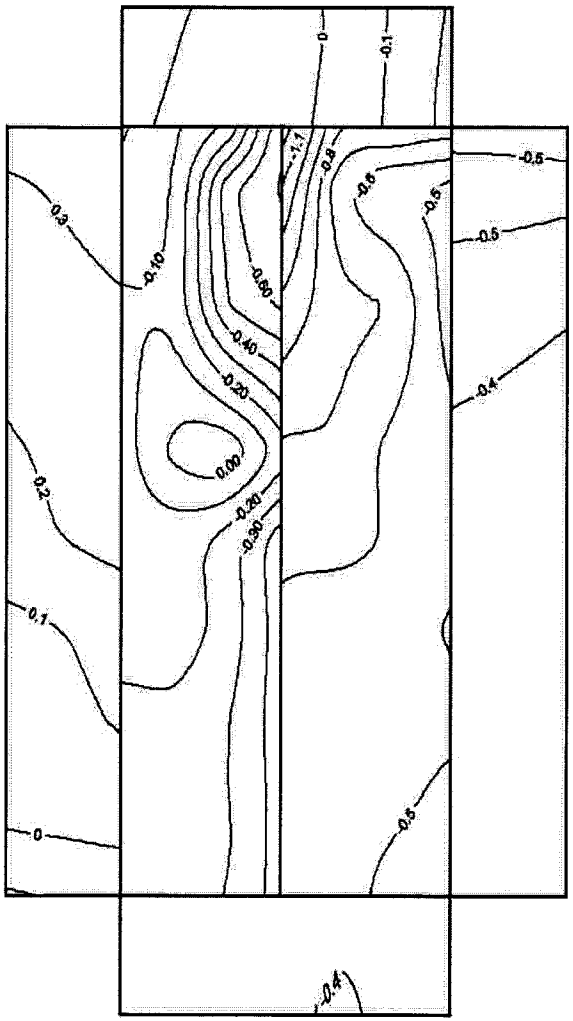

Minimum Pressure Coefficient

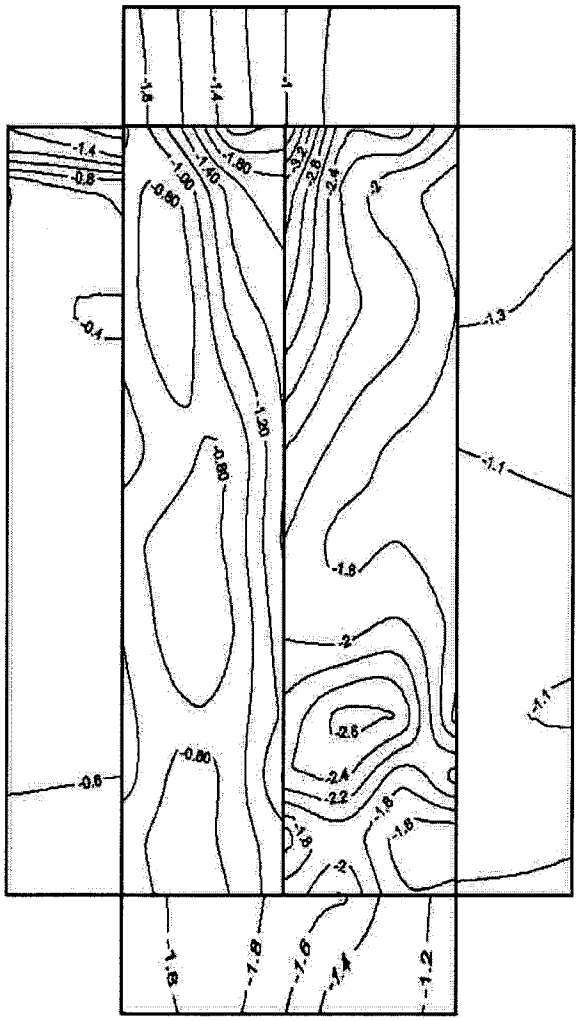

Maximum Pressure Coefficient

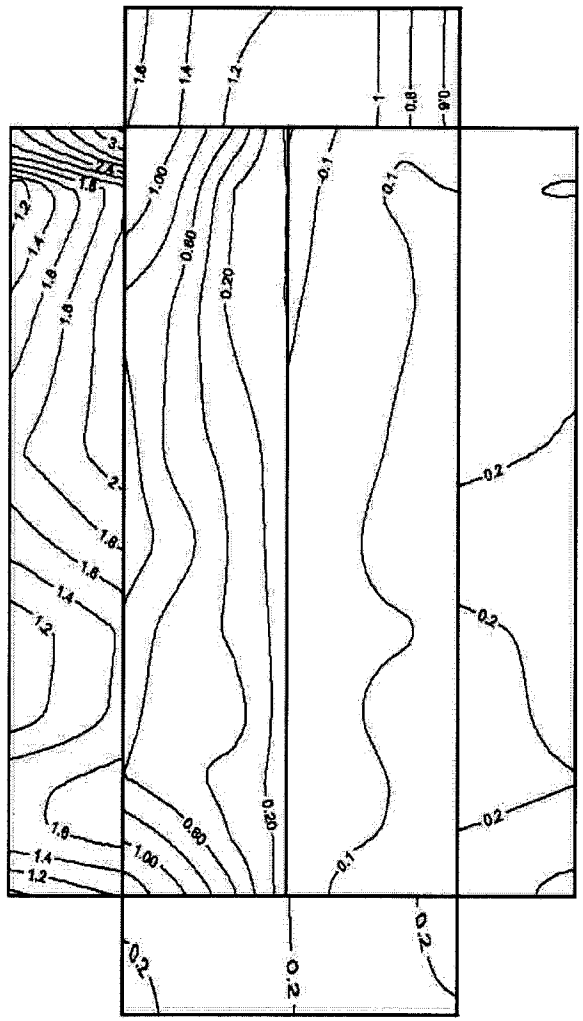

340 DEGREES

Mean Pressure Coefficient

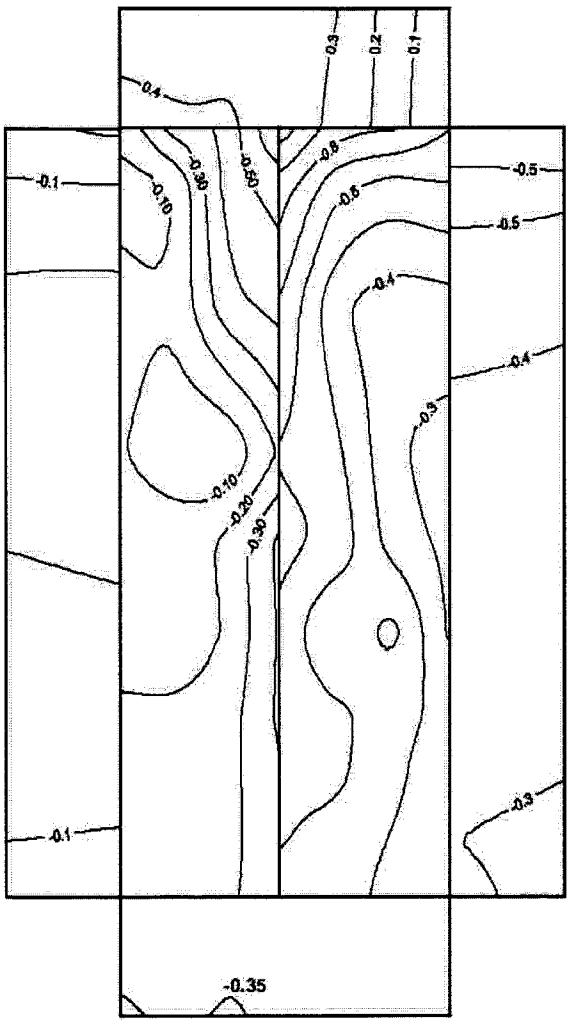

Minimum Pressure Coefficient

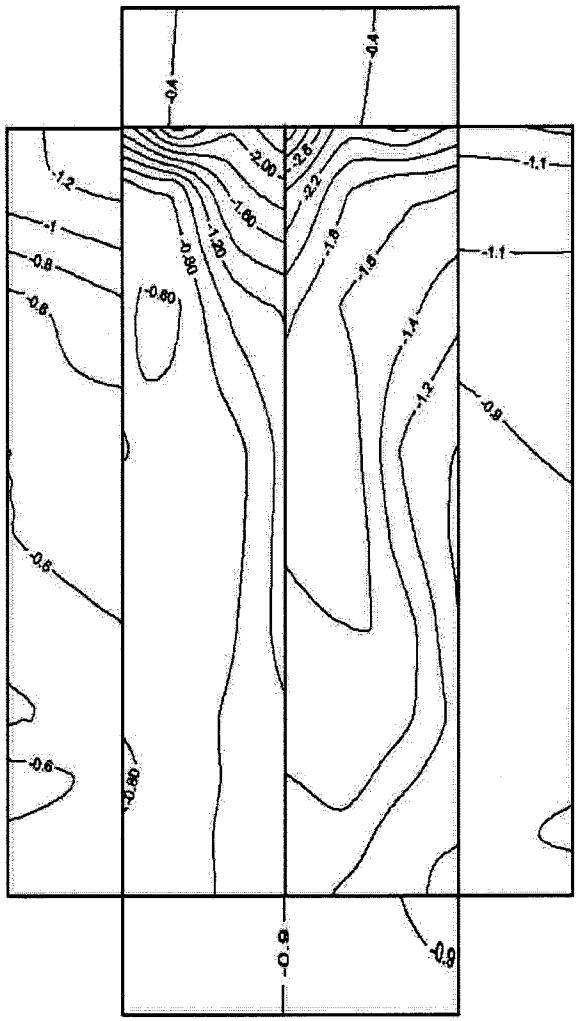

Maximum Pressure Coefficient

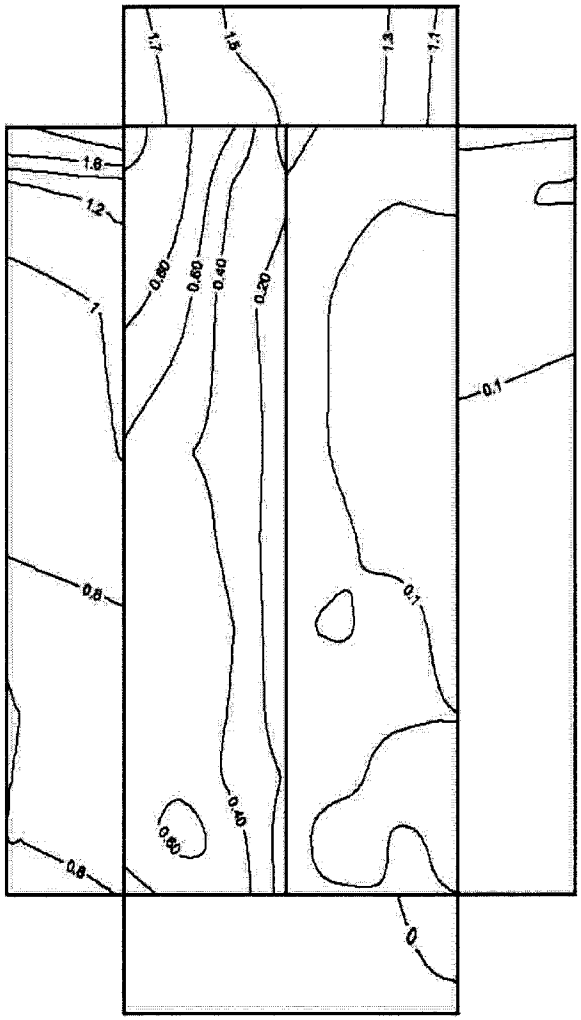

APPENDIX B

The input material, frame and shell properties for SAP2000 analysis (S2K file) are as follows:

MATERIAL

NAME=WOOD1 IDES=N M=.42 W=4.12 E=9500000 U=.3 A=.0000117
NAME=OSB IDES=S M=.6 W=5.886 E=5500000 U=.3 A=.0000117

M: Mass per unit Volume
W: Weight per unit Volume
E: Modulus of Elasticity
U: Poisson's Ratio
A: Coefficient of Thermal Expansion

FRAME SECTION

NAME=3X89X38 MAT=WOOD1 SH=R T=.089, .114 A=.010146 J=1.402084E-05
I=6.697206E-06, 1.098812E-05 AS=.008455,.008455
NAME=38X89 MAT=WOOD1 SH=R T=.038,.089 A=.003382 J=1.191204E-06
I=4.069673E-07, 2.232402E-06 AS=2.818333E-03,2.818333E-03
NAME=89X38 MAT=WOOD1 SH=R T=.089,.038 A=.003382 J=1.191204E-06
I=2.232402E-06, 4.069673E-07 AS=2.818333E-03,2.818333E-03
NAME=2X38X89 MAT=WOOD1 SH=R T=.076,.089 A=.006764 J=6.327345E-06
I=3.255739E-06, 4.464804E-06 AS=5.636666E-03,5.636666E-03
NAME=2X89X38 MAT=WOOD1 SH=R T=.089,.076 A=.006764 J=6.327345E-06
I=4.464804E-06, 3.255739E-06 AS=5.636666E-03,5.636666E-03
NAME=3X38X89 MAT=WOOD1 SH=R T=.114,.089 A=.010146 J=1.402084E-05
I=1.098812E-05, 6.697206E-06 AS=.008455,.008455
NAME=19X89 MAT=WOOD1 SH=R T=.019,.089 A=.001691 J=1.76121E-07
I=5.087092E-08, 1.116201E-06 AS=1.409167E-03,1.409167E-03
NAME=IJOINT MAT=WOOD1 SH=I T=.508,.09,.035,.01,.09,.035 A=.01068
J=2.086138E-06 I=4.230394E-04, 4.289E-06 AS=.00508,.00525
NAME=STPLATE MAT=WOOD1 SH=R T=.038,.089 A=3.382 J=1.191204E-06
I=4.069673E-04, 2.232402E-06 AS=2.818333,2.818333

MAT: Material
SH: Section Type
R: Rectangular
T: Depth, Width
A: Cross-section Area
J: Torsional Constant
I: Moment of Inertia about axis-3, Moment of Inertia about axis-2
AS: Shear Area in direction-2, shear area in direction-3

SHELL SECTION

NAME=WALL	MAT=OSB	TYPE=Membr	TH=.0095
NAME=ROOF	MAT=OSB	TYPE=Membr	TH=.0013

MAT: Material
TYPE: Shell type
TH: Thickness

APPENDIX C

Appendix B includes:

- Mean force coefficients (Cf,x – Cf,y – Cf,z) based on finite element analysis for the following wind directions : 20°, 60°, 90°, 110°, 150°, 180°, 200°, 225°, 240°, 255°, 270°, 290°, and 315°.
- Individual load cell mean force coefficient variation over direction based on finite element analysis.

Mean Force Coefficients based on F-E analysis

20 DEGREES

Cf,x

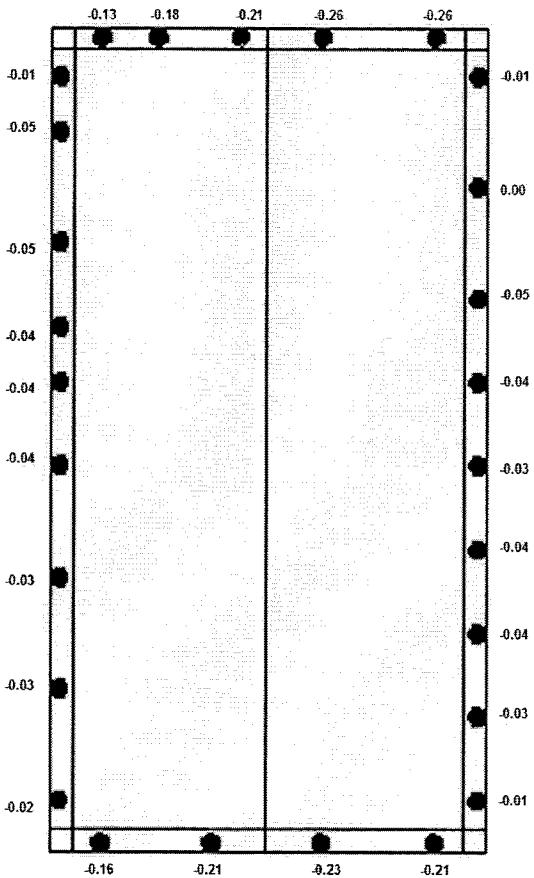

Cf,y

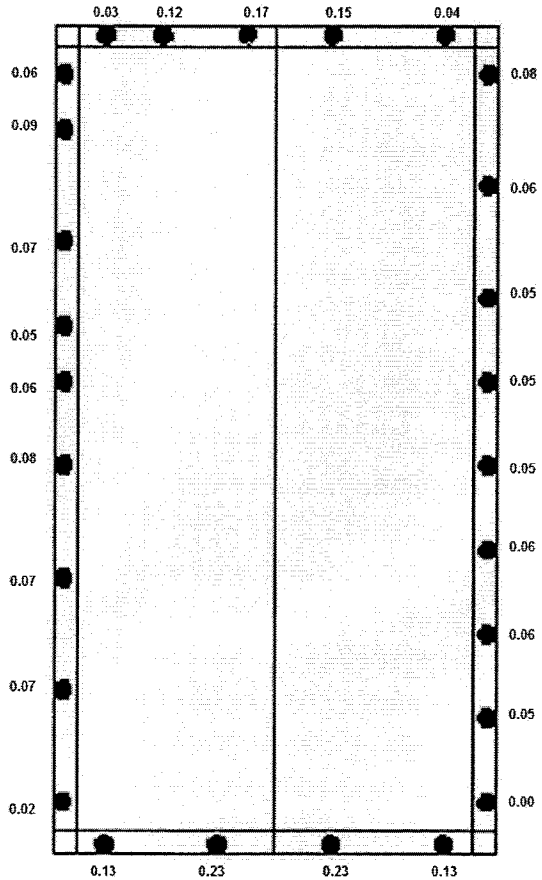

Cf,z

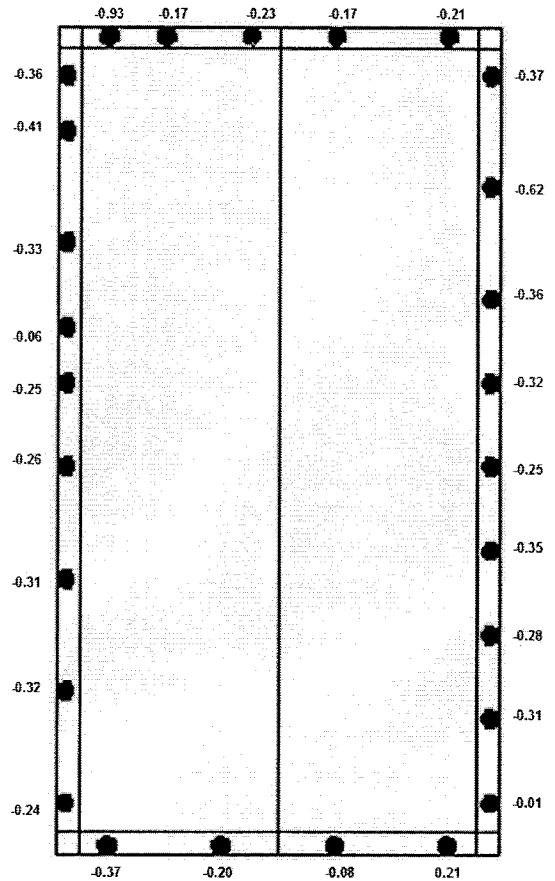

60 DEGREES

Cf,x

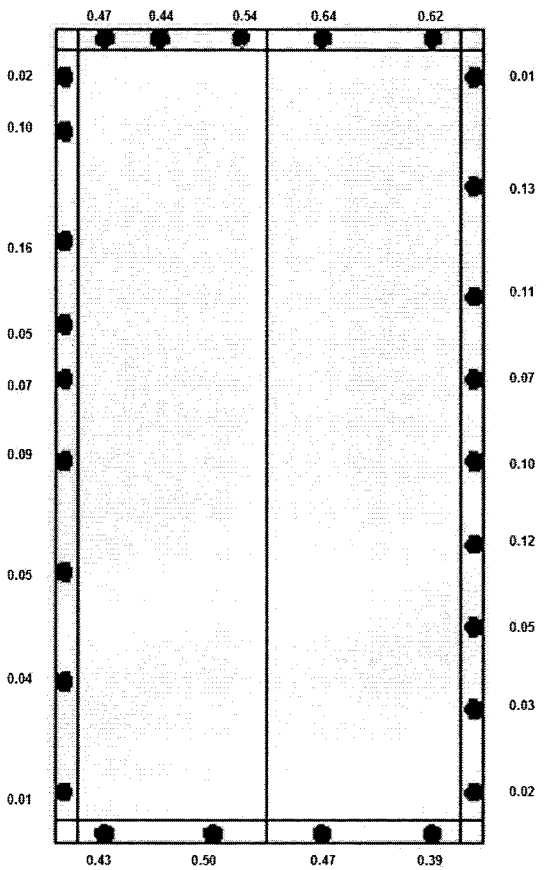

Cf,y

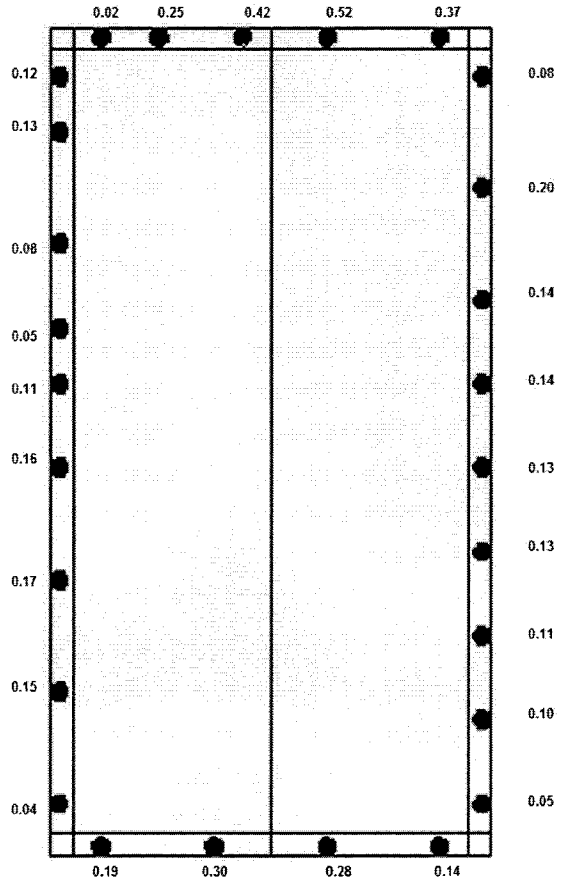

Cf,z

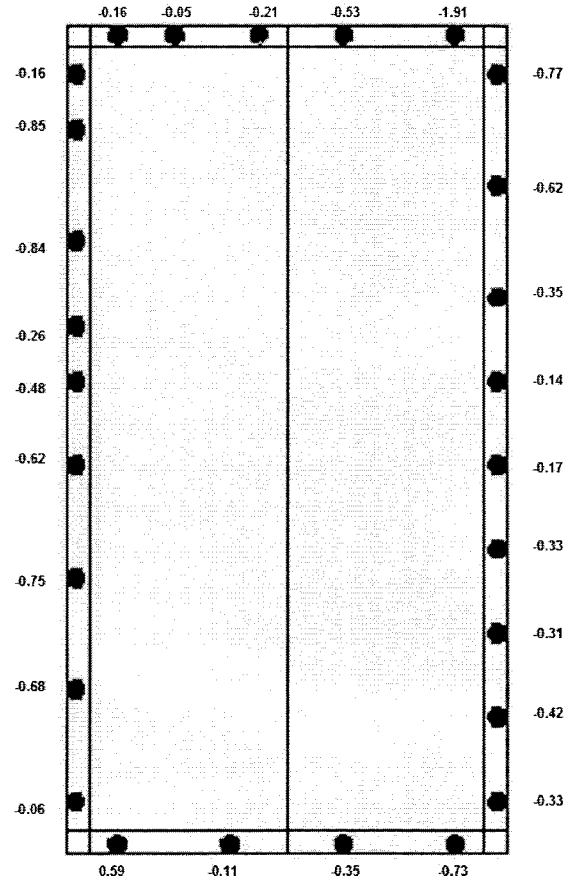

90 DEGREES

Cf,x

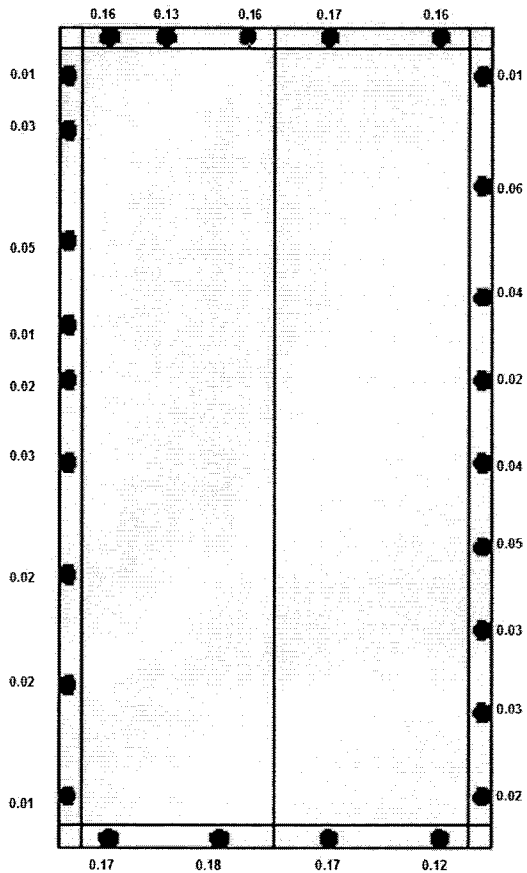

Cf,y

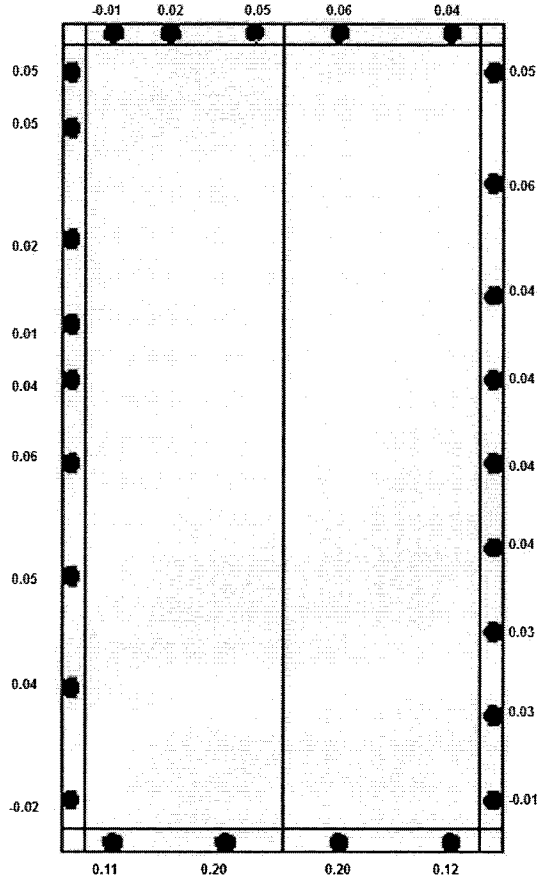

Cf,z

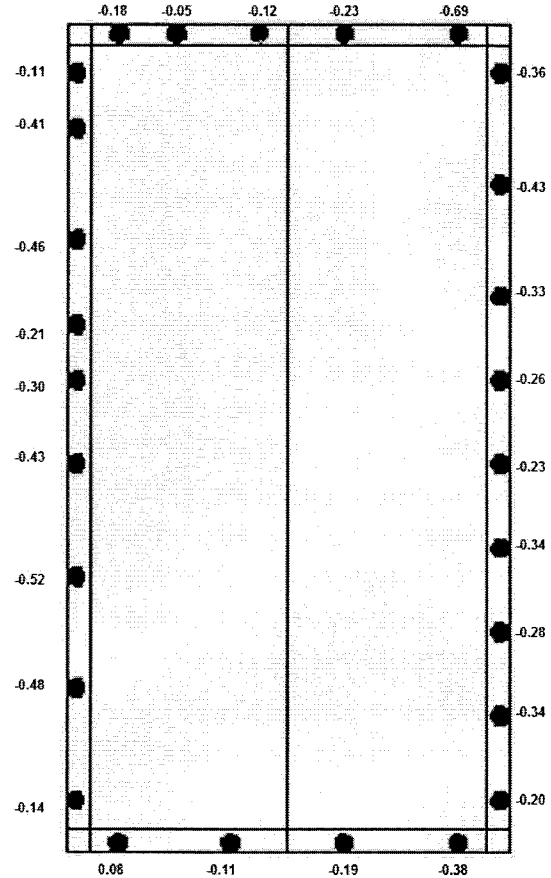

110 DEGREES

Cf,x

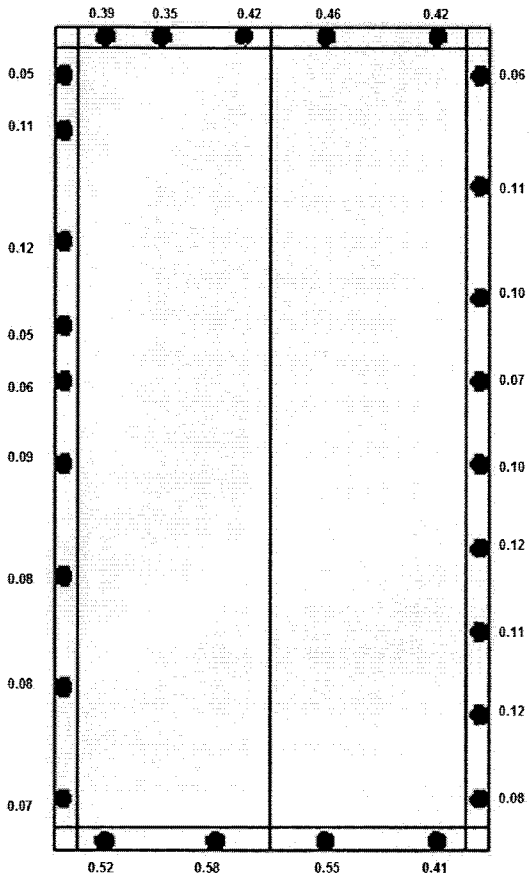

Cf,y

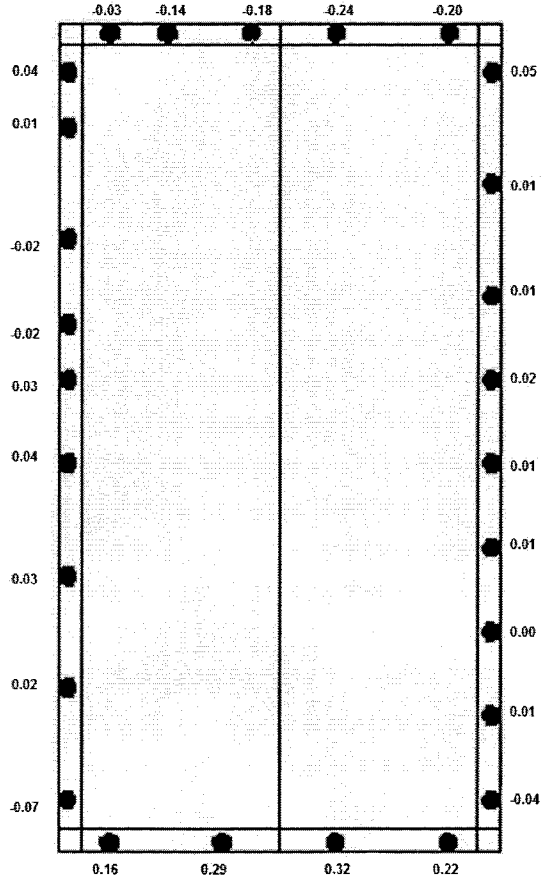

Cf,z

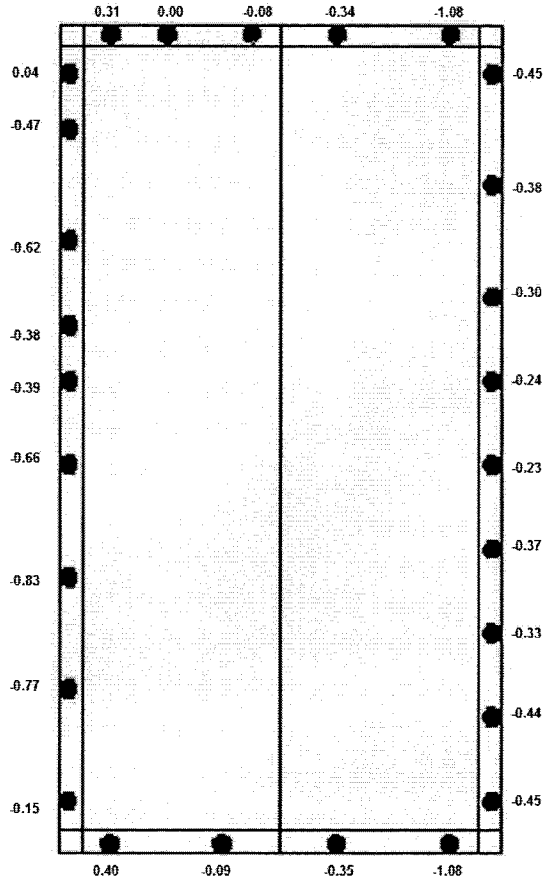

150 DEGREES

Cf,x

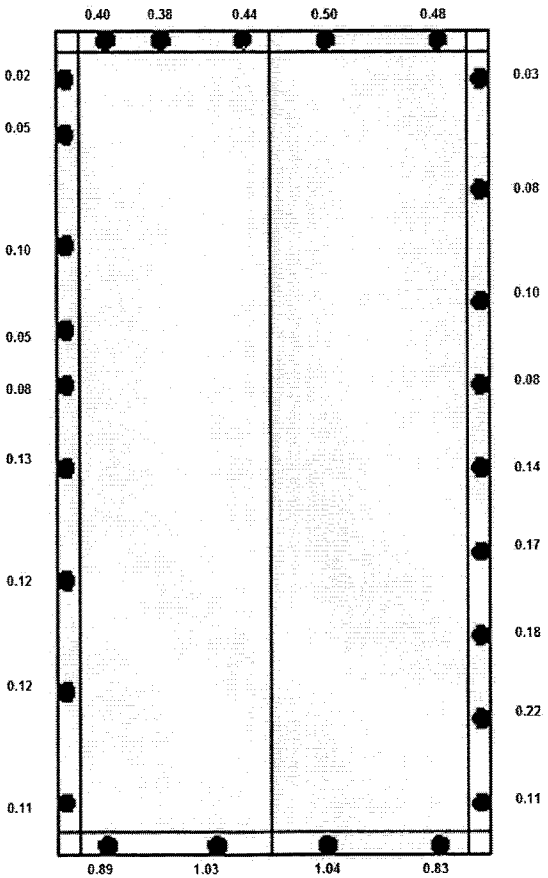

Cf,y

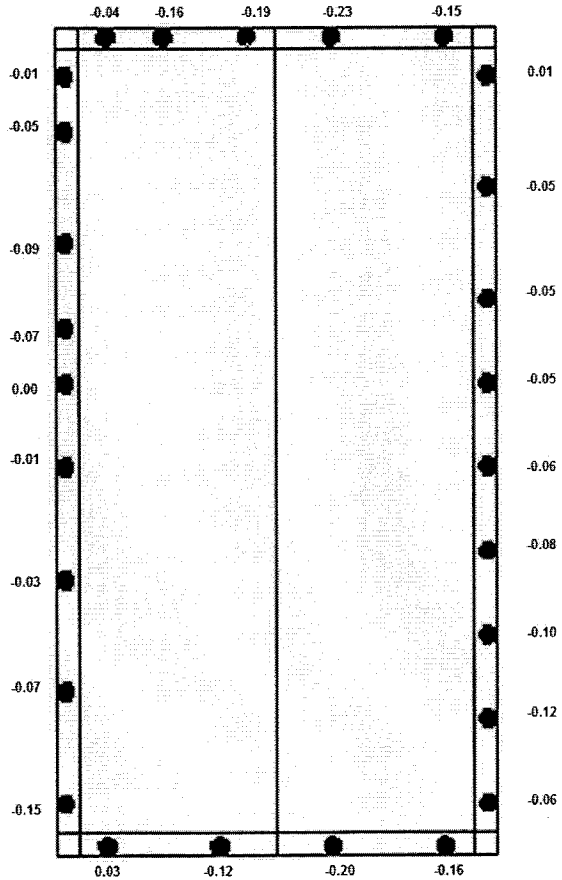

Cf,z

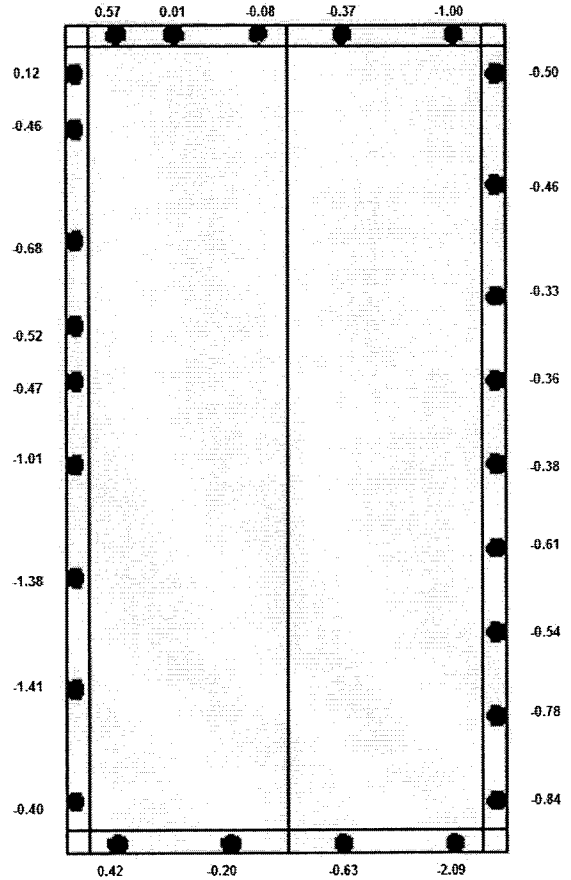

180 DEGREES

Cf,x

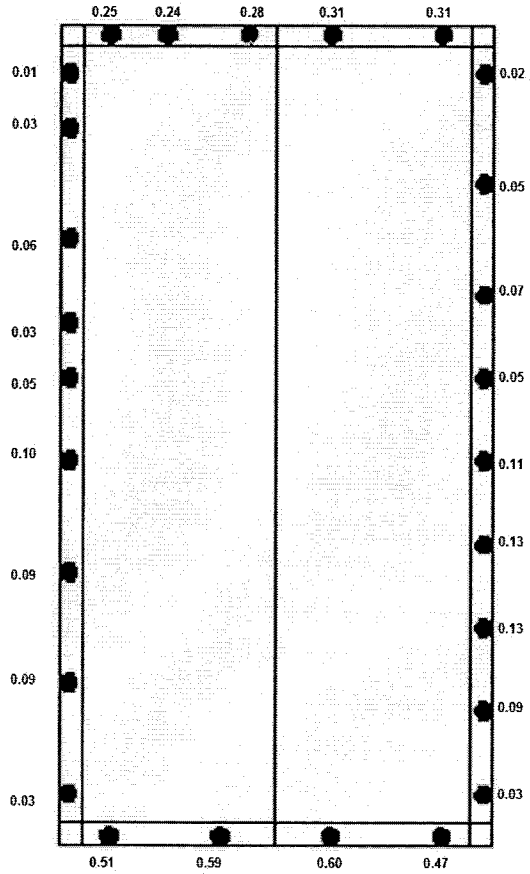

Cf,y

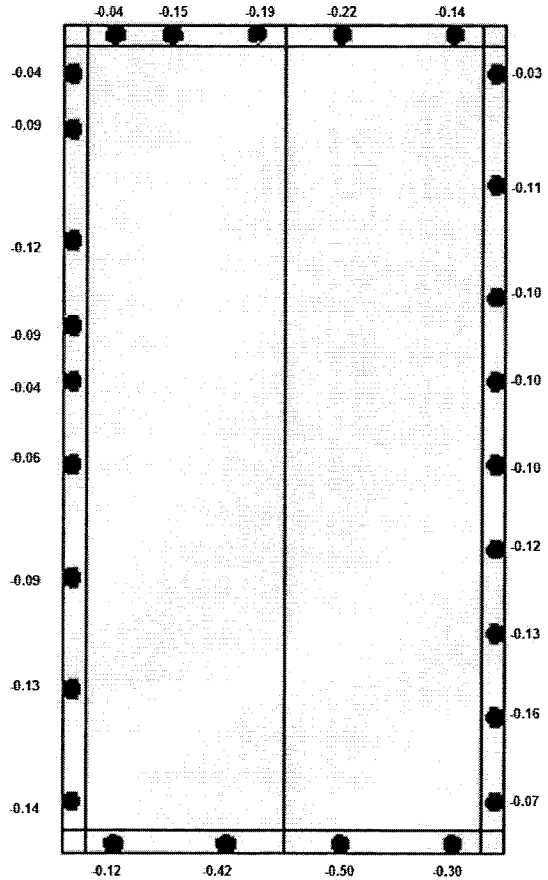

Cf,z

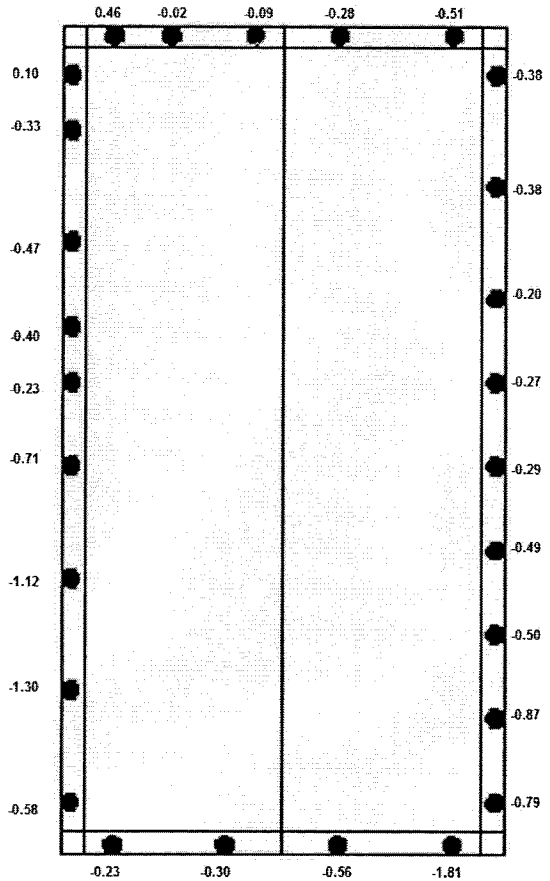

200 DEGREES

Cf,x

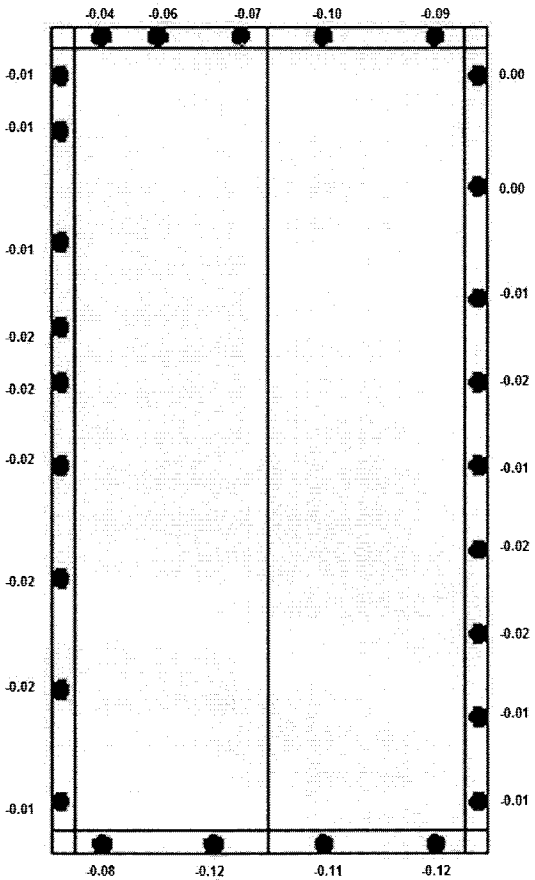

Cf,y

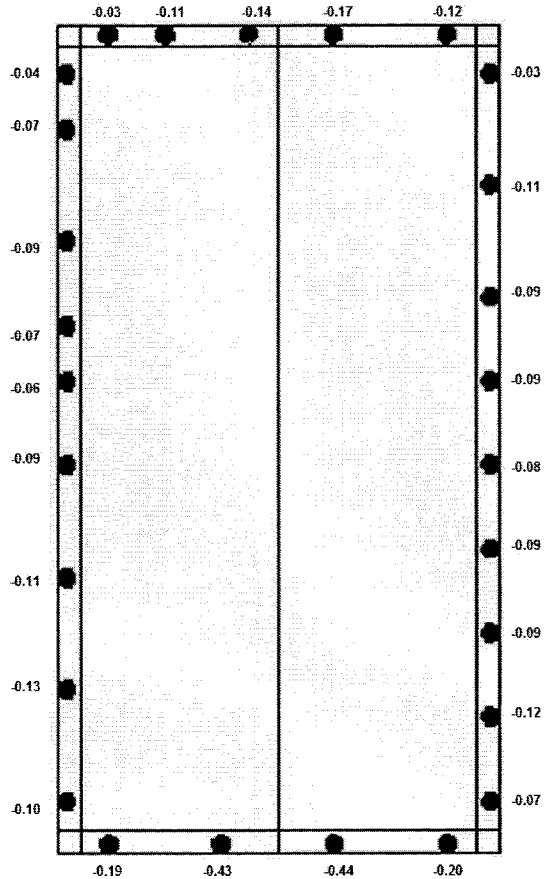

Cf,z

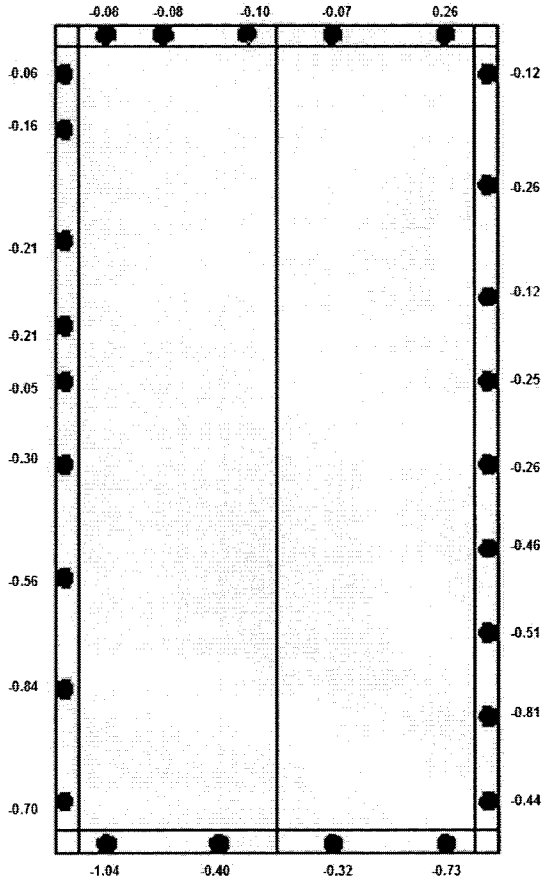

225 DEGREES

Cf,x

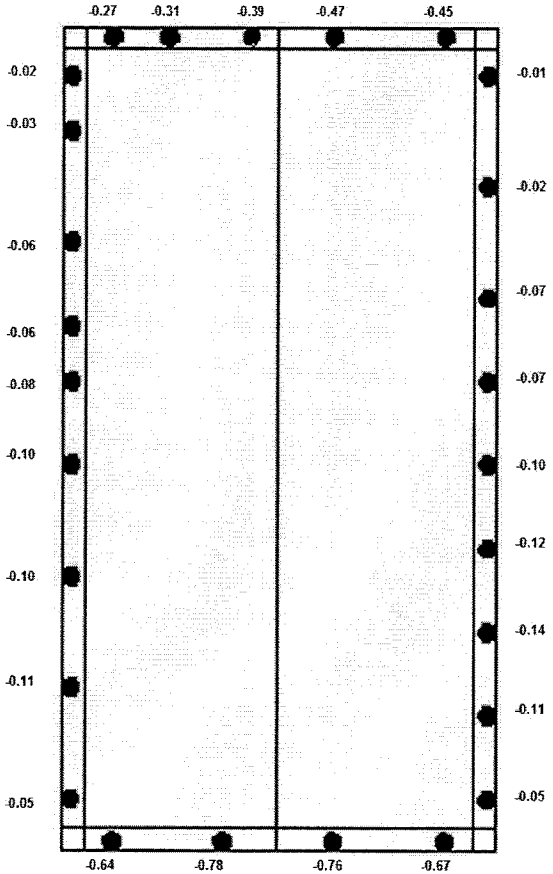

Cf,y

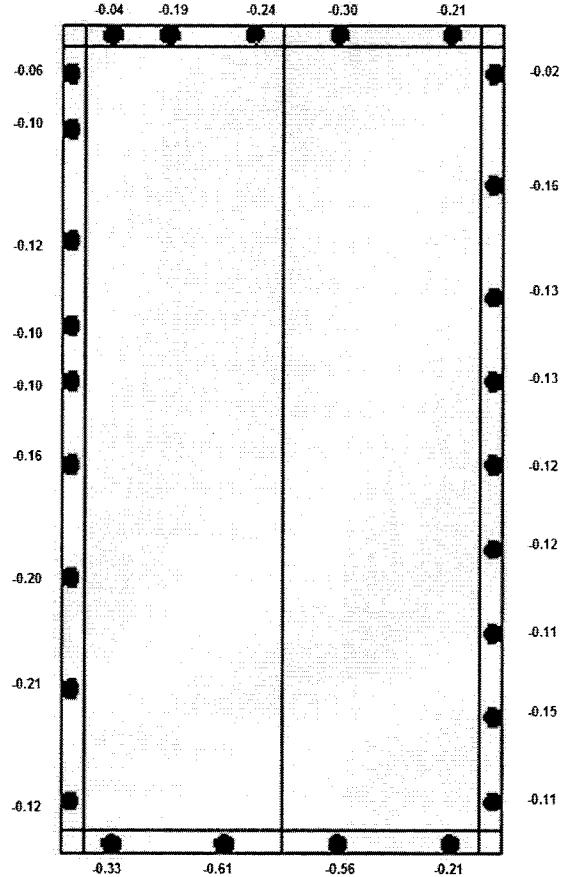

Cf,z

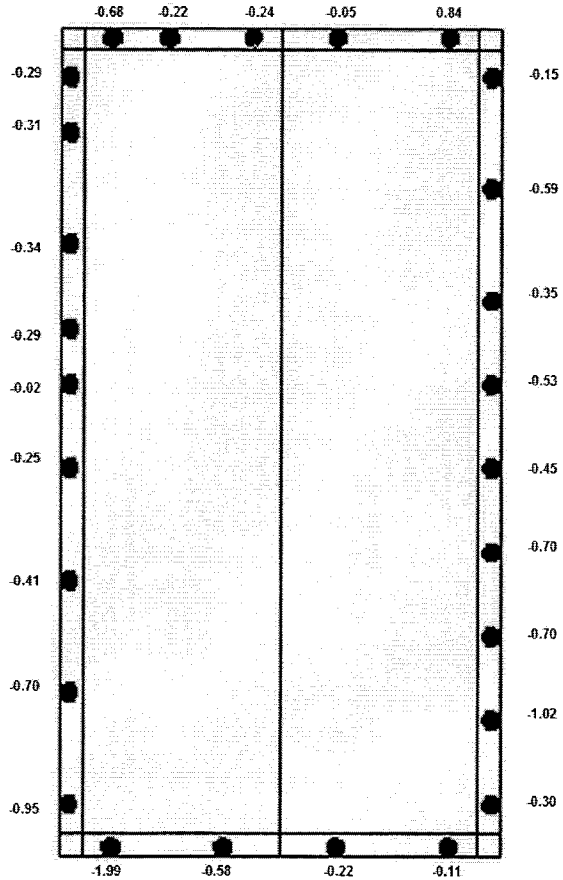

240 DEGREES

Cf,x

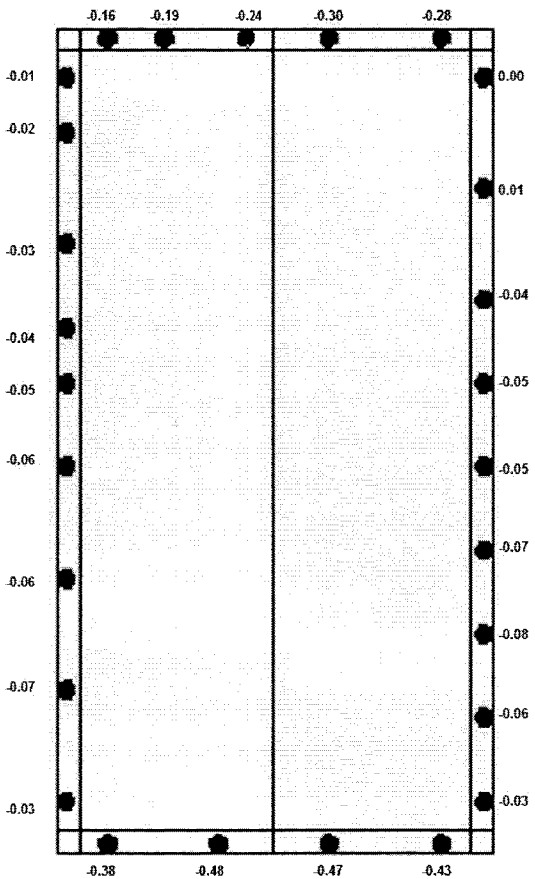

Cf,y

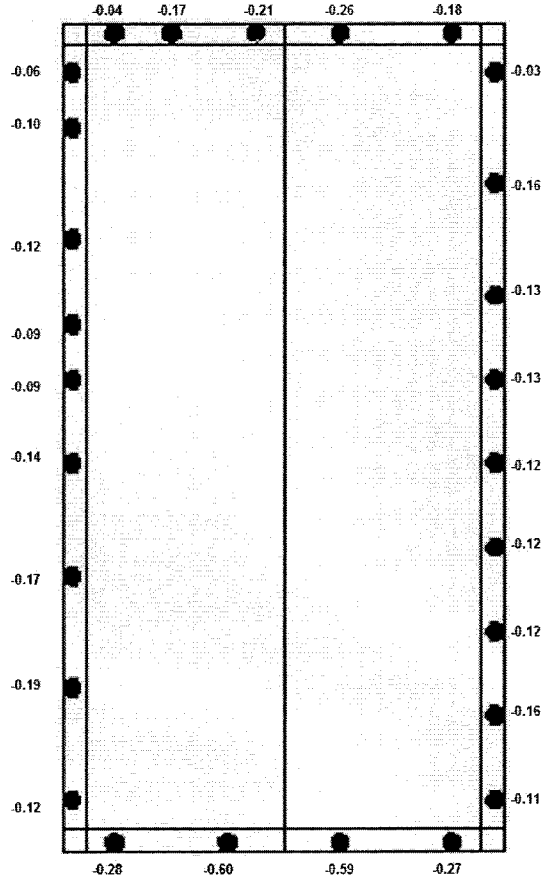

Cf,z

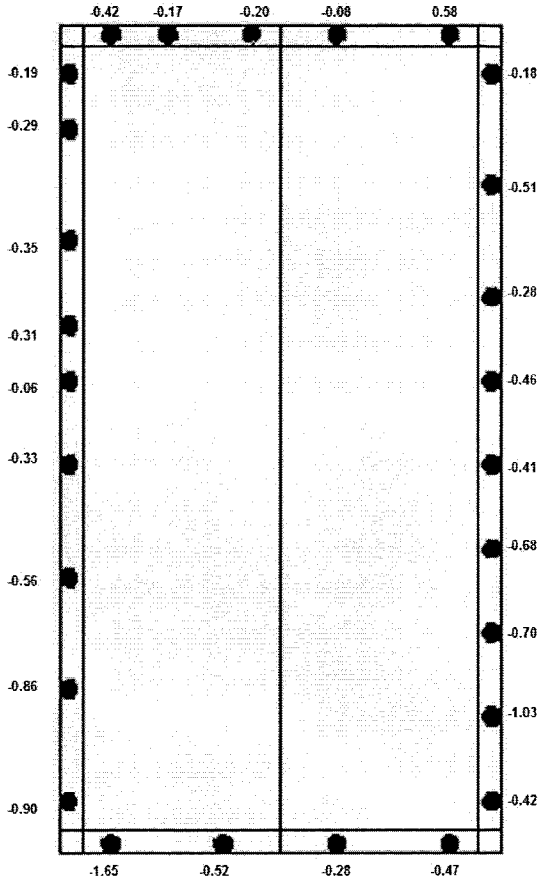

255 DEGREES

Cf,x

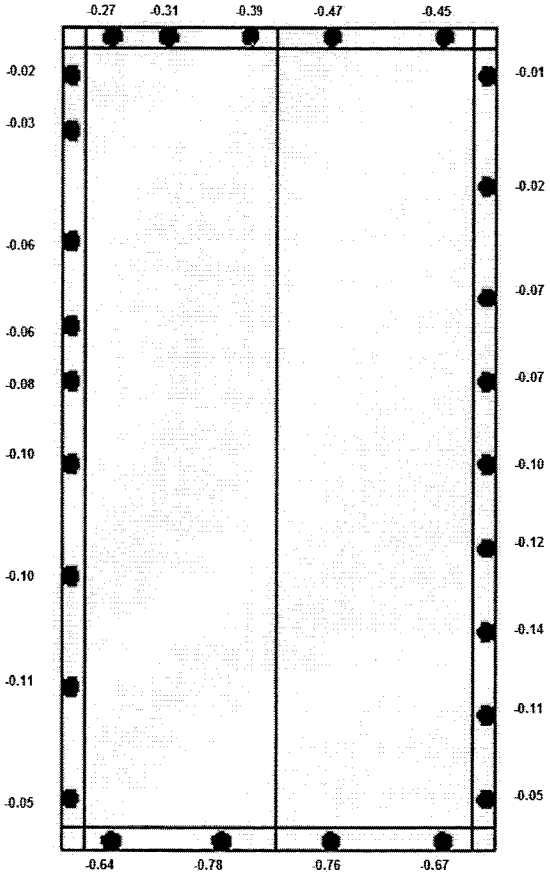

Cf,y

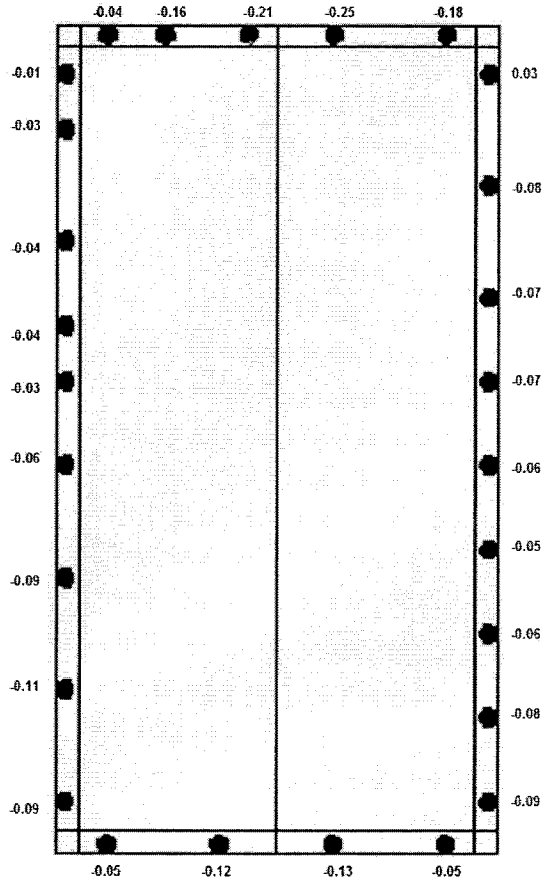

Cf,z

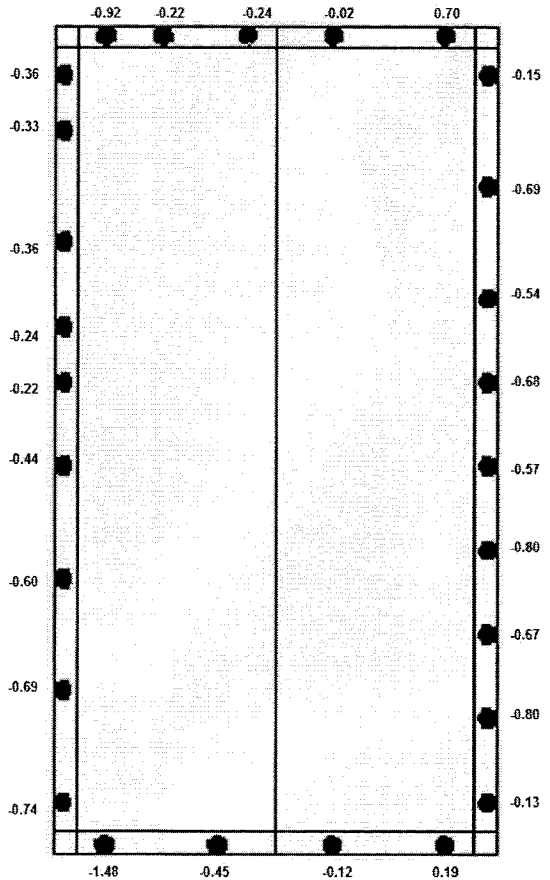

270 DEGREES

Cf,x

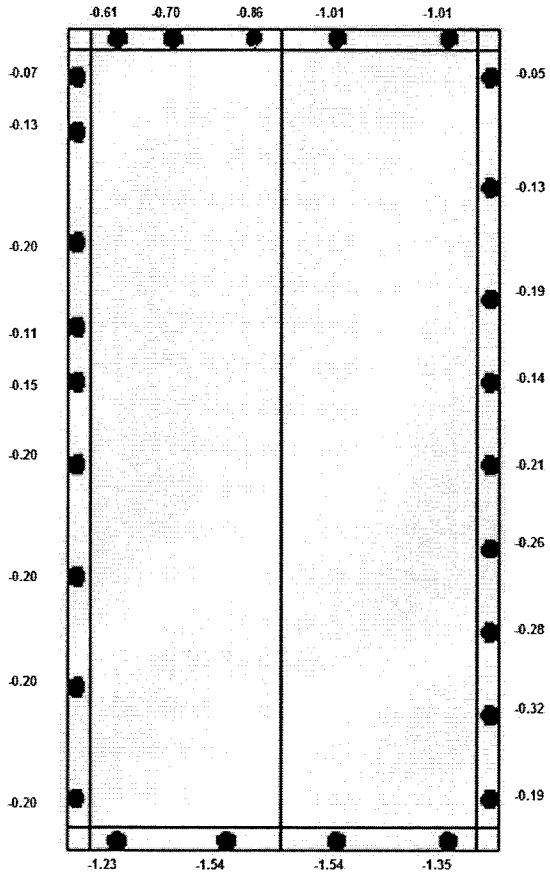

Cf,y

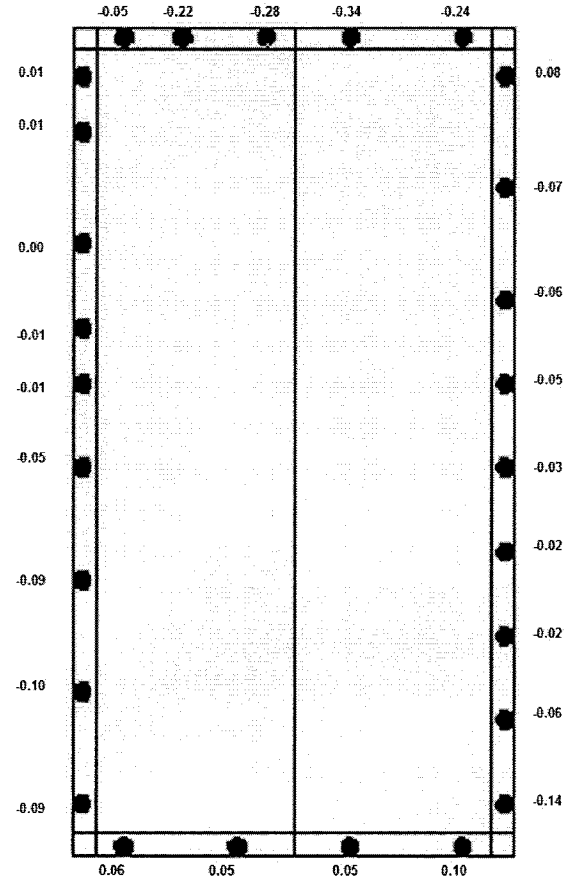

Cf,z

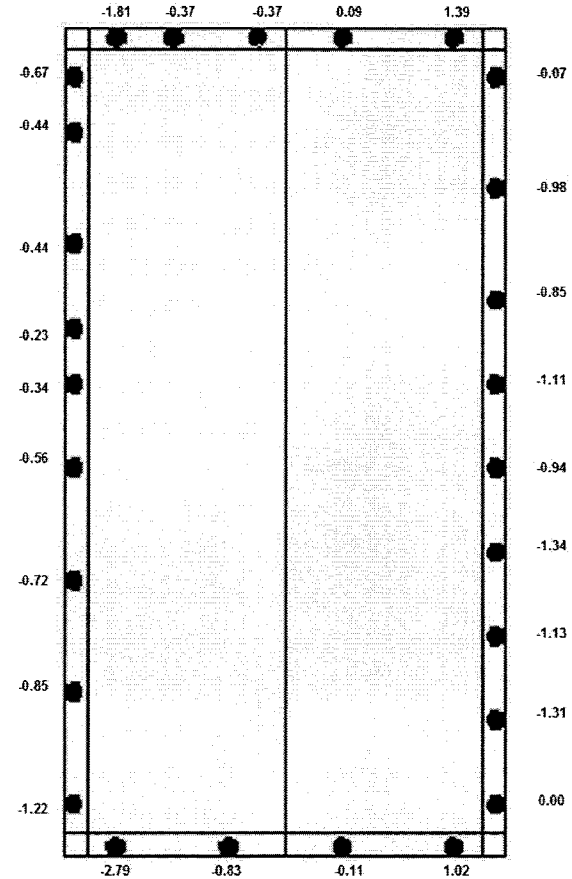

290 DEGREES

Cf,x

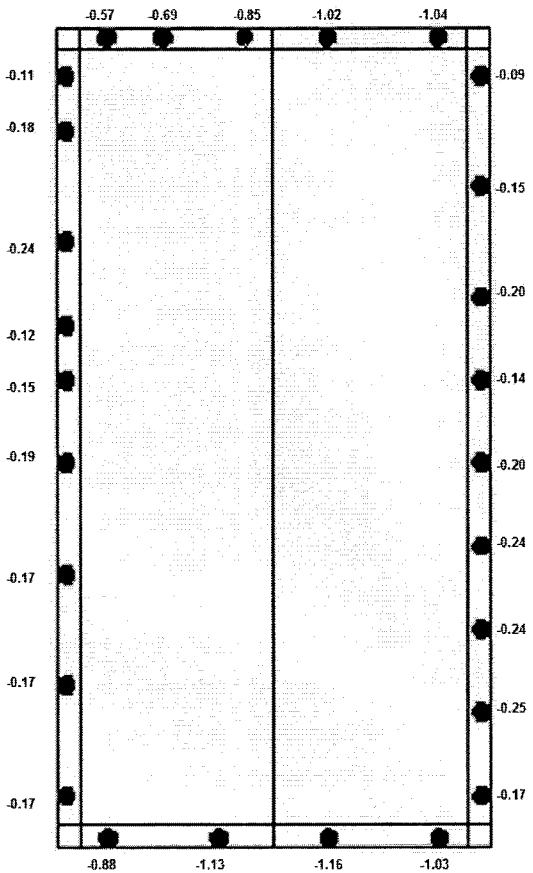

Cf,y

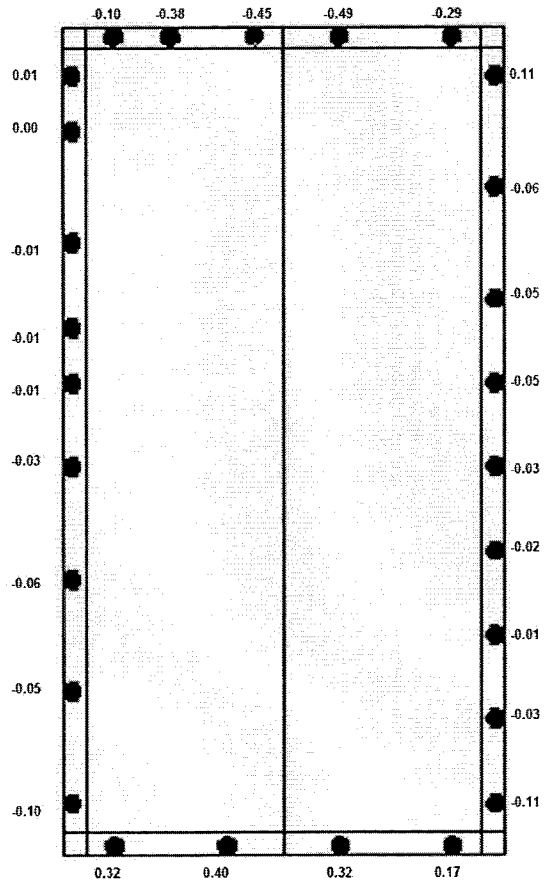

Cf,z

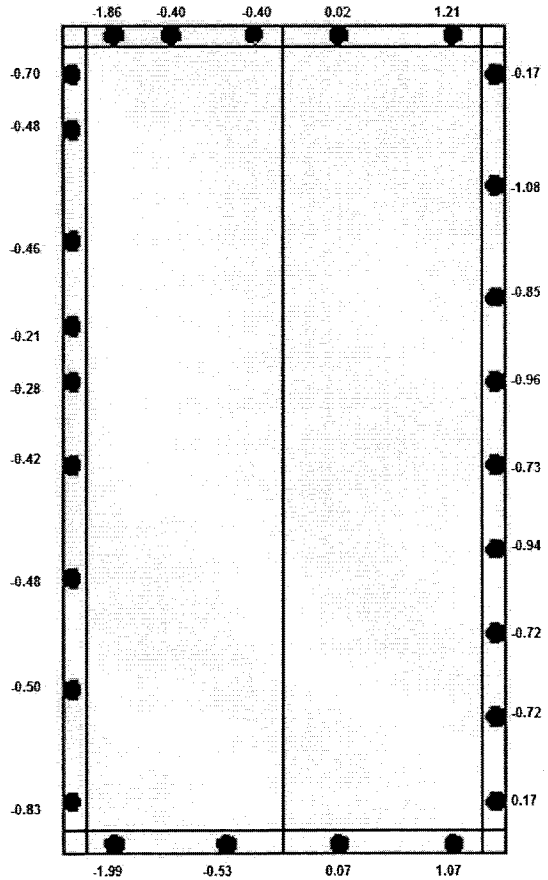

315 DEGREES

Cf,x

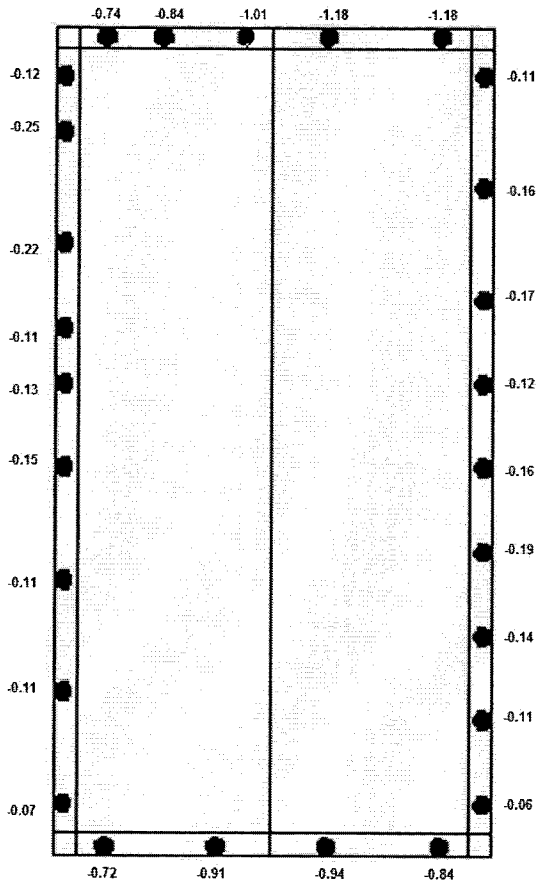

Cf,y

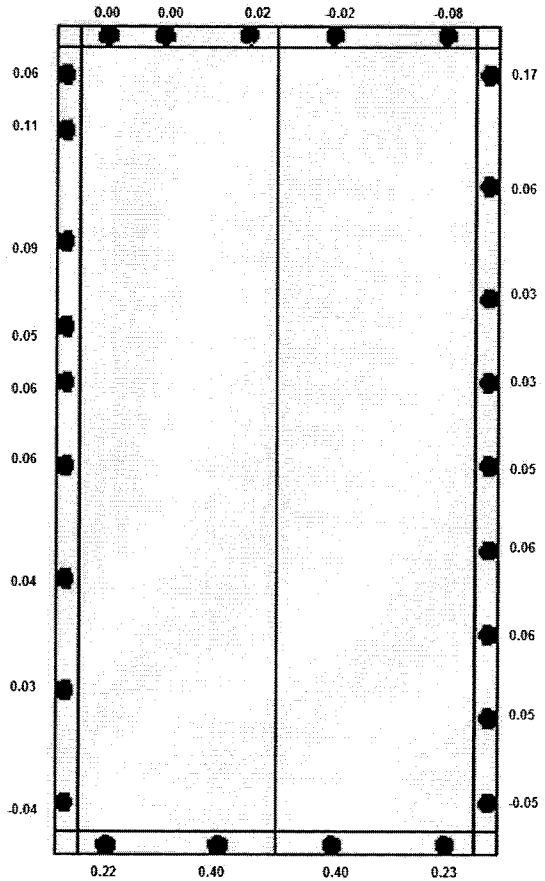

Cf,z

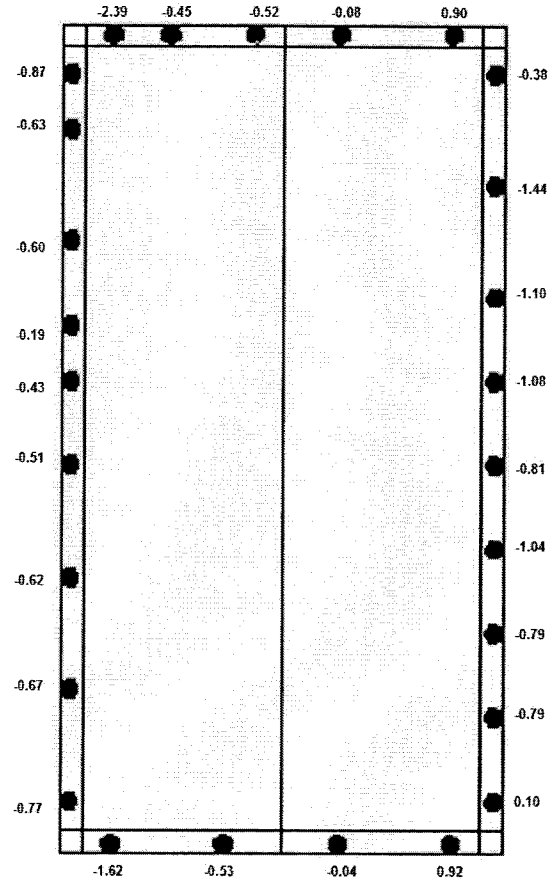

Individual load cell force coefficient variation over direction (based on F-E analysis)